NOVA SCHOOL OF SCIENCE & TECHNOLOGY

Department of Life Sciences

MIGUEL ÂNGELO MAGALHÃES PATRÍCIO

Bachelor in Cellular and Molecular Biology

DENDRITIC CELLS, BRIDGING NEUROMODULATION AND IMMUNITY

Master in Molecular Genetics and Biomedicine

NOVA School of Science & Technology | FCT NOVA

September, 2023

NOVA SCHOOL OF SCIENCE & TECHNOLOGY

Department of Life Sciences

Dendritic cells, bridging neuromodulation and immunity

Miguel Ângelo Magalhães Patrício

Bachelor in Cellular and Molecular Biology

Supervisor: María Martínez-López,
Postdoctoral researcher in the Immunophysiology laboratory at Champalimaud Foundation

Co-supervisor: Paula Videira,
Associate Professor of Glycobiology & Immunology at NOVA School of Sciences and Technology | FCT NOVA

Examination Committee:

Chair: Doctor Margarida Casal Ribeiro Castro Caldas Braga,
Assistant Professor at NOVA School of Science & Technology University| FCT NOVA

Rapporteur: Doctor Maria de Guadalupe Gonçalves Cabral,
Guest Assistant Professor at NOVA Medical School, Lisbon

Adviser: Doctor María Martínez-López,
Postdoctoral researcher at Champalimaud Foundation

Master in Molecular Genetics and Biomedicine

NOVA School of Science & Technology | FCT NOVA

September, 2023

Dendritic cells, bridging neuromodulation and immunity

Acknowledgments

First of all, I would like to praise Henrique Veiga-Fernandes for the great opportunity to welcome me to the immunophysiology laboratory at the Champalimaud Foundation, in which I was able to connect to an extraordinary group of people on both personal and professional levels.

Additionally, I want to thank my supervisor María Martínez-López for all her guidance through the dissertation period, for her patience in explaining every procedure, for showing me how a functional laboratory works, and for being always available to help me, even while on maternity leave, when I was feeling stressed or overwhelmed. Moreover, I am very thankful for the constant meetings that kept track of the project's progress. I learned a lot since the first day that I joined the laboratory, and I evolved as a scientist and a person. Therefore, I deeply appreciate you for investing in me and for all your attention. This project, alongside your generosity, kept motivating me to pursue a research career and for that, I am very grateful.

Moreover, I want to display appreciation to Raquel Silva, for all her availability during the whole dissertation and for assisting and teaching me several techniques related to laboratory work, especially during María maternally leave period in which all her help was crucial.

I also want to thank Bruno Raposo for always helping me in the laboratory. When I had doubts regarding the location of a machine or a certain reagent or even basic things regarding the laboratory, he was always there to assist me. I consider him a great friend that I hope to keep for the rest of my life. We exchange good periods both inside and outside the laboratory, and I am grateful for your kindness, and making me laugh, and for spending great times together.

Additionally, I want to thank my colleagues Beatriz Alves and Lynn Vermeer, we three formed the master's group which was very helpful throughout the whole period both professionally and personally. We spent so much fun time together in this period and our friendship facilitated my experience in the laboratory.

Moreover, I want to thank Paula Videira, my co-supervisor for your help during this period, and for keeping track of my thesis progression. You introduced me to dendritic cells in the first place and accepted me in the bachelor's project, which further explored my likeness to these cells.

I also want to thank my extraordinary parents and my girlfriend Vera Zöhrer, for always being ready to help and calming me down on days that I was more stressed than usual.

Furthermore, I want to give general gratitude to the whole immunophysiology group, you are a very fun group which I had the pleasure to spend time with.

Finally, I want to express my gratitude towards the GlassWash Platform, for your help with media preparation and glasswash cleaning, the ABBE Plataform for your constant assistance in confocal microscopy, the Vivarium Facility for managing the mice colonies, and the Flow Cytometry Plataform for their help in the flow cytometry machines.

Abstract

The neuroimmune system is an emerging investigation area, in which neurons and immune cells bidirectionally interact, modulating each other's cell function. Dendritic cells (DC) rely on their capacity to sense several environmental cues, and function by priming T cells therefore play pivotal roles in orchestrating immunological responses. The autonomic nervous system (ANS) comprises the parasympathetic and sympathetic branches. The last mediates "flight or fight" responses upon stress, influencing overall physiology, including immunity. Whether the DCs are able to integrate ANS-derived signals and how this affects DC functionality is the thesis' main goal. Advances in this field are limited by the use of *in vitro* approaches and unspecific DC genetic models *in vivo*. Hence, how ANS peptides impact DC function and host physiology is vastly unexplored. To address conventional DC type 1 (cDC1) functionality impact of sympathetic peptides, DC function was investigated upon norepinephrine and β2-adrenergic receptor (*Adrβ2*) agonist administration. Additionally, *in vivo* migration assays were conducted utilizing *Adrβ2* antagonists. Moreover, genetically engineered mice that devoid *Adrβ2* expression solely in cDC1 were analyzed. We observed that cDC1s lacking *Adrβ2* are more activated. Furthermore, DC1 migration increased upon *Adrβ2* antagonist administration. Henceforth suggesting that DC1, following *Adrβ2* signaling, suffers a phenotypical shift towards an immunosuppressive state. These results hold promise in developing innovative cancer immunotherapies by blocking DC *Adrβ2* signaling or limiting inflammation excess in an autoimmune disorder by promoting DC *Adrβ2* signaling. Deciphering the molecular and cellular intervenients of this neuroimmune crosstalk can revolutionize health and science, offering avenues to enhance physiological well-being.

Keywords: Dendritic cells, Sympathetic neurons, *Adrβ2*, Neuroimmune axis, Immunophysiology

Resumo

O sistema neuro-imune é uma área de investigação emergente, na qual neurónios e células imunes interagem bidireccionalmente, modulando a função celular um do outro. As células dendríticas (DC) baseiam-se na sua capacidade de detetar várias pistas ambientais e funcionam ativando células T, portanto, desempenham um papel fundamental na orquestração de respostas imunológicas. O sistema nervoso autónomo (SNA) inclui ramos parassimpáticos e simpáticos. Este último medeia respostas "fuga ou luta" em caso de stress, influenciando a fisiologia geral, incluindo imunidade. O principal objetivo da tese é saber se as DCs são capazes de integrar sinais derivados do SNA e como isso afeta a sua funcionalidade. Os avanços neste domínio são limitados pela utilização de abordagens *in vitro* e de modelos genéticos inespecíficos de DC *in vivo*. Por conseguinte, a forma como os péptidos ANS afetam a função das DCs e a fisiologia do hospedeiro é pouco explorada. Para abordar o impacto dos peptídeos simpáticos na funcionalidade das DC-convencional tipo 1 (cDC1), a sua função foi investigada após administração de norepinefrina e agonistas do recetor β2-adrenérgico (*Adrβ2*). Além disso, foram realizados ensaios de migração *in vivo* utilizando antagonistas de *Adrβ2*. Adicionalmente, foram analisados ratinhos geneticamente modificados que não têm expressão de *Adrβ2* apenas em cDC1. Observámos que cDC1s sem *Adrβ2* são mais ativas. Além disso, a migração de DC1 aumentou com a administração do antagonista *Adrβ2*. Sugerindo assim que DC1, após a sinalização de *Adrβ2*, sofre uma mudança fenotípica para um estado imunossupressor. Estes resultados são promissores no desenvolvimento de imunoterapias inovadoras contra cancro, bloqueando a sinalização DC *Adrβ2* ou limitando o excesso de inflamação numa doença autoimune, promovendo a sinalização DC *Adrβ2*. A decifração dos intervenientes moleculares e celulares desta interação neuro-imune pode revolucionar saúde e ciência, oferecendo vias para melhorar o bem-estar fisiológico.

Palavras-chave: Células Dendríticas, Neurónios simpáticos, *Adrβ2*, Eixo Neuro-Imune, Imuno-Fisiologia,

Content index

Figure Index

Table index

Abbreviation list

6-OHDA	6-hydroxydopamine
Ach	Acetylcholine
AChE	Acetylcholinesterase
Adrα1	α1-adrenergic receptor
Adrα2	α2-adrenergic receptor
Adrβ1	β1- adrenergic receptor
Adrβ2	β2- adrenergic receptor
Adrβ3	β3- adrenergic receptor
ALDH	Aldehyde dehydrogenase
ANS	Autonomic nervous system
APC	Antigen-presenting cells
Baft3	Basic Leucine Zipper ATF-Like Transcription Factor 3
BDCA3	Blood DC antigen 3
Btla	B-and T-cell lymphocyte attenuator
CD103	E-cadherin–binding integrin αE
cDC	Conventional dendritic cells
cDC1	Conventional dendritic cells type-1
cDC2	Conventional dendritic cells type-2
CDP	Common dendritic cell progenitor
CGRP	Calcitonin gene-related protein
ChAT	Choline acetyltransferase
Clec9a	C-type lectin domain containing 9A
CLPs	Common lymphoid progenitors
CLRs	C-type lectins receptors
CMP	Common myeloid progenitors
CNS	Central nervous system
CpG	Unmethylated cytidine-phosphate-guanosine
CpG-ODN	CpG oligodeoxynucleotides
CT	Cycle threshold
CTL	Cytotoxic T cells
DAMPs	Damage-associated molecular patterns
DBP	Dibutyl-phthalate
DCs	Dendritic cells
EDTA	Ethylenediaminetetraacetic acid
ENS	Enteric nervous system
Epi	Epinephrine
FACS	Fluorescence-activated cell sorting
FBS	Fetal Bovine Serum
FITC	Fluorescein isothiocyanate isomer I
Flt3	FMS-like tyrosine kinase 3
Flt3L	FMS-like tyrosine kinase 3 ligand
GM-CSF	Granulocyte-macrophage colony-stimulating factor
HBSS	Hanks' Balanced Salt Solution
HEPES	4-(2-hydroxyethyl)-1-piperazineethanesulfonic acid
HSCs	Hematopoietic stem cells
i.d	Intradermally

i.p	Intraperitoneally
ID2	Inhibitor of DNA binding 2
IFN-III	Type III interferon
IL	Interleukin
ILC	Innate lymphoid cells
IRF8	Interferon regulatory factor 8
L-DOPA	L-dihydroxyphenylalanine
LN	Lymph node
LPS	Lipopolysaccharide
mAChRs	Muscarinic acetylcholine receptors
MACS	Magnetic-activated cell-sorting
MF	Macrophages
MHC	Major histocompatibility complex
Mo	Monocytes
Mo-DC	Monocyte-derived dendritic cells
nAChRs	Nicotinic acetylcholine receptors
NE	Norepinephrine
Nfil3	Nuclear factor, interleukin 3 regulated
NICUs	Neuroimmune cell units
NK	Natural Killer cells
NLRs	Nucleotide oligomerization domain - like receptors
NOD	Nucleotide oligomerization domain
PAMPs	Pathogen Associated Molecular Patterns
PaNS	Parasympathetic nervous system
PBS	Phosphate Buffered Saline
pDC	Plasmacytoid dendritic cells
PNS	Peripheral nervous system
Poly (I:C)	Polyinosinic:polycytidylic acid
PRRs	Pattern Recognition Receptors
RA	Retinoic acid
RLRs	RIG-I-like receptors
RT	Room temperature
RT-qPCR	Reverse transcription quantitative real-time PCR
SIRPα	Signal regulatory protein α
SNS	Somatic nervous system
SP	Substance P
SyNS	Sympathetic nervous system
TCEP	Tris (2-carboxyethyl) phosphine
TCR	T-cell receptor
TE	Tris-EDTA
Tfh	T Follicular Helper
TGF-β	Transforming growth factor beta
Th	T-helper cells
TH	Tyrosine hydroxylase
Th1	T-helper cells type 1
Th17	T-helper cells type 17
Th2	T-helper cells type 2
TLRs	Toll-like receptors

TNF-α	Tumor necrosis factor-α
Treg	Tolerogenic T cells
TRPV1	Transient receptor potential vanilloid 1
VIP	Vasoactive intestinal peptide
VPAC1	Vasoactive intestinal peptide receptor type 1
XCL1	X-C motif chemokine receptor ligand 1
XCR1	X-C motif chemokine receptor 1

1. Introduction

1.1 Immune System

The immune system is a vast and complex set of cells and their molecules that aim to protect the host from various unknown entities, including infectious microorganisms, toxins, allergens and tumor cells, while maintaining the balance between tissue homeostasis and host defense[1].

In our day-to-day life, every time we breathe, eat, cut ourselves, touch surfaces, and interact with people or animals, we are in continual and constant contact with various organisms, naive or nocive, which may require immunological action. Hence, this continuously evolving system has the key ability to discriminate between patterns and molecules of the body itself or "self", and foreign "non-self" to be able to induce tolerance or elicit an efficient effector response respectively[1].

Nonetheless, two distinct but synergistic immune responses are required: the innate response that acts immediately upon contact with the threatening organism displaying no antigen specificity, and the adaptive response, a late-phase reaction that exhibits specificity to the immunogen and produces immunological memory being more prone to better defend against a subsequent invasion[1].

These immunological phases, despite their differences in their mode of action, duration, and specificity to the immunogen, need to act in a concise and balanced manner to not overwhelm the inflammatory response. If this equilibrium is compromised, and the immune system is left unchecked, the body can lose control of homeostasis, likely leading to severe immunopathologies.

1.1.1 Innate Immunity

The innate immune system is the organism´s first line of defense providing a rapid and non-specific response. It employs mechanical, chemical, and biological defensive barriers preventing the pathogen mode of action[2]. Immune cells like granulocytes, monocytes (Mo), dendritic cells (DCs), macrophages (MF), natural killer cells (NK) and innate lymphoid cells (ILC) alongside cytokines and the complement system, are included in this immune branch[2]. To recognize colonizing microbes, the immune cells express various Pattern Recognition Receptors (PRRs) that bind to specific Pathogen Associated Molecular Patterns (PAMPs)[3], this culminates in the secretion of pro-inflammatory cytokines and chemokines that result in increased phagocytic activity and migration into the site of injury to clear the threatening pathogens[4].

1.1.2 Adaptive Immunity

On the other hand, unlike innate immunity, adaptive immunity requires days to be elicited. Nonetheless, it is highly specific to the hazardous pathogen and has the unique ability to mount immunological memory. This immune branch englobes two major subtypes of response: the humoral immune response, executed by B cells, and the cell-mediated immune response which is carried out by T lymphocytes[5].

Humoral or antibody immune response involves activation of B cells and, through the release of cytokines produced by T-helper cells (Th), the differentiation into plasmocytes[4]. These immune cells produce and release soluble immunoglobins targeting the specific antigen[4]. The cell-mediated immune response relies on T cells interacting with the immunogenic peptides, displayed by antigen-presenting cells (APC) via the major histocompatibility complex, and the polarization into effector T cells that will clear virus-infected or tumoral cells and will assist other immune cells to perform their function[4].

1.2 Dendritic cells – origin and their subtypes

DCs are potent APC[6,7] presented in all mammalian lymphoid and non-lymphoid tissues bridging the innate and adaptive immunological arms together[8]. There are different subtypes of DCs, namely, plasmacytoid DCs (pDC), monocyte-derived DCs (Mo-DCs), and the conventional DCs (cDC), that can be subdivided into type-1 (cDC1) and type-2 (cDC2)[7–9].

DCs can be generated in the bone marrow from both common lymphoid progenitors (CLPs) and common myeloid progenitors (CMP). pDCs, a particular $CD11c^{low}$ $MHC\text{-}II^{low}$ DC, excels in the production of type I interferons which are crucial for anti-viral immunity[10–13], are mainly derived from CLPs, however increasing evidence supports that they can also emanate from CMP[7,10,13–17].

On the other hand, Mo-DC are derived from monocytes that upon inflammation originate DC-like cells, whose function remains unclear but it's thought to complement the function of cDC and also act as APC in the skin[8,18]. cDCs derived from CMP, and posteriorly from an intermediate state into common dendritic cell progenitor (CDP)[7,8,12,14] in a process that is highly dependent on the FMS-like tyrosine kinase 3 (Flt3) receptor and its ligand Flt3L[7,8,13] (Figure 1.1). Furthermore, it is further improved by Granulocyte-macrophage colony-stimulating factor (GM-CSF) and tumor necrosis factor-α (TNF-α), although being fl3tl the crucial cytokine[8,19,20]. cDC1 and cDC2 are the most studied DCs, being present in lymphoid or non-lymphoid tissues, being the ones with higher antigen processing and migration capacity[8,10]. Henceforth, cDC will be the focus of this dissertation, and the type of cells analyzed in the experiments.

1.2.1 cDC1 and cDC2 - Identification

As previously referred to in section 1.2 the group of DCs most characterized are cDC1 and cDC2. These are classical DCs that resort more to the initial definition of DCs by Ralph Steinman and Zan Cohn back in 1973[8]. The two types of conventional DCs can be defined or distinguished by the expression of their surface markers, transcription factors, PRR sensing, and the immunological function they promote after activation, due to having more or less affinity to prime naïve T cells into distinct specialized Th subsets as well as cytotoxic T cells[8].

The earliest classification that can distinguish these two main cDCs remote to the hematopoiesis process immediately after CDP stage[8]. In which, there are early markers that make a preliminary discrimination between committed pre-cDC1 lineage, like expression of CD117, CCR2 but not CD115 and double negatives for Ly6C and SiglecH markers[8,15,21], while pre-cDC2 committed cells express CD115 and Ly6C but not CD117 and SiglecH[8,15,21]. During the process of pre-cDCpoiesis, these cells become $CD11c^{+}$ but still lack expression of MHC-II[8,10,15], posteriorly, these cells will then migrate out of the bone marrow into the different mammalian tissues, posteriorly originating into the cDC1 and cDC2[8,10,14,15,21,] which then translates into $CD11c^{+}$ and $MHC\text{-}II^{high}$ immune populations[8] (Figure 1.1).

Additionally, it is also suggested that $CD24^{high}$ expressing splenic pre-cDC are more destinated to induce cDC1[14,21] while $CD24^{low}$ splenic pre-cDC lead to cDC2 genesis, moreover, it is suggested that $CD24^{int}$ have the plasticity to generate either subtype of cDC[14].

As previously stated, these cells share common progenitors with other myeloid cells (CMP stage), however, several genes have been identified that selectively distinguish between cDC and the other myeloid immune compartments, such as macrophages, like Zbtb46[8,10,15,16,21,22] and Flt3[8,10,15,16] transcription factor as discussed in section 1.2; Ccr7[8,10,15,16], the chemokine receptor with high impact in the migration into the lymph node (LN) as pointed in section 1.2.3; Btla (B-and T-cell lymphocyte attenuator or CD272)[15,16], an inhibiting immunoglobulin protein blocking T and B-cell receptor signalling[16]; c-kit[8,10,15,16] a stem-cell factor receptor, however, its role in cDC is unidentified[16]; Dpp4 (CD26) that transduces dipeptidyl peptidase protein also with unknown function in cDC compartment[15,16]; and more[16]. These selected genes/transcription factors can thus be good markers to distinguish such populations.

Furthermore, all conventional mouse DCs have general expression CD45, CD135 (Flt3 receptor) $CD11c^{+}$, an integrin alpha X[23], and $MHC\text{-}II^{+}$ in the plasma membrane and are negative for the phenotypic marker proteins of other immune cells such as lymphocytes and granulocytes as well as the hemocytes lineage[8,10,17]. However, the expressions of CD11c and MHC-II, despite being widely used in the

identification of classical DCs, are very heterogeneous among tissues and between immune cells since some tissue-specific macrophages can express such proteins[8,14–16]. Thereafter, the use of other markers can further promote better discrimination is sometimes needed, for instance, CD135[10], CD24[7] (mostly expressed in cDC1), and CD26 (mostly expressed in cDC2)[7,17].

Nonetheless, CD11c and MHC-II are still undisputed and key markers to target cDCs being highly used in flow cytometry. However, advances in the discovery of new markers could lead to even more robust and precise tissue cDC identification. Human cDCs are also $CD11c^+$, $HLA\text{-}DR^+$ (MHC-II human counterpart), and highly dependent on Flt3L[7,8,17], in addition, similar to mouse cDC[8,17], also lack other immune cell lineage markers.

As elicited in the introduction, cDCs can be subdivided into cDC1 and cDC2. Regarding transcription factors, the origin of cDC1 is heavily dependent on Basic Leucine Zipper ATF-Like Transcription Factor 3 (Baft3), interferon regulatory factor 8 (IRF8) in both humans and mouse[8], Nuclear factor, interleukin 3 regulated (Nfil3), and inhibitor of DNA binding 2 (ID2)[8,14,21]. On the other hand, cDC2 development is mainly regulated by Zeb2, IRF4[8,14,21], and IRF2[8,14]. It is further known that Notch2 receptor and Klf4 protein can display a role in regulating mouse cDC2 differentiation in other tissues like the spleen[8,14].

cDC1s are the least expressed cDCs in the tissues[7,8], accounting for 30% of total resident cDCs in non-lymphoid tissues[8] and 40% in secondary immune organs[8] (20% of total splenic DCs[17], however they are enriched in Thymus and Peyer patches[8]).

These cells are characterized by the expression of unique markers such as X-C motif chemokine receptor 1 (XCR1)[7,8,17] which will bind to X-C motif chemokine receptor ligand 1 (XCL1) mainly expressed by $CD8^+$ T cytotoxic effector cells[7,8] and NK cells[7], favoring its interaction. DNGR- 1, commonly known as C-type lectin domain containing 9A (Clec9a), is another good marker to exclusively target cDC1 from cDC2[7,8,17,24]. This C-type lectin is involved in binding to filamentous actin exposed by necrotic cells[8,24]. This interaction facilitates dead-antigen internalization promoting cross-presentation of cDC1 to $CD8^+$ T-cells resulting in cytotoxic adaptive response[7,8,24].

Furthermore, all lymphoid cDC1 are also $CD8^+$ cells, foreshadowing its role in cross-presentation to T cells[7,8,17]. Additionally expressed by cDC1 are the E-cadherin–binding integrin αE (CD103) mainly in peripheral tissues, hence this integrin is connected to the migration capability of cDC1 into draining lymph nodes[7,8,17]. Nonetheless, there is a defined subpopulation of cDC2 that expresses this molecule in the intestine[7,8,17]. Furthermore, CD24 is usually higher expressed in cDC1 (like in pre-cDC1 already depicted), although lung[8,17] and intestine[17] cDC2 also express this molecule[8]. One important note is that cDC1 is characterized also by higher protein levels of Flt3 (CD135)[7,8].

cDC2s on the other hand are a well-represented heterogeneous group of cDCs[7,8,17] (account for 80% of total splenic DCs[17]). These cells are characterized by expression of $CD4^+$ in secondary lymphoid organs, therefore also indicating its role in priming naïve T cells and eliciting adaptative CD4-type immunological responses[7,8,17]. Additionally, Signal regulatory protein α (SIRPα) and CD11b are the usual markers to target cDC2[7,8,17]. It is important to point out that the markers of both cDC1 and cDC2 are mutually exclusive, being XCR1 and SIRPα the gold standard to identify cDC1 and cDC2 respectively[7,8,25] (Figure 1.1).

Many similarities can also be traced in humans, for example, like mice, there is a pre-cDC stage that branches into pre-cDC1 and pre-cDC2[8]. Moreover, cDC1 expression is lower than cDC2 like the murine counterparts in the organs[7,8] and blood (the first corresponds to approximately 0.03% and the latter 1% of human PBMC[17]) and are also less heterogenous[8]. Again, in line with mice cDC1, human cDC1 also expresses XCR1 and Clec9a[7,8,17] and human cDC2 possesses SIRPα[7,8,17]. Furthermore, human cDC1 differentiation also requires Baft3 and IRF8 transcription factors[8]. In humans, blood DC antigen 3 ($BDCA3^+$) or CD141 is an additional marker for blood cDC1, widely used in human cDC studies, that displays similarities with $CD8^+$ mouse cDC1 being its human equivalent immune cell[7,8,17].

There have been papers hinting at their immense potential role in immunotherapies and cancer studies. Hence further studies are always required to fully comprehend these cells, take advantage of their immunological properties, and promote science and health.

1.2.2 DCs as environmental surroundings sensors

DCs are crucial for the shaping of the specific adaptive response against a harmful pathogen or for maintaining tolerance to a self-antigen or commensals thus playing a key role in preserving the organism's homeostasis[6,7,26,27].

After the differentiation event in the bone marrow, the immature DCs reside in various peripheral tissues susceptible to pathogen encounter, such as the lungs, intestine, and skin[6,8]. These resting DCs exhibit long protrusions, functioning as sentinel cells with great antigen-sampling capacity[6,8] but lack antigen presentation competence, therefore, having downregulation in the molecules and receptors needed for the T-cell clonal expansion and achieve their biological active state[28–30].

Given the high diversity of microorganisms and cellular components, DCs possess an immense array of PRRs, specifically recognizing different PAMPs. Thus, DCs excel in the function of sensing environmental surroundings with high plasticity. The family of PRR is very broad and includes both membrane-bound receptors like Toll-like receptors (TLRs) and C-type lectins receptors (CLRs), and intracellular proteins such as RIG-I-like receptors (RLRs) and nucleotide oligomerization domain(NOD)-like receptors (NLRs)[8,31–34].

Different TLRs are recently being explored to achieve DC activation in an inflammatory scenario. For instance, Polyinosinic:polycytidylic acid (Poly(I:C)), a synthetic double-stranded RNA molecule serves as TLR3 agonist to induce cDC1 stimulation[8] and consequent release of soluble cytokines such as interleukin (IL)-12[34] and type III interferon (IFN-III)[35,36]. Moreover, studies showed that TLR3 enhances cDC1 cross-presentation to $CD8^+$ cells in an anti-viral response[8,37]. It is also known that both human and mouse cDC1 express high amounts of TLR3[7,8,17]. Henceforth, Poly(I:C) administration is being very utilized in cancer studies[36,38] and adjuvants in vaccines[39–41] as well as boosting anti-viral strategies[42]. Additionally, unmethylated cytidine-phosphate-guanosine (CpG) is a target of TLR9 to distinguish mammalian DNA from bacterial DNA[34]. CpG oligodeoxynucleotides (CpG-ODN) molecules have also been used as an immunostimulatory agent triggering activation of DCs via TLR9[43] for vaccine purposes and immunotherapy[41,44–47].

Furthermore, lipopolysaccharide (LPS), a well-known bacterial membrane component is selectively targeted by TLR4[43,48,49] contributing to DCs activation[8] being more primed to perform cross-presentation[48,49].

Nevertheless, besides PRR triggering being a necessary key player in DC activation, sometimes is not sufficient[33]. In those scenarios, damage-associated molecular patterns (DAMPs) derived from infected cells, necrotic cells, and also from PAMP recognition, play a role in boosting DC activation[33,50,51]. These danger signals are very diverse and can include: ATP[50,51], nucleic acids[51], filamentous actin[8], uric acid[51], proinflammatory cytokines like TNF-a, IFN-I[33,51] as well as lymphocyte-derived activators such as CD40-L[51] that combines with IL-1 inducing a potent immunogenic DC[52,53]. The synergized action of all these parameters fully reaches the activation state of DCs.

Once DCs integrate the molecular information coming from pathogens together with danger signals via these diverse selective receptors they undergo a process of activation associated with upregulation of co-stimulatory markers and MHC and increase cytokine production[8] while losing endocytic ability. This process is termed maturation, therefore the DCs are with the necessary conditions to migrate into secondary lymphoid organs, such as draining lymph nodes, spleen, and Peyer patches via lymphatic vessels to present the specific immunogens to lymphoid cells hence the starting point to an effective adaptive immunological response.

1.2.3 DC migration through chemokines and their lymph node localization

As previously mentioned to prime naïve lymphocytes and trigger either a cellular immune response or a later humoral response, DCs require to migrate via lymphatic vessels into secondary lymphoid organs[6,54–56]. This crucial event is tightly modulated by chemokines, small soluble molecules released

by immune, endothelial, and epithelial cells following infection or damage[6,54–56], being its main function to govern migration events of immune cells, guiding them to the site of infection[6,54–56]. This is regulated by differential amounts of chemokines released, resulting in a chemoattractant gradient modulating the chemotaxis event after recognition by chemokine receptors on the surface of immune cells[6,54–56].

cDCs express the chemokine receptor CCR7[6,8,54–59]. This protein alongside its main ligands, CCL19 and CCL21 creates a chemokine axis crucial for the migration into the lymph node and therefore the initiation of an adaptive immunity[6,8,54–59]. CCL21 is involved in guiding the mature DCs alongside the lymphatic vessels while both CCL19 and CCL21 promote movement inside the lymphoid organ[55]. CCL21 is secreted by the afferent lymphoid vessels and CCL19 is released by matured DCs[57,60]. Furthermore, CCL21[6,8,54–57,60] and CCL19[57,60] are highly expressed in lymphoid stromal cells. Therefore, these chemokines will promote and guide, CCR7-DC dependent migration in a haptotaxis[6,8] manner, attracting the DCs into the draining lymph node where the expression of these molecules is more persistent (Figure 1.1).

The DCs additionally express CCR6[55,56,61–63] which together with its ligand CCL20, secreted in high amounts following an inflammation reaction by the epithelial cells[61–63], induce immature CCR6-DC dependent migration into the infected tissues, triggering immunity [61,62] (Figure 1.1).

Interestingly, in the lymph node, there are two populations of cDCs that can be distinguished regarding if they emanate from the tissues or "migratory cDC" and lymph node tissue-resident cDC that came after the bone-marrow differentiation phenomenon[8,10,64]. Migratory cDCs can be discerned from the resident cDCs due to the former typically expressing larger amounts of MHC-II protein and lower CD11c levels than the second population[8,10,64]. However, this discrimination is only viable in steady-state scenarios, as in an inflammation or challenge scenery using these general markers it is unfeasible to label these populations[10,64]. Like previously stated, $CD8^+$ cDC1 are from lymphoid origin, therefore are considered lymph node resident-cDC, while $CD103^+$ is a good marker to target migratory cDC1 in the lymph node[8,10,64]. However, up to date, there are no markers to apply the same discrimination of migratory and resident in cDC2[10,64].

After acquisition of the antigen, the migratory cDCs will, via afferent lymph vessels move into the lymph node to prime naïve T cells directly, or indirectly, in which it is hypothesized that they can transfer the immunogen to the resident cDC as an amplifier of the presentation event and thereafter the immune response[8]. Posteriorly, once the migrating CDCs have migrated and introduced the antigen, it is believed that they will die and be recycled[8]. The lifetime of cDC can be visualized in Figure 1.1.

One interesting notion is that lymph node cDC1 localized preferentially in the paracortex in a T-cell-rich area thus interacting more with $CD8^+$ cells mirroring its location[8,64]. cDC2 preferentially position themselves in the cortex or follicular zones in the T-B cell border, hence mirroring $CD4^+$ T cells[8,64].

After the migration event the DCs display the antigen to prime naïve T cells, this event is classified as antigen presentation. To prime effector lymphocytes successfully, the joint action of 3 distinct signals is required: antigen presentation via major histocompatibility complex (MHC); presence of co-stimulatory molecules; and release of soluble cytokines[65,66]. Ablation of any of these signals results in tolerance immunity.

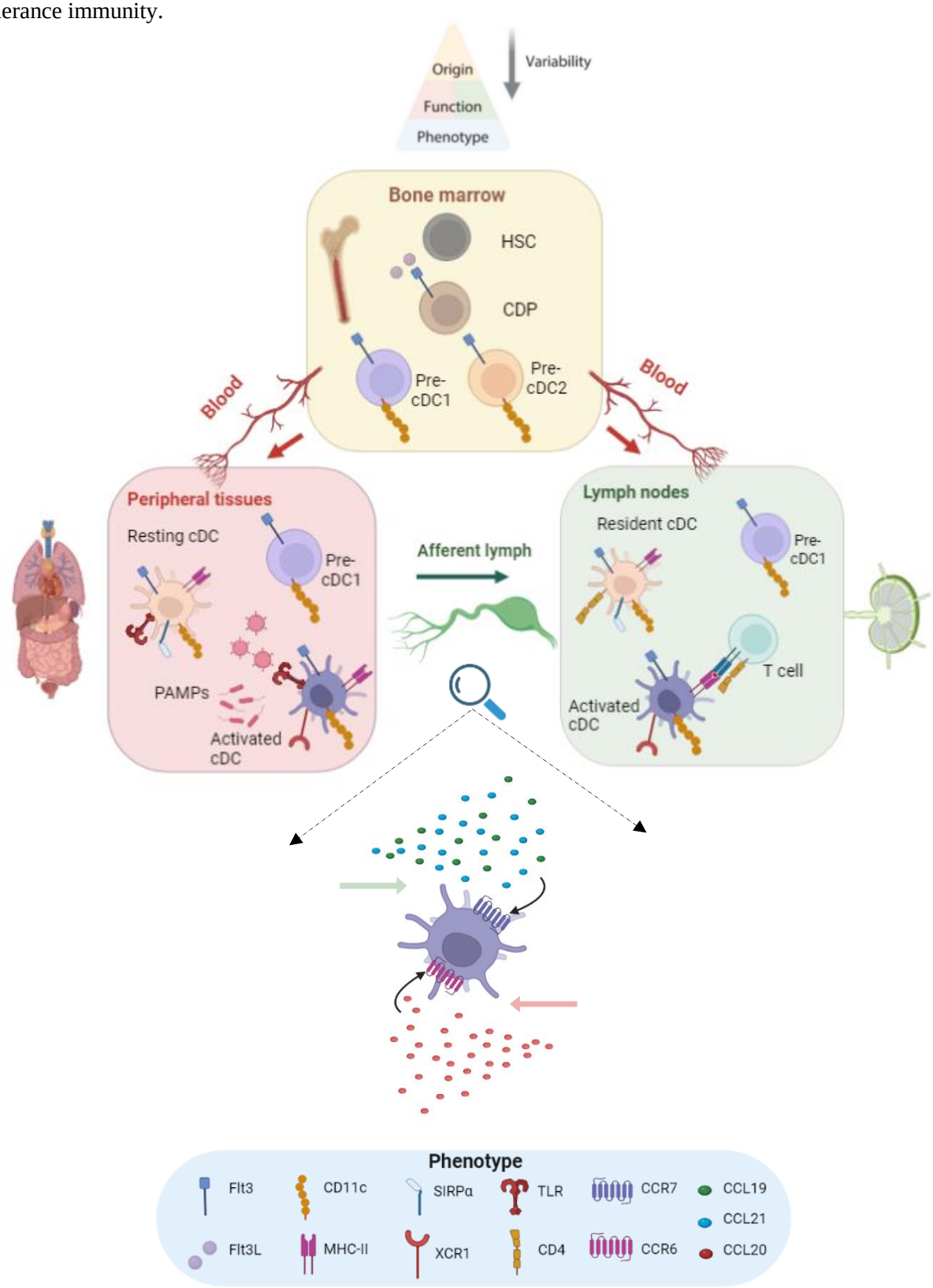

Figure 1.1 Lifetime period of a cDC. The cDCs originate in the bone marrow from hematopoietic stem cells (HSCs), and suffer differentiation, with prior intermediate stages, into CDP and pre-cDCs. These events are highly dependent on Flt3 receptor and its ligand Flt3L. In the pre-cDC stage, there are already some markers distinguishing pre-cDC1 and pre-cDC2 described elsewhere (not shown for simplicity reasons). Moreover, both are characterized by increased expression of CD11c marker. Posteriorly, these cells will egress from the bone marrow into both lymphoid and non-lymphoid tissues via blood circulation, finalizing the differentiation into cDC ($CD11c^+$ and MHC-II^+). cDC can be subdivided into cDC1 ($XCR1^+$) and cDC2 ($SIRP\alpha^+$). These resident cells will act as sentinel cells. After pathogen encounter via PAMPs recognition by PRR (TLR4 depicted), the cDC become active and suffer phenotypic changes characterized by increased expression of key molecules required from priming of T cells, like MHC, co-stimulatory molecules, and cytokines in a process denominated maturation. The active cDC will then migrate via afferent lymphatic vessels in a chemotactic manner via CCL21 and CCL19 chemokines, being both highly expressed in the lymph node, chemoattracting cDC via recognition by CCR7. Moreover, other cDC can be recruited to the skin via CCR6 recognition of CCL20, released by the epithelial cells following inflammation. After reaching the lymph node the active cDC can prime distinct naïve T cells into highly specific effector cells and trigger the beginning of an adaptive immunological response. For simplicity, in the figure illustrated, only cDC1 are active, migrate, and prime T cells, being cDC2 the resting and resident cell. However, all these physiological events can occur in both cell types. All images were created by using Biorender adapted from Cabeza-Cabrerizo, M., Cardoso, A., Minutti, C. M., Pereira Da Costa, M. & Reis E Sousa, C. Dendritic Cells Revisited. Annu. Rev. Immunol. 39, 131–166 (2021)[8].

1.2.4 Antigen Presentation via MHC – first signal

The first crucial signal needed in the naïve T cell activation event in the lymph nodes is the presentation of the sampled antigens, which normally are peptides, via MHC molecules[65,66].

This process can be carried out in two distinct mechanisms depending on the origin of the antigen: the intrinsic or cytosolic pathway that displays cytosolic/intracellular antigens via MHC class I molecules, and cross-presentation with $CD8^+$ lymphocytes, and the extrinsic or endocytic pathways that present internalized antigens in the context of MHC class II molecules to $CD4^+$ lymphocytes. Both MHC molecules with the loaded antigen will bind to the TCR (T-cell receptor)-CD3 complex in the surface of T cells, and alongside the other signals will activate downstream signaling cascades leading to T cell activation[1].

The cytosolic or intrinsic pathway is characterized by proteomic ubiquitination of intracellular-derived peptides through the proteasome. Posteriorly, the degraded peptides are translocated into the endoplasmic reticulum, to assemble with MHC class I molecules. Furthermore, this complex will then be released from the endoplasmic reticulum and migrate into the cellular membrane which will interact and activate $CD8^+$ T cells, eliciting cytotoxic immunological responses, crucial in the elimination of virus-infected and tumor cells[67,68].

On the other hand, the endocytic or extrinsic pathway is defined by the presentation of extracellular-derived antigens. These immunogens are endocytosed and later processed in endosome vesicles with proteases. The resulting peptides will be loaded with MHC-II molecules, also in the endosomes. Posteriorly the peptide-MHC complex will be transported to the plasma membrane to associate with

$CD4^+$ T cells[67,68]. These immune populations will assist other immune cells, enhancing/activating their functions, thus displaying a key central role in modulating the immune responses.

Focusing now on the function of cDC1s and cDC2s, the general dogma indicates that the former excels in cross-presentation of antigens via MHC-I to prime $CD8^+$ T cells eliciting cytotoxic immune responses[7,8,17,69,70], thus displaying key role mainly in inducing anti-viral[71–74] and anti-tumoral processes[75,76]. As previously stated, cDC1s has the key characteristics to cross-present the antigens to cytotoxic T cells: the expression of Clec9a that uptakes necrotic components, cDC1s locates in rich T-cell areas in the lymph node and displays XCR1 that binds XCL1 highly expressed by $CD8^+$ T cells as well as higher amounts of TLR3. Therefore, this suits the enhanced ability of cDC1 to prime $CD8^+$ lymphocytes in the lymph nodes. Furthermore, it is generally known that cDC1s are the major producers of IL-12[7,8,17] and IFN-III[17,35,36] while also releasing TNF-α[17].

On the other hand, it is stipulated that cDC2s are more efficient in priming via MHC-II, naïve $CD4^+$ T cells[7,8,17], leading them to act mainly against anti-parasitic immune responses in a Th-type 2 (Th2) response[77] against *Leishmania* for instance[78]. Furthermore, cDC2s can also induce other Th responses, like Th-type 17 (Th17)[7,17,77] by the high production of IL-23[7,17,79] and IL-6[7,17] cytokines against extracellular pathogens (*Citrobacter rodentium*)[79] and fungal microrganisms[7]. Furthermore, cDC2s can also produce TNF-α[17].

However, this idea, although generally accurate, cannot be oversimplified. It is true that cDC1s are experts in inducing cytotoxic responses due to priming $CD8^+$ lymphocytes, but they can also induce $CD4^+$ lymphocytes[80,81], to induce Th-type 1 (Th1) responses that can further help $CD8^+$ T cells cytotoxic responses[8,80]. Moreover, is it known that cDC1 produces high amounts of IL-12 thus supporting Th1 immunity also against the parasites *Leishmania major*[82] and *Toxoplasma gondii*[83], sustaining also cytotoxic T cells (CTL) action. Moreover, focusing now on human cDC1 despite being optimal in cross-presentation to $CD8^+$ T cells, this effect is less restricted than mice cDC1, and induces lower IL-12 amounts than for instance their cDC2 counterparts[8,17,84].

Although this priming ability of cDC1 to $CD4^+$ lymphocytes is less efficient than cDC2, following CpG stimulation the effect was reversed since cDC1 could proliferate $CD4^+$ T cells and induce IFN-y release[85].

The other way around, cDC2 has been found to promote both types of adaptive immunological events, and present to both $CD4^+$ and $CD8^+$ T cells, following inflammation[86]. Additionally, it is known that human blood cDC2 can cross-present soluble antigens and release high amounts of IL-12 thus behaving like a cDC1, therefore human cDC1 are less restricted in their functionality[8,17,84]. Hence both cells are very versatile contributing to host homeostasis.

1.2.5 Co-stimulatory molecules – second signal

The second signal or co-stimulatory signal required for the activation of naïve T cells is the expression of co-stimulatory molecules such as CD80, CD86, and CD40 on the surface of antigen-presenting cells such as DCs[65].

CD80 (B7-1) and CD86 (B7-2) molecules are part of the B7 family, that serve as ligands to CD28 receptor in naïve T cells, providing the necessary co-stimulatory signal, enhancing CD4/CD8 T cell proliferation and cytokine release[87].

The CD40 belongs to the TNF superfamily receptor, being highly expressed by DCs and B cells that interact with CD40L, being highly displayed by activated $CD4^+$ T cells. CD40 signaling promotes up-regulation of CD80/CD86 co-stimulatory molecules on DCs as well as increases cytokine release, like IL-12, thus enhancing the ability of DCs to activate effector T cells[88].

1.2.6 Cytokines as the third signal

The third and final signal, also known as the polarization signal, results in the action of soluble cytokines, acting as immune mediators to differentiate naïve $CD4^+$ or $CD8^+$ T cells (Figure 1.2).

Importantly, DCs are shown to release mediators that promote the differentiation of naïve $CD4^+$ T cells into differentiated Th1, Th2, Th17, T Follicular Helper (Tfh) as well as tolerogenic T cells (Treg) subsets, acting in a repertoire of different effector immunological responses[8,89,90] (Figure 1.2). For instance, DCs release high amounts of IL-12 polarizing naïve $CD4^+$ T cells into Th1 cells, which results in higher production of IFN-γ and TNF-α, assisting cytotoxic $CD8^+$ T cells and efficiently eliminating intracellular pathogens and cancer cells[66,90,91]. Interestingly, NK cells can release IFN-γ enhancing the DCs ability to produce high amounts of IL-12 and increase the polarizing of Th1 cells[65,90,91].

Furthermore, Th17 is polarized by the release of IL-6[89–91], IL-23[89–91], IL-1β[90,91], and Transforming growth factor beta (TGF-β)[89,90] by DCs. Th17 secretes IL-17, as well as IL-22, and excels in immunological action against extracellular pathogens and fungus[90,91]. Furthermore, DCs can also prime Tfh through the release of IL-6[89,90]. This immune cell releases IL-21, inducing B cell proliferation and survival[90] while enhancing antibody class switch[89], production and affinity[90], thus helping B-cell function. Additionally, DCs can also promote Treg by the release of IL-10[8,91], TGF-β, and retinoic acid (RA)[8,89–91]. Treg subset further releases both IL-10 and TGF-β thus promoting anti-inflammatory properties, inducing an anergy state[8,90,91].

Interestingly, it is still unknown the exact cytokine mediators released by DCs that differentiate Th2. Th2 cells result from the differentiation of naïve T cells upon the action of mainly IL-4 but also IL-2[90].

This immune population is characterized by the production of IL-4, IL-5, IL-13[66,89–91] enhancing immunological actions against parasites, venoms, and allergens[89,90]. However, it is widely known that DCs are essential to prime Th2 as previously depicted, nonetheless, there are still no studies indicating that DCs secrete IL-4[65,90], therefore, to prime Th2 it is thought that other immune cells, like basophils, mast cells[90,91] and other already polarized Th2 cells[65], are likely participating as third parties releasing IL-4, helping DC function in activating Th2 cells[65,90,91]. Furthermore, it is also thought that low levels of IL-12 released by DCs can contribute to priming Th2[89,90].

The combined action of these 3 signals is necessary to activate and differentiate naïve T cells into specialized T effectors cells, translating into an appropriate immune response to the type of invading pathogen. A generalized scheme can be seen in Figure 1.2.

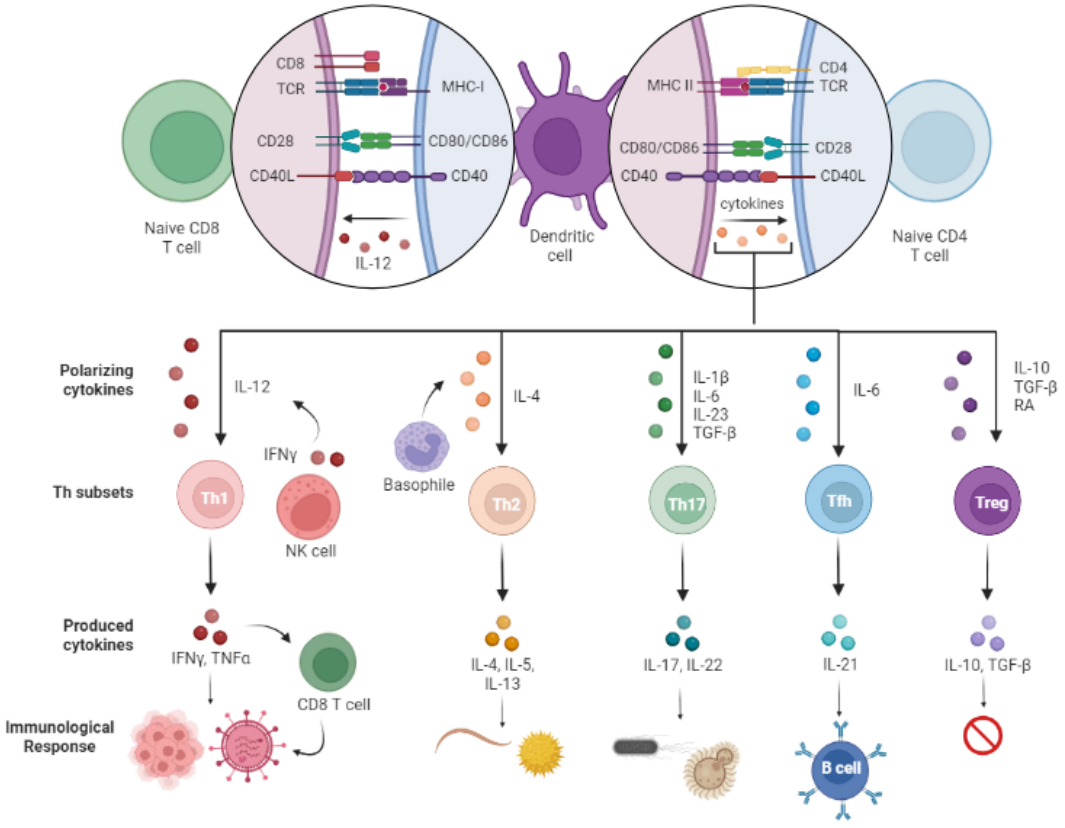

Figure 1. 2 The activation of naïve T lymphocytes and their polarization requires 3 signals presented by DCs. The first signal is the antigen peptide presentation via MHC-I or MHC-II that activates cytotoxic $CD8^+$ T cells or $CD4^+$ T helper cells. The second signal is the expression of co-stimulatory molecules CD80/CD86 and CD40 from the DCs that bind to the CD28 receptor and CD40 ligand respectively on T cells. The third signal needed for T cell polarization is the cytokine release. DCs produce cytokines such as IL-12 that polarize $CD8^+$ T cells promoting cytotoxic immune responses. Moreover, IL-12 release by DC also differentiates naïve $CD4^+$ T cells into Th1 cells assisting, with $CD8^+$ T cells, in the elimination of tumor or viral-infected cells as well as intracellular pathogens via IFNγ and TNFα production. NK cells can release IFNγ enhancing IL-12 release by DC. Th2 polarization by DCs requires assistance from an IL-4-producing immune cell, like basophiles. Th2 immune cells release IL-4, IL-5, and IL-13 aiding in the elimination of allergens and parasites. DCs can also prime naïve $CD4^+$ T cells into Th17 immune cells by secreting IL-1β, IL-6 IL-23, and TGF-β. Th17 excels against extracellular and fungi pathogens by the production of IL-17 and IL-22. Additionally, through the release of IL-6, DCs can polarize Tfh, leading to IL-21 production, helping B-cell proliferation and functions like antibody class-switch and promoting their production and affinity. Moreover, IL-10, TGF-β, and RA secretion by DC induce differentiation into Tregs leading to a tolerance state, damping down immunological responses. All images created by using Biorender adapted from Yin, X., Chen, S. & Eisenbarth, S. C. Dendritic Cell Regulation of T Helper Cells (2021)[90]; Hilligan, K. L. & Ronchese, F. Antigen presentation by dendritic cells and their instruction of $CD4^+$ T helper cell responses. Cell. Mol. Immunol. 17, 587–599 (2020)[89] and Walsh, K. P. & Mills, K. H. G. Dendritic cells and other innate determinants of T helper cell polarization. Trends Immunol. 1–10 (2013)[91].

1.3 Nervous System

Our body is heavily innervated by an elaborate and complex network of neurons. These basic constituent units of the nervous system carry messages by communicating with each other either through electrical synapses via ions or chemical synapses through the release of neurotransmitters to various anatomical regions of the body[92]. These soluble molecules are released by presynaptic neurons and bind to receptors on the postsynaptic cell, which can be either other neurons, effector muscle, glands, or even immune cells[93], thus playing a strong modulatory role in the functionality of these cells. These relationships govern and influence the capacity for voluntary and involuntary movements, affect the organism's senses, the capacity to make decisions, and how the system should respond to certain environmental stimuli.

Therefore, the nervous system senses, transports, integrates, and processes diverse signals, stimuli, and messages in a highly coordinated and refined way, to regulate and maintain the body in a state of homeostasis. Dysregulation of the balance between synthesis and degradation of neurotransmitters can lead to neurological disorders and neuropathies[94].

1.3.1 Central and Peripheral nervous system

In this sense, the nervous system is divided into two large sections: the central nervous system (CNS), and the peripheral nervous system (PNS). The first is constituted by the brain, being the body's control center, responsible for various vital functions such as control of heart rate, breathing, blood pressure, and temperature as well as general functions like awareness, balance, coordination, movement, emotions, thought processing, memory[95]. Also included in the CNS, the spinal cord acts as a passage of

the great ascending and descending pathways transmitting information from sensory organs through sensory or afferent nerves to the brain or sending motor signals from the brain to the peripheral body using motor or efferent nerves[95,96].

Furthermore, the remaining constituent part of the nervous system is the PNS, which innervates all regions and organs outside the CNS, being divided into the somatic nervous system (SNS) and the autonomic nervous system (ANS) featuring both sensory and motor nerves[93,97]. The SNS regulates and controls voluntary movements[93,96] while the ANS influences involuntary movements and physiological parameters (e.g. heart rate, blood pressure, respiration, digestion, and thermoregulation[98,99]).

The ANS is further subdivided into sympathetic nervous system (SyNS), parasympathetic nervous system (PaNS), and the enteric nervous system (ENS)[93,96–98,100,101]. The SyNS is the largest ANS component, and its innervation is seen in the whole body, including secondary lymphoid organs, a feature that is not applicable for parasympathetic innervation[101,102].

1.3.2 Parasympathetic and Sympathetic nervous system

In emergency situations and exercise, the sympathetic system becomes dominant, being responsible for preparing the body for physical activity, commonly known as the "fight-or-flight" response. Specifically, it increases blood pressure, heart rate and glycogenolysis to promote the supply of well-oxygenated and nutrient-rich blood to the tissues thus supplying energy to the cells[98,99].

On the other hand, during calm periods or rest, the parasympathetic system takes precedence. Its overall effect is to conserve energy, also known as the "rest and digest" response, which regulates the heart rate and blood pressure into normal values and restarts body physiological processes like digestion[98,99].

In synaptic transmission both SyNS and PaNS release acetylcholine (Ach) in presynaptic neurons, however postsynaptic neurons of the former use mainly, the catecholamine norepinephrine (NE) as the effector neurotransmitter while the latter continue to use Ach as signaling molecule[93,96,98,99].

Although SyNS neurons mainly release NE, the synthesis of this molecule is derived from Dopamine, (that comes from L-dihydroxyphenylalanine (L-DOPA) following DOPA decarboxylase), after the action of dopamine beta-hydroxylase enzyme. Furthermore, NE can originate epinephrine (Epi), the end-product, following phenyl ethanolamine-N-methyltransferase activation. All these 3 neurotransmitters are dependent on Tyrosine and the enzyme Tyrosine hydroxylase (TH)[103].

Acetylcholine molecules can be recognized by either ion-channel/nicotinic receptors or muscarinic receptors which are g-coupled receptors. NE can be recognized by adrenergic receptors on the surface of effector cells which are all g-protein coupled receptors[98,99]. These protein complexes are seven-transmembrane receptors that when triggered, following neurotransmitter ligand-bound, induce

conformational change in a G protein, activating it. The activated G protein either induces or inhibits a further signaling cascade, being dependent on the type of G protein. There are 3 main types of adrenergic receptors, α1-(*Adrα1*); α2-(*Adrα2*); and β-adrenergic receptors, (subdivided into *Adrβ1*, *Adrβ2* and *Adrβ3*)[102,103]. α1- and β-adrenergic receptors are associated with activation of phospholipase C and adenylate cyclase, respectively that will later activate protein kinases C and A, respectively which phosphorylate several other cellular proteins and transcription factors, leading to the regulation of nuclear genes controlling cellular functions[102–104]. α2-adrenergic receptor is associated with an inhibitory G-protein, hence has opposite effects compared to β-adrenergic activation[102–104].

1.4 Neuroimmune system - a synergistic interaction of two independent systems

The immune and nervous systems were first analyzed independently as two autonomous separated fields in science[105,106]. However, these two systems share similar features[107], display high plasticity, and have been co-evolved in a complex sensory/motor system, both can perceive and integrate internal signals and environmental stimuli[107] being tightly linked in detecting (input) and acting (output) against a diverse portfolio of naïve or danger inputs that could threaten tissue physiology. Moreover, another similar aspect is that both systems communicate through the releases of soluble chemical molecules, that extend the message to distant parts of the body[107] and mount effective responses creating memory and learning abilities[96,108–110], hence both systems are indispensable to maintaining the tissue proper functionality and species survival[108,109].

Therefore, due to the immense analogies and similar characteristics, nowadays attention in the science community is focused on the neuroimmunology field in a variety of scenarios and organs[101,111–113]. This recent area has been gaining new insights into the molecular and cellular components of the neuro-immune crosstalk[101,114] and increasing evidence acknowledges this synergistic bidirectional interaction[101,114] and how it has evolved to face ever-challenging conditions participating in health and disease[101,112,115,116]. Nonetheless, dysfunction of this very synergistic interaction has been involved in a wide range of disorders[101,114,117–121], including cancer[101,116]. Therefore, acquiring new insights into the ability to potentially modulate this crucial communication can lead to a revolution in health and science and create new therapy opportunities.

1.4.1 Cells and molecules involved in the neuroimmune crosstalk

The neuroimmune crosstalk can occur systemically, meaning the whole body, or in defined anatomical locations deemed neuroimmune cell units (NICUs) in which both cells colocalize and functionally interact[101,115]. Evidence of these precise areas of crosslinked has been characterized in different barrier surfaces[97,101,108,111,112,122,123], like skin and mucosa, visceral organs as well as lymphoid organs.

This bidirectional interplay can occur through the non-synaptic release of soluble chemical molecules derived from both the immune (mainly cytokines and chemokines) and nervous systems (neuropeptides and neurotransmitters), hence such signaling compounds can influence the activity of both systems and how they perceive and respond to diverse stimuli[101,106–108,114,124]. One key aspect of this co-modulation remains that despite cytokines being mainly synthesized by immune cells, neurons can also release these soluble compounds[107,114,125] thus likely mediating immune cells and communicating with other neurons.

Nonetheless, immune cells can also *de novo* synthesize classical neuronal-released compounds, like neurotransmitters[101,106,109,114,124–126] possibly regulating nerve cells, other immune cells, or even modulating their own cell-autonomous functions, likely indicating an autocrine self-modulating system and paracrine, modulating surrounding cells[114,124,126].

Additionally, to further emphasize the interdependence of these two systems, immune and nerve cells are equipped with the specific receptors of both classical released ligands of either system. For instance, several neurotransmitter receptors, that are typically expressed in neurons, have also been found on the surface of immune cells[101,106,108,109,114,120,124,127]. Indeed, as an example, T cells and DCs are among those immune populations, expressing receptor subtypes of classical neurons-released ligands such as glutamate, acetylcholine, serotonin, dopamine, and adrenergic[114].

Moreover, a vast array of immune cells, express neuronal receptors, such as adrenergic[101,103,109,124,128] and cholinergic receptors[101,109,124,129] being sensitive to NE and Ach inputs. On the other hand, neurons have been known to express the immune-classical receptors[106,109,114,118,120,130,131]. Therefore, as well as immune cells can receive and integrate neurotransmitters, being sensitive to neuronal innervation, nerve cells function can also be altered following immunological processes.

Thereafter, a cross-link can be traced between nervous-mediated regulation of immunity, and immune modulation of the nervous system and its feedback modulation is of vital importance in the body's general homeostasis and protection. Overall, further advancements in the study of neuroimmune cell units and deciphering the intervenient players, the molecular insights, and their complex bidirectional interplays may lead to new therapeutic approaches contributing to both science and clinical departments focusing on the organism's health.

1.4.2 Neuroimmune system effects on barriers and physiological organs

NICUs, as stated previously, are defined anatomical places in which neurons and immune cells interact and modulate each other function[101,115]. Thus, nervous and immune systems have a co-evolved relationship in various barriers surfaces and organs resulting in a neuroimmune axis. This axis hence provides a quicker anticipatory immunological response and properly fine-tunes it to constantly changing conditions[115].

1.4.2.1 Lungs

The lungs are a gateway to the entry of harmful pathogens and the possibility of the beginning of an infection. In addition, the lungs and respiratory tract are barrier surfaces filled with resident immune cells and are densely innervated by sensory/nociceptor neurons and sympathetic and parasympathetic afferent nerves, regulating lungs and airways proprieties. Therefore, there is an indication that the lungs and respiratory tract are particularly rich in NICUs, likely regulating their barrier integrity and physiological processes. Dysfunction in the neuroimmune communication in the lungs can lead to asthma, allergy, and chronic obstructive pulmonary disease[111,123].

Nociceptors are a subset of sensory neurons that are specialized in inducing pain sensitivity to protect the host from different damage inputs either environmental or biological[132,133]. In the case of inflammation, these specialized neurons are able to respond to immune-derived mediators produced like cytokines and alarmins triggering quick response and increased pain sensitivity. On the other hand, nociceptors following activation are also capable of releasing neuron-mediators, like substance P (SP), calcitonin gene-related protein (CGRP), and vasoactive intestinal peptide (VIP) that can modulate various immune cell populations, emphasizing this bidirectional neuro-immune communication in peripheral organs[122,134].

DCs can migrate into airway sensory ganglia, following allergic inflammation challenge, being this phenomenon possibly linked to promoting interactions with CGRP-neurons[135], as both these cells are in close proximity[123,135]. Nonetheless, the effects of CGRP in DC in an airway scenario are contradictory being the CGRP able to promote DC migration at lower doses[136] whereas it reduces DC migration upon physiological conditions[134,136]. Moreover, it is being reported that CGRP-treated DCs induce either Th2 immunity or Tregs proliferation[123]. Additionally, lung DCs treated with nociceptor-derived neuropeptides, including CGRP reduced their antigen phagocytic capability[136].

1.4.2.2 Intestines

The intestine is densely innervated by its own intrinsic nervous system, the enteric nervous system (ENS) that can communicate directly with CNS[137], while being also susceptible to extrinsic sympathetic and parasympathetic neuronal innervation[101,112,122] as well as sensory signaling[122,127]. All this innervation has been linked to modulating gut physiological events like intestinal motility, peristaltic contractions as well as gut secretions[101,112,138].

This visceral organ englobes the biggest immune compartment in the whole body[101,112,122] full of innate and adaptive immune cells[138,139], the last are mainly present in Peyer Patches which are lymphoid compartments in the intestines[101]. Besides that, the gut is a mucosal organ surrounded by an extensive microbiota and possible harmful pathogens that also modulate due to their metabolites or antigens,

intestinal neuroimmune axis, barrier integrity, and tissue inflammation[123,138–140]. Furthermore, NICUs in the gut can also receive nutrient-derived cues that can further regulate the intestinal physiological parameters[138]. Hence intestinal NICUs are of major importance in the body's homeostasis[101,112,113,122]. Understanding the gut neuro-immune complexes can then promote new therapies, contributing to the organism's health. Dysregulation of these bidirectional interactions could be a factor in inducing inflammatory bowel diseases[101,112,122] like Crohn's Disease[101].

Intestinal DCs are very heterogeneous acting as sampling immune cells and can induce both regulatory, for instance, in steady state scenarios and by release of RA, and effector T cells, for instance, through intestinal pathogenic sensing[137,141]. However, there is still limited information about how these cells are sensitive to gut neuronal inputs[138]. In literature, VIP is shown to modulate DCs functionality after TLR4 stimulation via VIP receptor type 1 (VPAC1), leading more to an immunosuppressive[101,137,142] state due to downregulation of co-stimulatory molecules and pro-inflammatory cytokines, induction of IL-10 cytokine release and less migration, due to downregulation of CCR7[137]. Furthermore, the endocytic process by VIP-treated DCs increased. Additionally, VIP-treated matured DCs also lead to an increase in anti-inflammatory cytokines secretion such as IL-10 and TGF-b by co-cultured T cells.

Curiously, this phenomenon only occurs with mature DCs (after TLR stimulation), since immature non-treated DCs followed VIP treatment led to increased expression of CD86 while also inducing type 2 cytokine production[137].

1.4.2.3 Skin

The skin is the largest organ in the human body, being highly dense with innate immune cells and vastly innervated by peripheral neurons. Hence it is expected to occur various neuroimmune interactions in the skin as part of physiological interactions in the organism's body that need constant readjustments and precise fine-tuning, following pathogen encounters, promoting homeostasis.

CD301b$^+$ dermal DCs a subpopulation of dermal migratory cDC2[143], can promote tissue immunity against *Candida albicans*, a fungal pathogen, infection[144]. These were dependent on Transient receptor potential vanilloid 1 (TRPV1) nociceptor neurons. These pain-associated sensory neurons are activated following microorganism challenge and release CGRP neuropeptide. This molecule can be recognized by skin-specific CD301b$^+$ DCs that will promote the release of Th-17-polarizing IL-23 cytokine. The immense production of this soluble molecule will drive IL-17 release by skin γδ T cells resulting in increased tissue immunity and pathogen clearance[101,112,144]. These findings were validated by inhibiting several steps of this pathway such as depleting the TRPV1$^+$ nociceptor neurons or by eliminating DCs, or using mice deficient for the cytokines[144]. CD301b$^+$ DCs were shown to co-localize TRPV1$^+$ sensory neurons, these nociceptors become activated with allergens and release substance P[145]. This molecule is

recognized by the dermal cDC2 promoting migration into draining lymph nodes to induce Th2 polarization and type 2 anti-allergen immunity[122,134,145].

Furthermore, it is also known that imiquimod-induced psoriasis, a type of skin inflammation, is enhanced by TRPV1$^+$ nociceptor neurons by inducing Th17 immunity derived from activated dermal DCs secretion of IL-23[101,112,122,143,146]. The IL-17 and IL-22 cytokines produced by activated skin γδ T cells recruit monocytes and neutrophils worsening inflamation[101,112,146].

Hence, the potential to induce inflammation by skin DCs can either be beneficial (in the case of *C. albicans* infection and allergen inflammation) or be unfavorable when worsening psoriasis by increasing the host immunity. Therefore, further studies should be conducted to improve and discuss novel immunotherapies against skin inflammation either by pathogen burden or a skin autoimmune disorder.

1.5 Cholinergic effects on DC functionality

It is known that DC expressed both muscarinic (mAChRs) and nicotinic (nAChRs) receptors hence, these cells can perceive and integrate parasympathetic-derived cues in both mice and humans[129,147]. Additionally, it is also demonstrated that DC expresses the enzymes needed to synthesize and degrade Ach such as choline acetyltransferase (ChAT) and acetylcholinesterase (AChE), respectively, in both mice and humans, suggesting a paracrine/autocrine role of Ach modulation[129,147]. However, no evidence of Ach synthesis and release was observed by DCs, being restricted to lymphocytes, mainly T-cells[129]. Also, the information regarding how the DC functionality is altered after acetylcholine signaling is very scarce[101,129].

There are some shreds of evidence suggesting that α7 nAChR signaling leads to suppressive DC function, likely inhibiting Th1 and Th2 differentiation and inducing Treg since an α7 nAChR KO mice promotes antigen-specific immunity[129].

In this regard, one study discovered that GTS-21, an α7 nAChR agonist drug, decreased the expression of CD80 and MHC-II molecules in splenic CD11c$^+$ DCs in a mouse model of induced rheumatoid arthritis[148]. GTS-21 also led to less amount of the same molecules in bone-marrow DCs in normal *C57BL/6 J* mice being this reversed by an α7nAChR antagonist[148]. Furthermore, it was also observed a decrease of TNF-α and IL-6 (pro-inflammatory cytokines), but not IL-10 (anti-inflammatory cytokine) in the serum of the autoimmune-induced mouse model after GTS-21[148]. Additionally, the researchers found less infiltration of DC into the synovium of the induced mice following the drug administration[148].

On the other hand, there are papers hinting that mAChR signaling induces pro-inflammatory properties of DCs. Backing this information, researchers elicited that carbachol, a synthetic Ach analog, promotes expression of CD86 and HLA-DR in human DCs, moreover, TNF-α and IL-8 suffered up-regulation[147]. These two phenotype findings were reversed with atropine, a mAChR blocker, but not with a nAChR

antagonist, indicating crucial roles of mAChR in eliciting pro-inflammatory DCs[147]. Interestingly, the authors pointed out that cholinergic signaling in mAChR affects human DC phenotype depending on their maturation status since opposite findings were shown with LPS[147].

Posteriorly, the same research group displayed that Ach-treated DCs, increased the release of CCL22 and CCL17 by co-cultured T-cells, two chemokines responsible for Th2 recruitment to allergenic inflammation tissues[149]. Moreover, it was also evidenced proliferation of T cells and induction of IL-2 when cultured with Ach or carbachol-treated DCs and IL-4, IL-5, and IL-13 but not TNF-α, IFN-γ or IL-10 with Ach-treated DCs, clearly indicating that Ach in DCs signaling promotes polarization into Th2 immune responses[149]. Furthermore, the same DCs also lead to increased expression of OX40L, a Th2-promoter, further validating the polarizing effect of Ach-treated DCs in inducing Th2 cells[149].

Moreover, after stimulation with a Th2-promoting mediator, HLA-DR, OX40L, and CD83 (human DC activation marker) expression by DCs were further improved with Ach, being the effect of the last two attenuated by a mAChR antagonist and not a nAChR blocker[149]. The same was observed for TNF-α and IL-8.

Later in another paper, the same authors also demonstrated that Ach increased murine DCs MHC-II expression and promote release of TNF-α and CCL2[150]. Moreover, the researchers displayed that Ach-treated DCs co-cultured with splenocytes promote their proliferation[150]. Interestingly, the findings observed were reversed by utilizing mAChR blockers and not with nAChR antagonists[150], matching the previous paper with human DCs[147], further indicating that mAChR signaling induces immunologically active DCs in both mice and humans.

At last, the authors evidenced that injecting Ach-treated DCs intranasally in a lung inflammation-induced mice model promotes lung tissue recruitment of $CD11b^{+}CD11c^{-}$ mononuclear cells while also boosting TNF-α release, therefore displaying a role in inducing inflammation[150].

However, there are also findings suggesting anti-inflammatory roles of mAChR triggering. It was observed that ablating hepatic vagal afferent nerves lead to decreased production of RA as well as reduced expression of their synthetic enzyme, aldehyde dehydrogenase (ALDH) by $CD103^{+}$ DCs ultimately leading to reduced amounts of gut Treg[151]. Additionally, the values of ALDH enzymes were brought to normal with a mAChR agonist, as well as number of Tregs, but not with an α7nAChR agonist, antagonist, or by genetical depletion[151].

Everything pooled indicates that mAChR signaling on the surface of DCs can lead to either a more immunologically active or immunosuppressed phenotype, while α7 nAChR signaling displays the latter outcome. However, most are *in vitro* studies with no specific targeting of DCs therefore more studies are necessary to fully determine the cholinergic effects in DC functionality. A summary of how Ach signaling modulates DC functionality can be visualized in Figure 1.3.

1.6 Sympathetic input on DC functionality

Sympathetic innervation has clear effects on immune cell function. As previously stated, various immune cell populations express adrenergic receptors and, therefore, are able to be modulated by sympathetic-derived signaling.

DCs express both α- and β-adrenergic receptors[102,103,152,153], being the β2-receptor adrenergic receptor highly expressed[154]. Therefore, DCs can specifically recognize sympathetic released adrenergic molecules such as NE and Epi[103,128]. Epi is mainly secreted by the adrenal medulla whereas NE is mainly local by the adrenergic nerves, which is ideal for studying neuro-immune interactions[119,155].

There have been papers suggesting that triggering of adrenergic receptors has effects in all aspects of DCs functionality, ranging from antigen uptake[102,156,157], migration[102,158], antigen presentation[102,154,156,159], and cytokine production[102,154,156,159,160].

It has been shown that activating *Adrβ2* signaling on DCs dampens its ability to cross-present to cytotoxic T cells[101,124,127,153,159]. Additionally, NE sensing by DCs leads to decreased production of pro-inflammatory cytokines, namely IL-12[124,159,161], TNF-α[124], and IL-6[124], suppressing Th1 responses[101,102,153,162], while also upregulating tolerogenic cytokines like IL-10[124,156,159,161] and Th2 polarizing cytokines like IL-33[124,] and a shift into Th17-polarizing cytokine IL-23[154]. Hence, stimulating this g-couple receptor promotes Th2[101,124,153,156,161] and Th17[101,102,153,160,162] responses while inhibiting Th1[101,102,124,153,161,162]. Additionally, due to the increased amount of IL-10, it could lead to a more immunosuppressive state of DCs and induction of tolerogenic T cells[124,156].

The findings of this paper[159] suggest that reduced cross-presentation is not due to down-regulating the essential molecules to prime $CD8^+$ T cells such as the co-stimulatory molecules and the MHC-I, since the expression of these molecules barely reduce (co-stimulatory) or remain intact (MHC-I), but due to inefficient antigen degradation[153,159]. These results were *Adrβ2* signaling-dependent since this finding was visible only after DC treatment with *Adrβ2* agonist (salbutamol) and reversed with an *Adrβ2* antagonist (ICI-118,551 hydrochloride)[159]. Interestingly, the paper also showed that after salbutamol, Th1-polarizing cytokine IL-12 was severely reduced and anti-inflammatory IL-10 was upregulated. The researchers also demonstrated that it is *Adrβ2*-dependent since it was reversible using the *Adrβ2* antagonist and an *Adrβ2* KO mice were insensitive to salbutamol changes of both cytokines[159].

Another paper demonstrates that *Adrβ2* stimulation, through epinephrine and salbutamol, reduces IL-12 while increasing IL-10[156]. These findings were brought to normal following propranolol, an *Adrβ2* antagonist. Interestingly, they also registered that epinephrine and salbutamol increased the release of IL-4 by Th2 cells. Thus antigen-presentation experiments of this paper suggest that Th2 and Treg are favored after *Adrβ2* activation[156].

In a normal scenario, LPS administration induces a potent IL-12 secretion compared to IL-23 production, hence leading to a Th1 scenario. However, this paper shows that following NE, together with LPS, the production of the Th1-polarizing molecule was severely reduced and the Th17-polarizing cytokine was not affected[154]. Therefore, led to a shift of paradigm into inducing more IL-23 than IL-12 indicating a Th17 response. Furthermore, the authors also observed that the effects of NE were reversed by adding an *Adrβ2* antagonist (ICI-118,551 hydrochloride) but not by an *Adrα2* antagonist (SKF 86466 hydrochloride)[154]. In cohesion with the findings, in parallel, the authors showed that the effects of NE in reducing IL-12 were reproduced by adding *Adrβ2* agonist (fenoterol hydrobromide)[154]. Therefore, seems that *Adrβ2* can have a role in the inhibition of pro-inflammatory type 1 cytokine and induce Th17 responses at the expense of Th1 inhibition. The authors defended that cultured T cells together with DCs that were treated with the NE or *Adrβ2* agonist molecules led to a decrease of IFN-γ, a specific Th1-response cytokine released by $CD4^+$ T cells, and in parallel increased IL-17 thus leading to increased Th17 response[154].

In cohesion, another paper stated that following treatment with NE, the DCs also displayed inhibited IL-12 secretion and improved IL-10 release, however, it was not receptor specific since this was reversed with both *Adrα2* antagonist (yohimbine) and propranolol (*Adrβ2* antagonist), although *Adrα1* does not seem to have a role since *Adrα1* antagonist (prazosin) was not able to reverse NE effects[161]. Furthermore, the same paper also demonstrates that in an antigen presentation assay with adoptive transfer of treated DCs with NE resulted in lower production of IFN-γ and higher IL-4 in the lymph nodes, thus promoting Th2 responses and suppressing Th1 immunity. These findings were reversed with the same previous antagonists[161].

Regarding alpha-adrenergic receptor stimulation, the papers listed indicate that DCs usually increase antigen uptake event[101,124,127,153], namely via *Adrα2*[124,153,157], as well as the migration capability into the lymph nodes[101,124,127], being this phenomenon responsible for triggering *Adrα1*[102,124,153,158]. This effect is receptor specific since *Adrα1* antagonist (prazosin) reverses this finding following FITC-skin sensitization, an *in vivo* migration experiment, while following administrations of *Adrβ2* antagonists (propranolol) and *Adrα2* antagonist (yohimbine) the migration was equal to control (former) or enhanced (latter)[158].

Additionally, the paper also showed that with NE alone the migration of DC is improved, however, when NE is together with prazosin the migration ability was reduced, indicating a role of *Adrα1* in the migration of DCs. Further on, another paper also showed that ICI-118,551 (*Adrβ2* antagonist) was consistent in inducing DC migration[163].

As previously addressed, the endocytic capacity of DCs correlates to *Adrα2* signaling, since *Adrα2* agonist (azepexole), and NE improved antigen endocytosis while *Adrα2* antagonist (yohimbine) and not

Adrα1 antagonist (prazosin) nor *Adrβ2* antagonist (propranolol) suppressed the actions of NE-improved antigen uptake[157].

All these results pooled indicate that the effect is dependent on the type of adrenergic receptor triggering, since α- and β-adrenergic receptors seem to have opposite effects, the former g-couple receptor usually leads to a more activation state while the latter induces a tolerogenic phenotype. A state-of-the-art of how NE signaling modulates DC functionality can be visualized in Figure 1.3.

Nonetheless, most of these studies are *in vitro* assays that use unspecific DC target techniques, like differentiation of bone-marrow-derived cells with cytokine cocktails such as GM-CSF, which is known that although being $CD11c^{+}$, these can include both cDC1, cDC2, and also macrophages[164], cells that can be modulated by sympathetic inputs[103,128]. Therefore, does not fully represent a distinct crosstalk between adrenergic neurons and DCs as well as does not clarify its precise molecular and cellular basis. Furthermore, all these papers do not use a specific genetic mouse model to *in vivo* target a population of DCs, thus most of the findings are not specific, moreover, are based on the use of the full KO animals, instead of a Cre-dependent line, and therefore the findings should not be generalized to DCs as a whole.

Thereafter, little is still known yet about the modulation abilities of adrenergic catecholamines and their impact on DC functionality and how this affects the host's physiology *in vivo.*

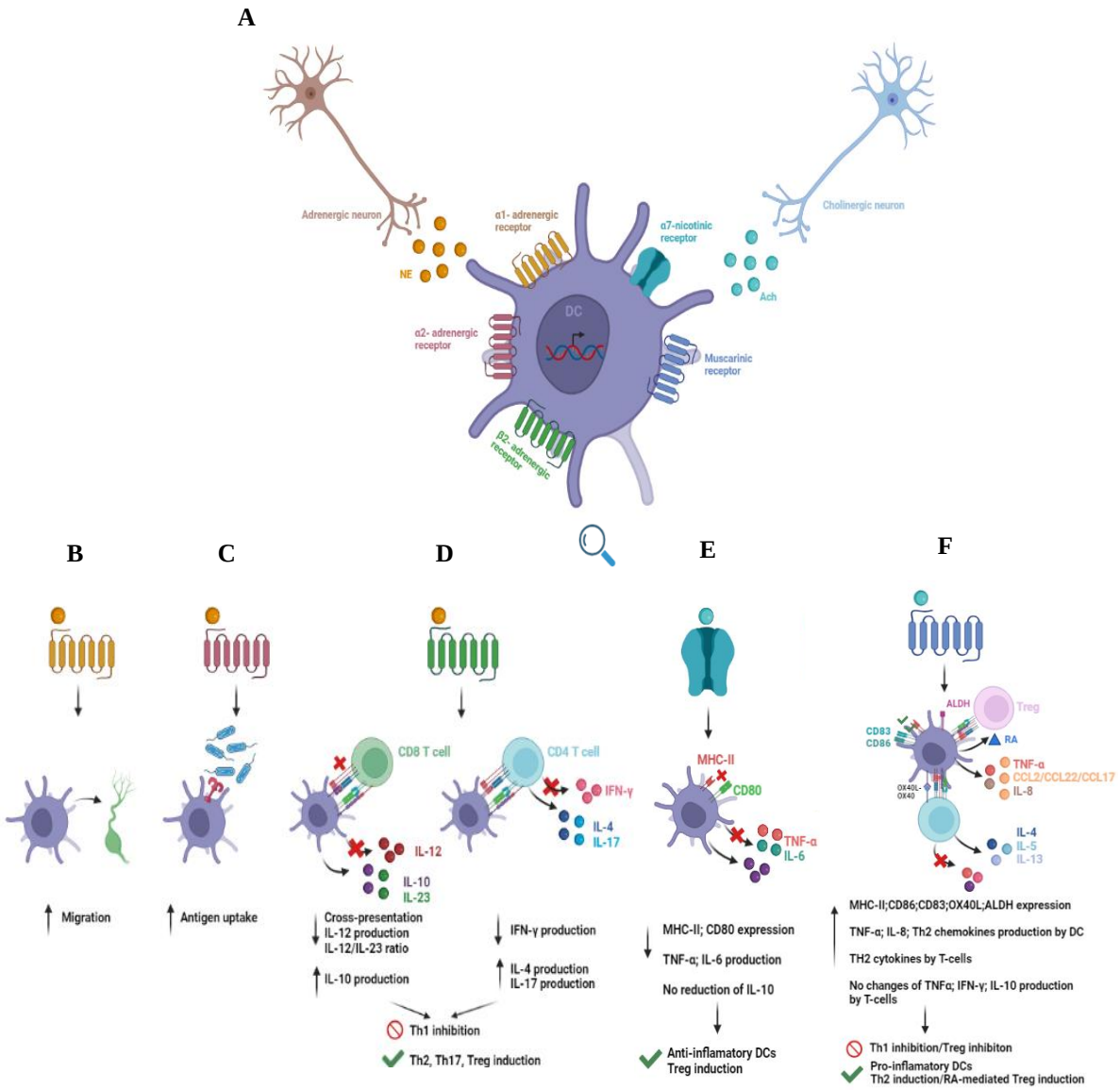

Figure 1.3 Modulation of DC functionality with adrenergic and cholinergic signaling. **A-** DCs express α1, α2, and β-adrenergic receptors being susceptible to NE input. DCs express α7-nicotinic and muscarinic receptors being sensitive to Ach signaling. **B**- NE sensing via α1-adrenergic receptor promotes DC migration. **C**- NE sensing via α2-adrenergic receptor enhances antigen endocytosis by DC. **D**- NE signaling via β2-adrenergic receptors leads to reduced cross-presentation capability of DCs. Moreover, IL-12 is reduced while IL-23 cytokine remains unaffected leading to a decrease in the IL-12/IL-23 ratio promoting Th17 immune responses at expense of Th1 immunity. Furthermore, IL-10 production is increased following β2-adrenergic receptor signaling promoting induction of Treg, inducing immunotolerance. β2-adrenergic receptor activation in the surface of DC induces IL-4 and IL-17 but not IFN-γ production by T-cells, promoting Th2 and Th17 immunity respectively while inhibiting Th1 responses. **E-** Ach sensing via α7-nicotinic receptors down-regulates the expression of MHC-II and CD80 molecules while also reducing the amount of TNF-α and IL-6 release but not IL-10, thus Ach signaling via α7-nicotinic receptors promotes anti-inflammatory properties of DCs and lead to proliferation of Tregs. **F-** Ach sensing by muscarinic receptors leads to increased expression of MHC-II and CD86, CD83 molecules and Th2 molecule, OX40L, moreover it increases the production of TNF-α, IL-8 and Th2 chemokines (CCL2, attracting monocytes and CCL22, CCL17 recruiting Th2 cells to site of injury), therefore Ach sensing by muscarinic receptors promotes pro-inflammatory properties of DCs. Moreover, T-cells cultured with Ach-DCs promote IL-4, IL-5, and IL-13 cytokine production without altering TNF-α, INF-γ, and IL-10 levels, thus promoting Th2 immunity and inhibiting Th1 and Treg immune responses. Nonetheless, it was also evidenced that Ach signaling via muscarinic receptors induces the expression of RA-synthetic enzyme, ALDH, promoting the proliferation of colonic Tregs. All images were created by using Biorender.

1.7 Thesis's goal

The immune and nervous systems throughout time were investigated as independent fields in science. Nevertheless, in recent years, there has been substantial emphasis on neuroimmune cellular units, their interactions, and functionality across a wide range of branches and scenarios. In-depth studies in the neuroimmunology department have broadened our knowledge of the synergy between these two systems, and it is with great interest to further characterize NICUS with an eye toward the evolution of science and potential clinical applications. The immunophysiology group is strongly committed to exploiting how the neuroimmune axis influences immunity, the phenotypical differences in immune cell populations, and how this influences organism homeostasis.

Since DCs have the capacity to integrate a wide range of environmental surroundings, regardless of whether pathogenic, commensal, self, or non-self-elements, thereby fine-tuning immunological responses by shifting the balance towards immunity and tolerance, it is hypothesized that they are the in the interface of the neuroimmune axis, being sensitive to neuronal-derived cues and adjusting the content and nature of host physiological/pathophysiological mechanisms accordingly.

Nonetheless, and much in line with the last chapter, studies in this area are focused on sensory neuronal input, and in the case of autonomic nervous system-derived signals, the results are based on non-specific targeting and differentiation of DCs as well as *in vitro* assays hence knowledge gaps persist regarding the crosstalk between neurons and DCs, and how this interaction affects DCs phenotype and its associated molecular changes and how this affects the host physiology.

Therefore, the main goal of this thesis is to uncover whether sympathetic neuron-derived signals affect the functionality of cDC1, and if it leads to a more immunologically active or immunosuppressive state. For this purpose, we are going to administer both *in vitro* and *in vivo*, the natural *Adrβ2* ligand (NE) as well as different antagonists and agonists of *Adrβ2*. To fully assess the range of how the functionality of DC is affected, the expression markers of several crucial DC parameters were analyzed via Fluorescence-activated cell sorting (FACS) methodology, in terms of expression of co-stimulatory molecules, shifts of MHC-I and MHC-II variability, as well as changes in cytokines and chemokines output. To provide extra information regarding DC migration, the gene expression of different chemokine receptors and their ligands were also investigated through qPCR methodology. Additionally, *in vivo* migration was also assessed with FITC painting experiments.

In parallel, with the specific gene targeting for cDC1 using a specific genetic mouse, it is possible to selectively target these cells *in vivo*, as of now there are still no specific genetic mice for cDC2.

The deciphering of the molecular and cellular components of this interplay can lead to the manipulation of these interactions, thus having vast potential to revolutionize the outcome in science and clinical in

numerous challenging diseases ranging from immunopathologies to cancer and beyond, contributing to improving the organism’s correct physiology.

2. Materials and Methods

2.1 Mouse lines

To address the biological question and to perform the scientific experiments described in the following sections, are required specific mouse lines. *C57BL/6J* (Jackson Laboratories); *Xcr1*^{Cre} [165]; *Xcr1/ksho*^{Cre} [166]; *TH*^{Cre} [167]; *Ai9(RCL-tdT)*^{fl} [168]; *Ai32(RCL-ChR2(H134R)/EYFP)*^{fl} [169] and *Adrβ2*^{fl} [170] were used. The Xcr*1*^{Cre} was imported from *Centre d'Immunologie de Marseille-Luminy* (CIML) in Marseille, France since the authors of this paper designed the genetic mouse[165]. *The Xcr1*^{Cre} was then crossed with *Adrβ2*^{fl} resulting in *Xcr1*^{Cre}*Adrb2*^{fl}.

Similarly, another *XCR1*^{Cre} construct, named *Xcr1/ksho*^{Cre}, developed by Tsuneyasu Kaisho, was kindly shared by the Laboratory for Immune Regulation, International Research Center Initiative, Immunology Frontier Research Center in Osaka University Suita in Japan, in which they designed the mutant[166]. These mice were also crossed with *Adrb2*^{fl} resulting in *Xcr1/ksho*^{Cre} *Adrb2*^{fl}.

Furthermore, *Xcr1*^{Cre} was also crossed with *Ai9(RCL-tdT)*^{fl} providing the cDC1 Cre-dependent specific tdTomato endogenous fluorescence. Following the same principle *TH*^{Cre} mice were then crossed with *Ai9(RCL-tdT)*^{fl}, or *Ai32(RCL-ChR2(H134R)/EYFP)*^{fl} hence targeting sympathetic neurons in a CRE-dependent fashion with endogenous tdTomato or yellow fluorescence, respectively. All mouse lines have *C57BL/6J* background.

All utilized mice were bred and maintained at the Champalimaud Centre for the Unknown (CCU) animal facility in Lisbon, Portugal by the Vivarium Platform team. The mice were kept at a constant 12-h light–dark cycle at normally 21ºC with around 50% humidity under specific pathogen-free conditions with food and water provided *ad libitum*. All mice cages were changed once a week by the Vivarium Platform team. Both males and females between 5 to 16 weeks of experimental mice were used. All animal experiments were approved by Direção Geral de Veterinária (DGAV) and CCU ethical committees.

2.2 *In vivo* substance administration

To assess the effects of acute and chronic NE in cDC1 functionality, *C57BL/6J* mice were submitted either to 4 mg /kg mice /day of NE (EMD Millipore) prepared fresh in 0.1% ascorbic acid and 0.9 % NaCl intraperitoneally (i.p) (200µL) during 3 consecutive days representing acute stress or 2 mg/kg/day of NE i.p (200µL) administered on 2 consecutive days with a resting period of 1 day for a total of 15 days simulating chronic stress. Furthermore, *C57BL/6J* mice were used as vehicles in which they were injected (200µL) with the vehicle solution. On the 15th day of the experiment, the experimental mice were sacrificed following CO_2 inhalation.

For local administrations of *Adrβ2* antagonists and NE in the ear, *C57BL/6J* or *Xcr1*^{Cre} *Adrβ2*^{fl} mice were anesthetized by inhaling 2-2.5% isoflurane in a mouse chamber in an anesthesia vaporizer system (VetEquip RC^{2+} Rodent Circuit Controller). The anesthetized mice were then placed in a heating pad and an isoflurane face mask was inserted in the nose of the animal. With the help of a microscope/magnifier (LEICA DFC7000 T or LEICA S9E) the mice were then intradermally (i.d) injected 25µL in both ears with propranolol (Alfa Aesar) 2.5 mg/kg, 1mM ICI 118,551 (EMD Millipore) or 2mM of NE freshly prepared in 0.1% ascorbic acid and 0.9 % NaCl during 3 consecutive days. As control, vehicle mice were 25µL i.d injected with a solution containing 0.1% ascorbic acid and 0.9 % NaCl. All solutions were prepared freshly with 0.1% ascorbic acid and 0.9 % NaCl.

When indicated a stimulation mix containing CpG (InvivoGen) (10µg/mouse) Poly(I:C) (InvivoGen) (25µg/mouse) and PBS 1X were also administrated intradermally (25µL/ear) following mouse anesthesia with inhaled isoflurane like previously described.

6-hydroxydopamine (6-OHDA) is a neurotoxic compound, widely used in research, that selectively targets and kills all adrenergic (tyrosine hydroxylase^{+}) neurons thus abrogating NE signaling[171]. For reverse transcription quantitative real-time PCR (RT-qPCR) analysis of chemokine content in whole tissue, *C57BL/6J* mice were i.p injected (200µL) with 100mg/kg of 6-OHDA hydrobromide (Sigma-Aldrich) for 5 consecutive days. As controls, *C57BL/6J* mice were i.p injected (200µL) with a solution containing 0.1% ascorbic acid and 0.9 % NaCl. On the following day, the mice were sacrificed with CO_2 inhalation and the ears and ear-draining lymph nodes were removed and placed in 1.5mL safe-lock eppendorf tubes (Eppendorf) in dry ice, the samples were immediately frozen in -80ºC until further usage.

For confocal imaging, *XCR1*^{Cre}*Ai9(RCL-tdT)*^{fl} mice were required. The cDC1s of these mice express Cre-dependent endogenous tdTomato fluorescence hence it is possible to visualize this immune population by confocal microscopy. The mice were further subjected to 200µL i.p injections of either 100mg/kg of 6-OHDA during 5 consecutive days or with vehicle in which they were injected with a solution containing 0.1% ascorbic acid and 0.9 % NaCl. Additionally, *XCR1*^{Wt}*Ai9(RCL-tdT)*^{fl} mice were also used serving as a control of the endogenous fluorescence. All 6-OHDA solutions were freshly prepared in a solution with 0.1% ascorbic acid and 0.9 % NaCl.

Moreover, 6-OHDA was also i.d administered, however, since is a novelty, and there are no literature findings on intradermal 6-OHDA injections, the dosage of 6-OHDA was based on this paper[172], in which 8µL of 12mg/mL 6-OHDA prepared in saline with 0.02% ascorbic acid was injected in iWAT fat pad. Hence, troubleshooting experiments were conducted utilizing *TH*^{Cre}*Ai9(RCL-tdT)*^{fl} and *TH*^{Cre}*Ai32(RCL-ChR2(H134R)/EYFP)*^{fl} reporter mice and assessed by confocal microscopy if the adrenergic neurons are abolished. These mice were then intradermally injected 25µL of 12mg/mL 6-OHDA or 2 shots of 25µL of 24 mg/mL 6-OHDA respectively, freshly prepared with a solution containing 0.1% ascorbic acid and

0.9 % NaCl during 2 consecutive days with a following rest day. As control of 6-OHDA injections, both *$TH^{Cre}Ai9(RCL\text{-}tdT)^{fl}$* and *$TH^{Wt}Ai9(RCL\text{-}tdT)^{fl}$*, *$TH^{Cre}Ai32(RCL\text{-}ChR2(H134R)/EYFP)^{fl}$* and *$TH^{Wt}$ $Ai32(RCL\text{-}ChR2(H134R)/EYFP)^{fl}$* were intradermally injected with one or two shots of 25µL in both ears, respectively with 0.1% ascorbic acid and 0.9 % NaCl. For the i.d administrations it was followed the same instructions as previously described. 2 days after the last intradermal injection the mice were sacrificed.

For FITC painting with intradermal 6-OHDA, *C57BL/6J* mice were i.d administered with 2 shots of 25 µL of 24 mg/mL 6-OHDA, freshly prepared with a solution containing 0.1% ascorbic acid and 0.9 % NaCl for 2 consecutive days. As control, vehicle mice were 25µL i.d injected with a solution containing 0.1% ascorbic acid and 0.9 % NaCl two times. On the afternoon of the following day, a stimulation mix containing CpG (10µg/mouse), Poly(I:C) (25µg/mouse) and PBS 1X was also applied intradermally (25µL/ear).

2.3 FACS buffer and DC media preparation.

FACS Buffer, composed of 900mL of Mili-Q Water, 100mL of PBS10X (Corning®), 2.5mM of EDTA(Corning®), and 2.5% of FBS (Corning®) was the recurrent buffer of choice for cellular suspensions, washing steps and extracellular antibody staining.

For *in vitro* stimulation processes, it was prepared a DC medium containing 200mL of RPMI 1X (Corning®), 2.5mL of L-Glutamine 100x (Corning®), Penicillin/Streptomycin Antibiotics 100X (Corning®), HEPES Buffer 100X (Corning®), non-essential amino acids 100X, (Corning®) Sodium Pyruvate 100X (Corning®), 0.25mL of B-mercaptoethanol 1000X (Corning®) and 20% of FBS (Corning®) being the last component previously filtered with a 0.45nm strainer.

2.4 Spleen and lymph node processing

The removed spleen and lymph nodes were placed in a 24-well plate name (Corning®) containing 1mL or 200µL respectively of Hanks' Balanced Salt Solution (HBSS) plus Ca^{2+} and Mg^{2+} (Corning ®) in ice.

Posteriorly, the organs were digested by using a mix of 250 µg/mL Liberase TL (previously suspended with 2mL HBSS) (Roche) and 67 µg/mL DNase I (AppliChem GmbH, ITW Reagents) digestion solution. In the case of the spleen, this mixture was injected inside the spleen at least 3 times.

Later, the spleen and lymph nodes were minced into small pieces and later transferred into an incubator (Thermo Scientific) for two periods of 15 and 10 minutes respectively. After the first incubation period, the samples were softly minced again. Posteriorly, after the incubation events, the digestion reaction was stopped by adding 100 µL/well of FBS (Corning®). Posteriorly, the splenic cells were filtered with a 70 µM cell strainer placed on top of a 50mL falcon tube (Corning®) whereas the digested lymph nodes

were filtered with a 30 µM cell strainer inserted in a new 24-well plate. The lymph node filtering process was conducted via a gauge 18-gauge needle (Terumo) at least 3 times.

The filtered splenic cells were later centrifuged at 700g for 3 minutes and the cell pellet was resuspended with 1mL of Red Blood lysis solution (BD bioscience) and incubated for 5 minutes at room temperature (RT), then the cells were washed with 4mL of FACS buffer and centrifuged at 700g for 3 minutes.

2.5 CD11c pre-purification

The splenic cellular suspension was resuspended in a solution containing 440 µL of FACS buffer and 60 µL of CD11c Microbeads UltraPure (Miltenyi Biotec) and incubated for 15 minutes at 4ºC. After the incubation with the beads, the cells were washed with 10 mL of FACS buffer and centrifuged at 700g for 3 minutes. The pellet was resuspended with 500 µL of buffer and was filtered using a 30 µM cell strainer before applying the sample to the magnetic activated cell sorting (MACS) columns (Miltenyi Biotec). The cells were purified following the manufacturer's indications.

2.6 Flow cytometry staining and sorting

Splenic cells were plated in 4 different readout panels to examine the different molecules that assess the functionality of cDC1. The panels with all the antibodies as well their fluorophore, dilution, and company used in staining of splenic cells can be depicted in Tables 2.1-2.4, and for lymphoid cells, in Table 2.5. All the antibody stainings were performed in round bottom 96-well plates (Corning®). 10 µL/sample of Brilliant Stain Buffer Plus (BD Biosciences) was added to the antibody mixes containing more than 2 BV antibodies. All washing events described in this section involve centrifugation at 700g for 3 minutes. Prior to the antibody staining, all wells were first stained with 50µL/well for 5 minutes at 4ºC with Aqua BV510 (Invitrogen, 1:1000), a live-dead dye that positively marks dead cells, and FcBlock (eBioscience, 1:100), reducing unspecific binding, prepared in PBS 1X. After washing with 100 µL of PBS 1X, the splenic and lymphoid cells were submitted to surface antibody staining mixes (50µL/well) prepared in FACS buffer for 20 or 15 minutes respectively, at 4ºC. In the case of the chemokine receptors panel (Table 2.2), the splenic cells were previously stained with CCR7 and CCR6 antibodies at 37ºC, washed with 100µL FACS buffer, and then labeled with the rest of the antibodies at 4ºC. After surface staining, the cells were further washed with 100µL FACS buffer and resuspended in a mixture containing FACS buffer (200µL/well) and counting beads (BD bioscience) (5µL/well).

For cytokines and chemokines analysis after *in vitro* stimulation, the splenic cells were labeled with Aqua and FC block and were subjected to surface antibody staining mixes (Table 2.3 and 2.4) (50µL/well) prepared in FACS buffer for 15 minutes at 4ºC. The samples were then washed with 100µL FACS buffer and were fixed 100µL/well for 40 minutes at RT with Fix/Perm (BioLegend) solution as indicated by the manufacturer. After the cells were incubated overnight at 4ºC with a mix containing the

intracellular antibodies (Table 2.3 and 2.4), washed, and resuspended with FACS buffer and counting beads before acquisition. The resuspended cells were then transferred into FACS tubes.

The acquisition of all the samples was conducted by BD LSRFortessaTM X-20 cell analyser and the results analysis was performed via FlowJo™ Software for Windows Version 10.8.1. Ashland, OR: Becton, Dickinson and Company; 2023.

For *in vitro* stimulation assays with clenbuterol, CD11c purified cells were resuspended with 500µL/sample of sorting mix of MHC-II, XCR1, and SIRPα (CD172α) from Table 2.6, prepared in FACS buffer with the aim of sorting and isolating cDC1 and cDC2. After 20 minutes staining at 4ºC, the cells were centrifuged at 700xg for 3 minutes. The cell pellet was resuspended with 200µL/well of Hoechst 33258 (Thermo Fisher Scientific) viability dye previously prepared in FACS buffer at 1:100. After resuspension the samples were then transferred to FACS tubes for the sorting process. The cell sorting was performed using BD FACS AriaTM Fusion Flow cytometer with the 100 nozzle by the Flow cytometry platform team at Champalimaud Foundation.

For every condition (*in vitro* stimulation with clenbuterol/ without clenbuterol) 10.000 cDC1 and cDC2 were collected in 1.5mL eppendorfs containing 100µL FBS in ice. Therefore, for every sample 20.000 cDC1 and 20.000 cDC2 were required. Additionally, a random sample Wt sample was selected to also serve as control wells (no stimulation) therefore to a random Wt sample it was removed 40.000 cDC1 and cDC2.

The Xcr*1*/ksho^{Cre}*Adrβ2*^{fl} were checked for *Adrβ2* depletion, for that different immune splenic cells were FACS-sorted into 1.5mL eppendorfs containing 100 µL RA1 + 2µL TCEP (Macherey-Nagel) in dry ice based on distinct surface markers expression: cDC1 (MHC-II$^+$ CD11c$^+$ XCR1$^+$); cDC2 (MHC-II$^+$ CD11c$^+$ SIRPα$^+$) macrophages (CD64$^+$), T (CD3$^+$) and B cells (CD19$^+$). The panels with all the antibodies as well as their fluorophore, dilution, and company used in staining and sorting splenic cells can be depicted in Table 2.6. The cell sorting was performed using BD FACS AriaTM Fusion Flow cytometer using the 85 nozzle.

2.7 CD11c *in vitro* stimulation

For MHC, co-stimulatory molecules and chemokine receptors output, after CD11c purified, the cells were directly analyzed, whereas the chemokines and cytokines were determined after culture and stimulation of the DCs. The cells were resuspended with DC medium and rested in an incubator with CO_2 for 15 minutes. Aftermath, a stimulation mix containing 0.5 µg/mL and 50 µg/mL of CpG ODNs (InvivoGen) (TLR9 agonist) and Poly(I:C) (InvivoGen) (TLR3 agonist) respectfully, was added to the cultured cells and incubated for 30 minutes. After Brefeldin A (Alfa Aesar) was added to the cells as indicated by the manufacturer for a 3-hour stimulation period.

For the clenbuterol *in vitro* assay, the cells were transferred into an incubator at 37ºC with CO_2 for 20 minutes. After the incubation period, the cDC1 were stimulated 100µL/well with a mix containing 0.5 µg/mL of CpG, 50µg/mL of Poly(I:C), and 0.5 mg/mL of clenbuterol (Sigma-Aldrich) prepared in DC medium and the cDC2 were stimulated 100µL/well with a mix containing 0.5 µg/mL of CpG, 100µg/mL of Poly(I:C), and 0.5 mg/mL of clenbuterol prepared in DC medium. The stimulated cells were placed in an incubator at 37ºC for 30 minutes. As control, there were sample wells that did not were submitted to clenbuterol (only went to the process of stimulation with CpG and Poly(I:C)). Furthermore, unstimulated wells were also conducted in which cells received only medium instead of a stimulation mix.

Posteriorly, after the 30-minute stimulation phase, all cultured cells were subjected to 20µL/well of Brefeldin A, 1:1000 previously prepared in DC medium. After a 3-hour and 30-minute stimulation period in the incubator with CO_2 the samples were fixed and permeabilized to label with the intracellular antibodies for cytokines and later analyzed by flow cytometry.

2.8 FITC painting assay

Mice submitted or not to CpG/Poly(I:C) intradermal administration were 2-3 hours later subjected to skin sensitization by topical administration of 1% Fluorescein isothiocyanate isomer I (FITC) (Sigma-Aldrich) prepared in acetone (Thermo Fisher Scientific) and dibutyl-phthalate (DBP) in a 1:1, volume: volume ratio. Using a micropipette, 20µL per ear of the solution was applied to fully cover the ears upon anesthesia in a biosecurity chamber. After "painting" with the FITC solution the ears were dried out using a fan. As controls of the experiment, there were mice that did not get the CpG/Poly(I:C) inflammatory mix and other mice that were painted in the ear only with acetone and DBP lacking FITC. Importantly, the FITC resuspension was prepared freshly immediately before the painting assay and covered in aluminum foil to preserve the fluorescence.

On the next morning, the mice were euthanized following CO_2 inhalation. Posteriorly, the mice were sprayed in the ears with 70% ethanol in the ears sections and the ear lymph nodes of both ears were removed with sharp-straight scissors and forceps (Terumo), the ear lymph nodes were then placed in a 24-well plate (Corning®) containing 0.2mL HBSS plus Ca^{2+} and Mg^{2+} (Corning ®) in ice.

2.9 RNA extraction from sorted cells

RNA from sorted cells was purified and extracted adapted from Macherey-Nagel manufacturer's protocol, being the only differences the filtration of the lysate with NucleoSpin® Filters, placed in top of 2mL collection tubes and centrifugation at 11.000xg for 30 seconds, and in the end the pure RNA was eluted with 12µL of RNase-free H_2O. Afterward, after RNA purification, 1µL of the extracted RNA

was checked for concentration and purity following Nanodrop Spectrophotometer (Nanodrop Technologies).

2.10 RNA extraction from tissues

RNA of whole ear and ear lymph node tissues was extracted, and the expression levels of the chemokine genes responsible for the migration capability were investigated through qPCR methodology.

Inside the chemical hood, 300µL of Trizol (Grisp) was added to the samples. Since the ears were too thick, they were minced with sharp-straight scissors into small pieces. Additionally, with forceps, it was added 1 Stainless 3mm diameter sphere per eppendorf. The samples were then placed and equilibrated in the 24 vortex adapters (Qiagen). The adapters were settled in the Tissue Lyser machine (Qiagen) and closed tightly so it doesn't get loose. After a program of 30 Hertz for 3 minutes the samples were recovered and later centrifuged at full speed (17000xg) for 3 minutes at 4ºC. Afterward, the supernatant was recovered (+/- 300µL) into newly labeled normal 1.5mL eppendorfs with extreme caution to not touch the cell pellet. To promote a good separation of aqueous and organic phases, 60µL of chloroform (Sigma-Aldrich), inside the chemical hood, was then added to the obtained supernatant and later vortex for 15 seconds. Furthermore, after a centrifugation of 12000xg for 15 minutes at 4ºC, it is visible the isolation of 3 different layers in the samples. The aqueous phase containing RNA was then recovered (+/- 150µL) into new eppendorf tubes while the rest of the sample with the white interphase ring containing the DNA and the organic phases containing cell debris proteins and lipids were discarded. This step needs to be conducted with extreme caution to avoid loss of RNA and contamination with the other substances.

After isolation of the aqueous layer, to promote good precipitation of RNA, 150 µL of isopropanol (Thermo Fisher Scientific), inside the chemical hood, was appended to the samples, and the tubes were inverted to mix. After an incubation period of 10 minutes at RT, the samples were centrifuged 12000xg for 10 minutes at 4ºC so that RNA could be precipitated. The supernatant was discarded by inverting the tube and the RNA pellet was washed with 300µL with ice-cold EtOH 75% and centrifuged again 12000xg for 10 minutes at 4ºC, further promoting precipitation of RNA. After washing, the supernatant was discarded, the eppendorf tubes were inverted and the pellet was left to dry for 5-10 minutes. To note, it is suggested that the RNA pellet does not completely dry otherwise the RNA could not be totally soluble. After the drying event, the RNA was resuspended with 50µL RNAse-free water. Posteriorly, the RNA was further purified following Macherey-Nagel manufacturer's protocol and checked for concentration and purity as described in the 2.9 section. All later events, mainly, RNA to cDNA conversion, pre-amplification of target chemokines and house-keeping genes, and RT-qPCR were conducted in a similar fashion to what is described in the 2.11 section. The chemokines and housekeeping probes list are displayed in Table 2.7 (B).

2.11 cDNA synthesis, pre-amplification, and reverse transcription quantitative real-time PCR (RT-qPCR)

High-capacity RNA-to-cDNA™ kit (Applied Biosystems) was used to convert the extracted RNA into cDNA following the manufacturer's instructions. Reverse-Transcriptase PCR was conducted using a SimpliAmp™ Thermal cycler (Applied Biosystems) according to the manufacturer's indications.

After that, cDNA pre-amplification was conducted by using TaqMan ™ PreAmp Master Mix (Applied Biosystems) manufacturers protocol. Briefly, a probe mix was prepared containing 15µL/sample of TaqMan ™ PreAmp Master Mix (Applied Biosystems), 0.125µL/sample of each probe gene, and 7,5µL – (0,125*probes) / sample of Tris-EDTA (TE) (Thermo Fisher Scientific) buffer. 22.5µL of this mixture was then micropipette into each PCR tube, in which later 7,5µL of extracted cDNA was added leading to a total of 30µL volume inside the PCR tube. The tubes were then spined down to guarantee a mixture of all components. Posteriorly the cDNA was then inserted in SimpliAmp™ Thermal cycler (Applied Biosystems) and the pre-amplification protocol was performed according to manufacturer indications.

For qPCR, the 30µL cDNA samples were firstly diluted 1:10 with 270µL of TE buffer. Individual probe mixes comprising 5 µL/sample of TaqMan® Gene Master Mix (Applied Biosystems), 0.5 µL/sample of each probe, and 2 µL/sample of RNAse-free water were prepared. All RT-qPCRs were performed in 384-well plates (Applied Biosystems) where 7.5 µL of the PCR reaction mix was added with a single automated pipette and 2.5 µL of each pre-amplified cDNA using a multichannel pipette thus each well in the end account for 10µL. The plates were sealed with a plastic cover (Thermo Scientific) and were then centrifuged at 700g for 2 minutes. RT-qPCR reactions were conducted in the QuantStudio™ 5 Real-Time PCR System (Applied Biosystems) according to the manufacturer's indications and the analysis was performed by the comparative cycle threshold (CT) method ($2^{-\Delta CT}$), in which, the CT values of the genes of interest are the mean CT values of the triplicate samples minus the mean CT values of the housekeeping genes. GAPDH and HPRT were the selected house-keeping genes. The list of probes used is illustrated in Table 2.7 (A).

2.12 Confocal imaging and immunofluorescence

After the indicated treatment or without any further action the *XCR1^{Cre} Ai9(RCL-tdT)^{fl}* , *TH^{Cre} Ai9(RCL-tdT)^{fl}* and *TH^{Cre}Ai32(RCL-ChR2(H134R)/EYFP)^{fl}* reporter mice were euthanized with 100µL i.p injection of sodium pentobarbital (Exagon, Richter pharma) or Ketamine (Nimatek, Dechra) /Xylazine (Rompun, Elanco) Mouse Mix (100µl/10g). The chest was opened, and a thin gauge needle was inserted in the left ventricle of the still-beating heart in order to promote systemic perfusion. Firstly, the mice were perfused with 2 minutes of PBS 1X to remove all the blood. If the liver immediately starts to get a white tone the perfusion is confirmed to be working. If any liquid is leaving the nose and mouth, probably the needle was inserted in the right ventricle, or it was too deep in the left ventricle that it

entered in right auricle leading to the pulmonary circulation. After the 2-minute perfusion with PBS 1X (Corning ®), it was followed by 5-minute perfusion with paraformaldehyde (PFA) 4% (Sigma-Aldrich) promoting tissue fixation. After the perfusion with the fixating agent, the spleen and mesenteric lymph nodes, of *XCR1*^{Cre}*Ai9(RCL-tdT)*^{fl} mice were removed using sharp-straight scissors and forceps and were attached to card pieces before transferred into 50mL Falcons (Corning ®) and 2mL eppendorfs with appropriate volumes of PFA 4%. In parallel, the ears of all reporter mice were also removed, the basal and peripheral sides of the ears were opened with forceps in the basal (white side) and another on the peripheral (darker side) and pulled in separate directions according to whole mount ear protocol[173]. Both opened ears were placed in card pieces, internal side up and later transferred into PFA 4%- containing 2mL eppendorfs. All the organs were then delivered to the histopathology platform for all the stainings with the desirable antibodies and mounting of the slices for confocal microscopy acquisition. Briefly, the dissected ears were fixed in 4% PFA. Fixation was followed by permeabilization through 2-hour incubation with 0.3% Triton X-100 in PBS, with 5% bovine serum albumin, 0,1M glycine and 0,1% sodium azide. Tissues were incubated overnight at 4°C with primary antibody for TH (Pel-Freez, Ref.: P40101-150), diluted at 1:1000 in 0.3% Triton X-100 in PBS with 0,1% sodium azide. Secondary antibodies conjugated with appropriate fluorophores were then applied for 2 hours at room temperature. After AlexaFluor 647 anti-goat secondary antibody incubation (Invitrogen, A21244), the tissues were stained with 4',6-diamidino-2-phenylindole DAPI at a concentration of 1µg/mL in PBS for 15 minutes to visualize cell nuclei. Tissues were mounted onto glass slides using a glycerol-based mounting medium. The slides were acquired by confocal microscopy with specific excitation and emission filters. Additionally, the results were analyzed by Zeiss Zen Blue or Fiji/ImageJ.

2.13 Statistical Analysis

The analysis of the experiment's findings was performed by using FlowJo™ Software for Windows Version 10.8.1. Ashland, OR: Becton, Dickinson and Company; 2023. The results are displayed as the mean values +/- standard deviation. These values were obtained by paired t-test when performing comparisons between two independent groups or an ordinary one-way ANOVA with multiple comparisons for more than 2 independent groups using GraphPad Prism version 8.4.3 for Windows (GraphPad Software, San Diego, California USA). The findings were considered statistically significant when p-value is lower than 0.05 (*), <0.01(**), <0.001 (***), and <0.0001(****).

Table 2.1. Antibodies used for staining of antigen-presentation and co-stimulatory molecules

Mix	Fluorochrome	Antigen	Dilution	Clone	Brand
Surface antibody staining for antigen-presentation and co-stimulatory molecules	PercPCy5.5	CD40	1:100	3/23	BioLegend
	FITC	CD80		16-10A1	
	BV650	CD86		GL-1	
	eF450	MHC-I		H-2Kb	Invitrogen
	PE	MHC-II	1:400	M5/114.15.2	BioLegend
	BV785	XCR1	1:100	ZET	
	APC	CD11b	1:200	M1/70	
	AF700	SIRPα (CD172α)		P84	

Table 2.2. Antibodies used for staining of chemokine receptors

Mix	Fluorochrome	Antigen	Dilution	Clone	Brand
Surface antibody staining - Chemokines receptors	AF700	CCR7	1:100	G043H7	BioLegend
	BV711	CCR6		140706	BD Biosciences
	BV650	XCR1	1:200	ZET	BioLegend
	PercPCy5.5	SIRPα		P84	BioLegend

Table 2.3. Antibodies used for staining of intracellular chemokines

Mix	Fluorochrome	Antigen	Dilution	Clone	Brand
Intracellular staining for chemokines	APC	CCL3	1:50	39624	Invitrogen
	PE	CCL5	1:100	2E9/CCL5	BioLegend
Surface staining	BV785	XCR1		ZET	
	AF700	SIRPα (CD172α)	1:200	P84	

Table 2.4. Antibodies used for staining of intracellular cytokines

Mix	Fluorochrome	Antigen	Dilution	Clone	Brand
Intracellular staining cytokines	PE	IL-12	1:50	C17.8	Invitrogen
	BV421	TNFα	1:200	MP6-XT22	BioLegend
Surface staining	BV785	XCR1	1:100	ZET	
	AF700	SIRPα (CD172α)	1:200	P84	

Table 2.5. Antibodies to stain the migratory cDC1

Mix	Fluorochrome	Antigen	Dilution	Clone	Brand
Surface antibody - FITC painting	AF700	MHC-II	1:600	M5/114.15.2	Invitrogen
	PercPCy5.5	CD40	1:100	3/23	BioLegend
	PE	CD11c	1:200	N418	eBioscience
	AF647	XCR1		ZET	BioLegend
	BV605	CD103		2E7	

Table 2.6. Antibodies used to identify and sort the different immune populations

Mix	Fluorochrome	Antigen	Dilution	Sorted cell	Clone	Brand
Staining for sorting of distinct immune cells populations	FITC	MHC-II	1:300	-	2G9	BD biosciences
	APC	CD11c	1:200	-	N418	BioLegend
	BV785	XCR1		cDC1	ZET	
	PercPCy5.5	SIRPα (CD172α)		cDC2	P84	
	BV711	CD64(FcγRI)		MF	X54-5/7.1	
	BV605	CD19		B cell	6D5	
	PE	CD3e	1:50	T cell	145-2C11	Invitrogen

Table 2.7. List of probes used for Real-time PCR. (**A**) Probes used to assess adrenergic receptors expression on the different immune sorted cells. (**B**) Probes to assess chemokine content in ears and lymph node tissue. The probes were obtained by obtained by Thermo Fisher Scientific.

(A)

Gene	Reference
Adrβ1	Mm00431701_s1
Adrβ2	Mm02524224_s1
Adrβ3	Mm02601819_g1
GAPDH	Mm99999915_g1
HPRT	Mm03024075_m1

(B)

Gene	Reference
CCR7	Mm99999130_s1
CCR6	Mm99999114_s1
CCL19	Mm00839967_g1
CCL20	Mm01268754_m1
CCL21	Mm03646971_gH
GADPH	Mm99999915_g1
HPRT	Mm03024075_m1

3. Results

3.1 *Xcr1/ksho^{Cre}Adrβ2^{fl}* genetic mice construct suffers germline deletion

Many findings of the laboratory were derived from the use of the genetic model *Xcr1^{Cre}Adrβ2^{fl}*, being the *Xcr1^{Cre}* imported from Marseille, France as said previously. However, there are some concerns regarding germline deletion in the CRE. Although, previously the lab performed qPCR and displayed that only cDC1s from CRE mice, the expression of the *adrβ2* gene is severely affected (unpublished) (Figure 7.1). Nonetheless, the group also decided to order other mice with the same construct but from different centers, being this one derived from Japan (*Xcr1/ksho^{Cre}*).

The *Xcr1/ksho^{Cre}Adrβ2^{fl}* were then checked for *adrβ2* depletion, in which there were sorted distinct splenic immune cell populations and through qPCR methodology, expression levels of *adrβ2* were investigated (Figure 3.1A). In parallel, to infer compensation over *adrβ2* loss, the expression levels of *adrβ1* and *adrβ3* were also examined (Figure 3.1B and 7.2 respectively).

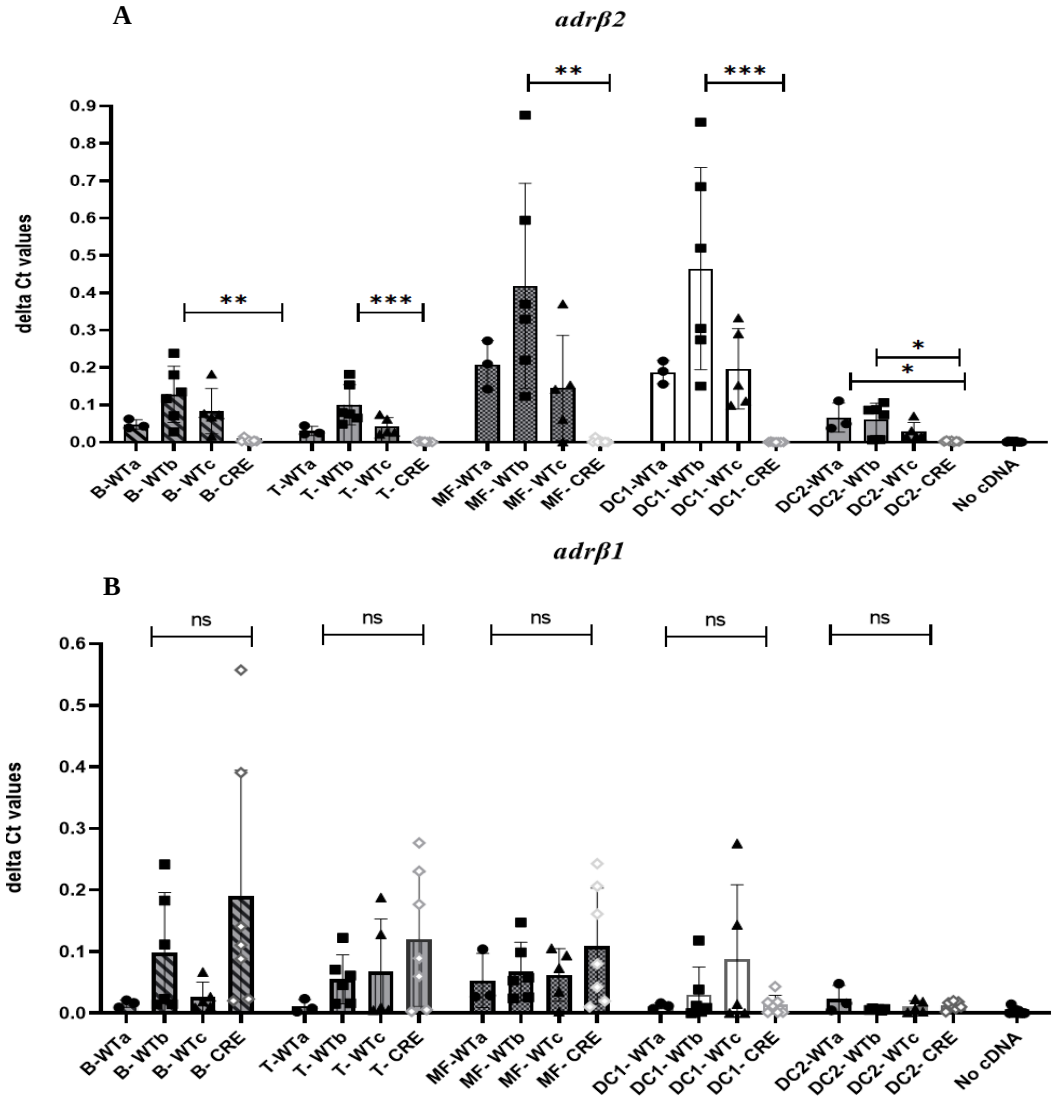

Figure 3.1. qPCR results of sorted splenic immune populations of *Xcr1/ksho^{Cre}Adrβ2^{fl}* and *Xcr1/ksho^{Wt} Adrβ2^{fl}* mice. **(A) –** *adrβ2* expression levels values in each sorted immune population: cDC1(MHC-II^{+} CD11c^{+} XCR1^{+}); cDC2 (MHC-II^{+} CD11c^{+} SIRPα^{+}) macrophages (CD64^{+}), T (CD3^{+}) and B cells (CD19^{+}) (Table 2.6). **(B) –** *adrβ1* expression levels values in sorted each immune population. The selected probes for qPCR reaction are illustrated in Table 2.7A. *gadph* and *hprt* were the chosen housekeeping genes. These plots were obtained by applying ordinary one-way ANOVA with multiple comparisons per immune population using GraphPad Prism 8.4.3 version for Windows (GraphPad Software, San Diego, California EUA). Abbreviations: ns- non-significant result (p-value>0.05). Wta- *Xcr1/ksho$^{Cre/Wt}$Adrβ2$^{Wt/Wt}$* mice. Wtb- *Xcr1/ksho^{Wt}Adrβ2$^{fl/Wt}$* mice. Wtc- *Xcr1/ksho$^{Wt/Wt}$Adrβ2$^{fl/fl}$* mice. CRE- *Xcr1/ksho$^{Cre/Wt}$Adrβ2$^{fl/wt}$* mice. B- B immune cell; T- T immune cell. MF- macrophage immune cell. DC1- cDC1 immune cell; DC2- cDC2 immune cell. These results are derived from two independent experiments which account for 3Wta, 6Wtb, 5Wtc, and 7 CRE mice. No cDNA values represent a control group, in which instead of cDNA plus RNAse-free, only RNAse-free were incubated with RT enzyme in the cDNA synthesis step.

Since *Xcr1/ksho^{Cre}Adrβ2^{fl}* is a Cre-dependent line it is theoretically supposed that only on XCR1^{+} cells (cDC1) the *adrβ2* receptor gene would be floxed. As seen in Figure 3.1A, the cDC1 of Cre-expressing mice have no expression of the g-couple receptor compared to all other Wt littermates. Nonetheless, this phenomenon also occurs in every other sorted immune cell, with expression levels of *adrβ2* suffering clear downregulation in comparison to all other Wt animals with significant p-values as displayed by the graph. This correlation could indicate that the genetic line is not specific to cDC1 since the *adrβ2* is cleaved in all isolated immune cells, hence suffering severe unspecific recombination. Thereafter, the imported Cre construct from the Japanese institute displays a tendency to be highly leaky therefore leading to severe germline deletion. Henceforth, this genetic line cannot be used for *in vivo* studies for testing the effects of *adrβ2* signaling on cDC1 functionality due to the genetic mice construct is not specific for cDC1.

In fact, Wta mice, which represent *Xcr1/ksho$^{Cre/Wt}$Adrβ2$^{Wt/Wt}$* animals, had reduced *adrβ2* gene expression at least on B and T cells compared to other Wt. Since these classified Wt mice are the ones that carry the Cre allele with no floxed allele on the *adrβ2* gene this could suggest that the Cre construct is responsible for the germline deletion event. Additionally, Wtc mice, which are classified as *Xcr1/ksho$^{Wt/Wt}$Adrβ2$^{fl/fl}$* animals, also have less expression than Wtb mice, which stands for *Xcr1/ksho$^{Wt/Wt}$Adrβ2$^{fl/Wt}$* mice, in every immune cell. Since it is a double flox allele in one gene, the *adrβ2* could display less relative values compared to a singular flox allele. This indicates that the chosen Wt mice of this line could be *Xcr1/ksho$^{Wt/Wt}$Adrβ2$^{fl/Wt}$* mice (Wtb). Additionally, the only significant statistical results displayed in Figure 3.1A come from the comparison of the mean values of Wtb with the Cre animals in every immune population, apart from cDC2 in which Wta vs. Cre is also significant. This provides strong confirmation that in fact, the germline suffers severe unspecific recombination due to the Cre construct being leaky and performing its cleaving action to remove the *adrβ2* gene in every immune population leading to germline deletion.

Moreover, as seen in Figure 3.1B, despite the results being non-significant there is a general tendency to increase expression amounts of *adrβ1* receptor in isolated splenic B, T, and MF cells Cre-expressing

mice compared to other Wt. These intriguing results could indicate that the expression of *adrβ1* is increased likely to compensate for the loss of *adrβ2*, further indicating that this NE receptor is indeed cleaved out in the surfaces of the immune cells. Interestingly in cDC1, there is a tendency to have decreased *adrβ1* expression in Cre-expressing mice while in cDC2, *adrβ1* values do not change.

Furthermore, as depicted in Figure 7.2, despite *adrβ3 gene* is barely expressed by immune cells, contrary to both *adrβ1 and adrβ2,* there is an indication that this gene is up-regulated in both T cells and cDC2, further indicating the compensation effect to overcome the loss of *adrβ2* gene.

Henceforth, all of these findings pooled confirmed that this genetic line cannot be used for *in vivo* studies for testing the effects of *adrβ2* signaling on cDC1 functionality due to the genetic mice construct is not specific for cDC1, suffering severe unspecific recombination.

3.2 Clenbuterol affects cytokines production by cDC1 *in vitro*

Measuring cytokine parameters is a good readout to assess cDC functionality. In this experiment, clenbuterol, an *Adrβ2* agonist was supplied together with CpG/Poly(I:C) in a stimulation mix to sorted cDC1 and cDC2 of both *Xcr1/ksho*^{Cre}*Adrβ2*^{fl} and *Xcr1/ksho*^{Wt}*Adrβ2*^{fl} to assess impact of TNFα and IL-12 production by these cells. The cytokine results can be visualized in Figure 3.2.

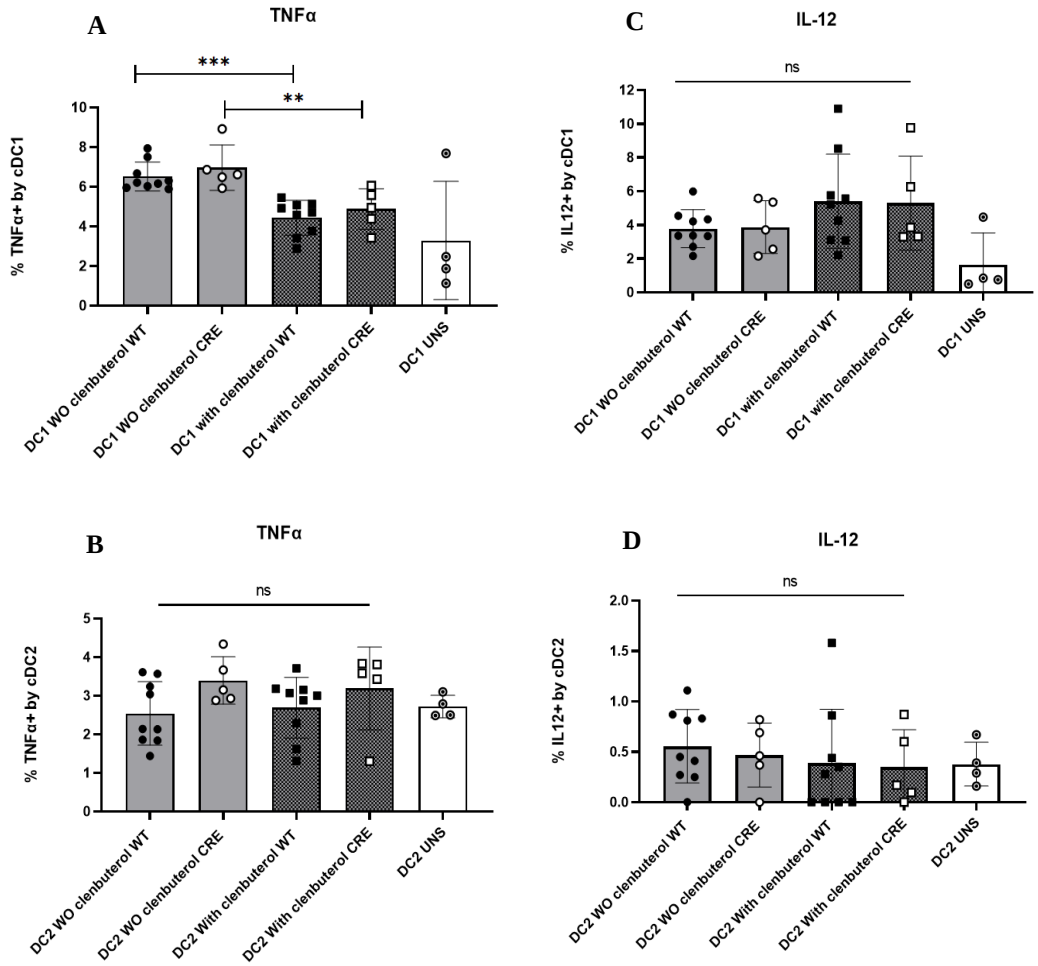

Figure 3.2. Alterations in cytokines expression in cDC1 and cDC2 following stimulation with (darker grey) or without (WO) (light grey) clenbuterol. Splenic cDC1(MHC-II$^+$ CD11c$^+$ XCR1$^+$) and cDC2 (MHC-II$^+$ CD11c$^+$ SIRPα$^+$) (Table 2.6) from both *Xcr1/ksho^{Cre}Adrβ2^{fl}* and *Xcr1/ksho^{Wt}Adrβ2^{fl}* were sorted and stimulated with CpG/Poly(I:C), apart from the unstimulated controls, in the presence or not of clenbuterol. Posteriorly, the cells were stained with TNFα and IL-12 intracellular antibodies (Table 2.4), and their cytokine expression was assessed by flow cytometry. (**A**)- changes in TNFα production by cDC1. (**B**)- changes in TNFα production by cDC2. (**C**)- changes in IL-12 production by cDC1. (**D**)- changes in IL-12 production by cDC2. The analysis was performed by using FlowJo™ Software for Windows Version 10.8.1. Ashland, OR: Becton, Dickinson and Company; 2023. These statistical values were obtained by using ordinary one-way ANOVA with multiple comparisons using GraphPad Prism version 8.4.3 for Windows (GraphPad Software, San Diego, California USA). Abbreviations: ns= non-significant results (p-value >0.05); UNS = unstimulated cells; DC1- cDC1 immune cell; DC2- cDC2 immune cell. These results are derived from two independent experiments which account for 9 *Xcr1/ksho^{Wt} Adrβ2^{fl}* and 5 *Xcr1/ksho^{Cre}Adrβ2^{fl}* mice.

Firstly, before analyzing the impact of *adrβ2* signaling through administration of the *Adrβ2* agonist (clenbuterol) and if it influences cytokine release by cDC, a parallel qPCR was conducted as a confirmation assay to confer if *adrβ2* was depleted in the isolated cells. As Figure 7.3 suggests, *adrβ2* is cleaved in both isolated cDC1 and cDC2. Despite cDC2 being a contradictory result is reproductive of Figure 3.1A further indicates the germline deletion problems. Nonetheless, *adrβ2* is floxed in Cre-expressing animals which validates the following findings.

As illustrated by Figure 3.2A, clenbuterol administration impacts TNFα production by cDC1 since Wt cells (cells that express *adrβ2* receptor) that were not subject to the *adrβ2* agonist synthesize more TNFα than the cells that were stimulated with the NE mimic being this a significant result (***). Furthermore, these findings are scientifically validated since the stimulated cells produce more TNFα cytokine than the unstimulated cells (white bar).

Moreover, through comparison of Wt and Cre cDC1 without clenbuterol treatment, there is a slight tendency that the Cre-expressing cDC1 (cells that lack *adrβ2* receptor) produce more TNFα than the Wt cDC1, meaning the purely the impact of the loss of *adrβ2* signaling promotes a higher production of the pro-inflammatory cytokine, a finding that will be further validated in following experiments. Furthermore, in cohesion with the expectation, when both cells are subjected to clenbuterol stimulation the tendency of higher production of TNFα by cells lacking *adrβ2* receptor remains, indicating that Cre-expressing cells are less sensitive to the clenbuterol inhibition due to the loss of *adrβ2* receptor, however, these last two results are non-significant.

Conversely, Cre mice that were *in vitro* submitted with clenbuterol produced fewer amounts of the pro-inflammatory cytokine than the Cre-cells that were stimulated with only CpG and Poly(I:C). Since neither group displays the adrenergic receptor, it would be expected similar values between the two groups since it would be expected that the clenbuterol inhibitory effects would not be addressed by these genetically modified cells.

As Figure 3.2B suggests, the cDC2 follow similar trends to the cDC1 counterparts, since both Cre groups treated with and without clenbuterol yield more TNFα than the *adrβ2*-expressing cells. However, in contradiction to cDC1, there is no clear impact of clenbuterol effects in TNFα synthesis, indeed it seems a small increase in TNFα production of Wt cDC2 following clenbuterol treatment. Nevertheless, all of these findings are non-significant and are not validated due to unstimulated cells (cells that were not submitted to TLR agonists) producing similar amounts of cytokine to the stimulated cells. The cDC2 serve as an internal control of the genetic model, since this model targets cDC1 and not cDC2 it is expected that are no differences in cytokine production by the cDC2 in Cre animals.

In opposition to the TNFα findings, the effects of clenbuterol administration in IL-12 production by the sorted cDC1 are unclear as visualized by Figure 3.2C. Although there is a general tendency that clenbuterol supplementation leads to an increase in the IL-12 production by cDC1 all these findings are non-significant. However, they are validated due to all stimulated cells producing more IL-12 than the unstimulated cells. Nonetheless, as Figure 3.2D displays, regarding the IL-12 production by cDC2, clenbuterol did not affect the output of the Th1-polarizing cytokine. Nonetheless, in a similar fashion to TNFα production by cDC2 these findings are not validated. These results indicate that cDC1s are the major producers of both cytokines, as depicted in the introduction, while cDC2s contribute very little to Th1 cytokine release.

Overall, all the findings pooled indicate that clenbuterol, an *Adrβ2* agonist, dampens down TNFα production by cDC1, being the only obtainable statistically significant finding, thus, triggering *adrβ2* signaling could lead to decreased functional ability of cDC1.

3.3 NE signaling induces tolerogenic properties of cDC1

As a way to debate regarding changes in cDC1 functionality following adrenergic signaling and assess the main differences in cDC1 phenotype following acute or chronic stress, NE was provided in two different scenarios and kinetics and the different functionality readouts were investigated. The results are displayed in Figures 3.3-3.7

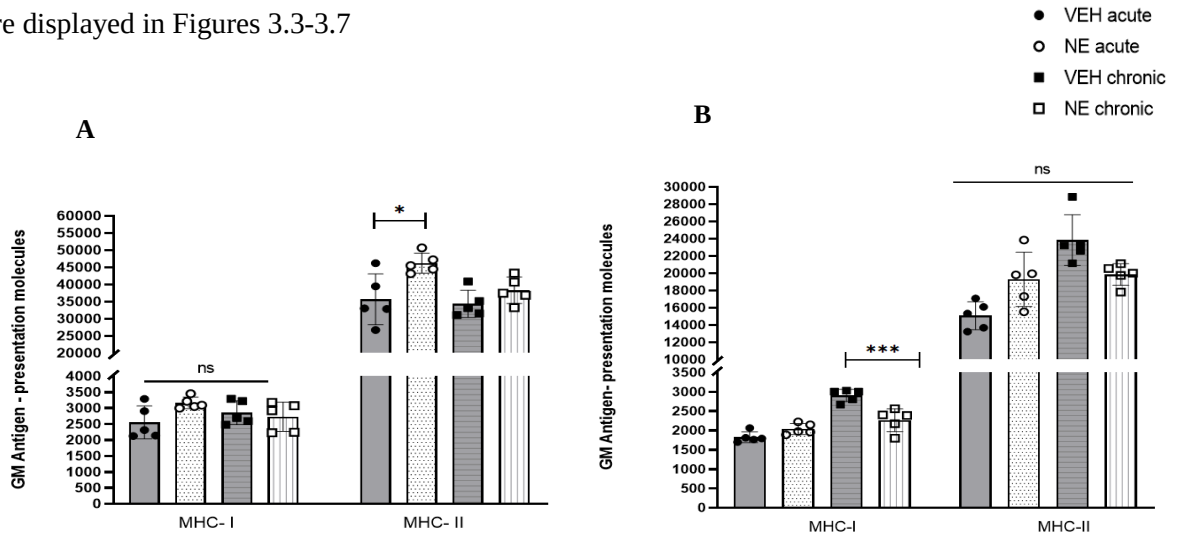

Figure 3.3. MHC values following acute vs. chronic NE treatment in I **(A)** and II **(B)** experiments. *C57BL/6J* mice were i.p injected with an acute dose (4 mg /kg mice /day) of NE for 3 consecutive days representing acute NE or with a chronic dose (2 mg /kg mice /day) administered in 2 consecutive days with a resting period of 1 day in a total of 15 days simulating chronic stress. As control there are *C57BL/6J* mice i.p treated with a vehicle solution containing 0.1% ascorbic acid and 0.9 % NaCl following the same described kinetics as the NE acute or chronic mice. CD11c purified splenic DCs were then stained with extracellular antibodies depicted in Table 2.1. A total of 5 mice were utilized per condition in both experiments. The y-axis represents the Geometric mean (GM) of the fluorescence. The analysis was performed by using FlowJo™ Software for Windows Version 10.8.1. Ashland, OR: Becton, Dickinson and Company; 2023. These values were obtained by using ordinary one-way ANOVA with multiple comparisons using GraphPad Prism version 8.4.3 for Windows (GraphPad Software, San Diego, California USA). ns- non-significant results (p-value >0.05).

As depicted by Figure 3.3, there is a slight indication of upregulation of the expression of both MHC-I and MHC-II molecules in an acute setting in both conducted experiments compared with vehicle acute findings. Although the increase in MHC-I expression is non-significant, the MHC-II variation is the most prominent and characterized as statistically significant in the first experiment (3.3A), while in the second one (3.3B) experience also a substantial increase in the $CD4^+$ presentation molecule. Regarding the chronic scenario, in the first experiment, there were barely any clear visible differences, only a small increase in MHC-II surface molecule. Nonetheless, in the second performed experiment MHC-I suffered a clear downregulation, furthermore, despite being non-significant, the levels of MHC-II also displayed a reduction compared to chronic vehicle values.

These findings polled suggest that a short acute stress tends to elicit the cDC1s into an activated state, however, following constant exposure to stress, in chronic events the cDC1s tend to be more immunosuppressed.

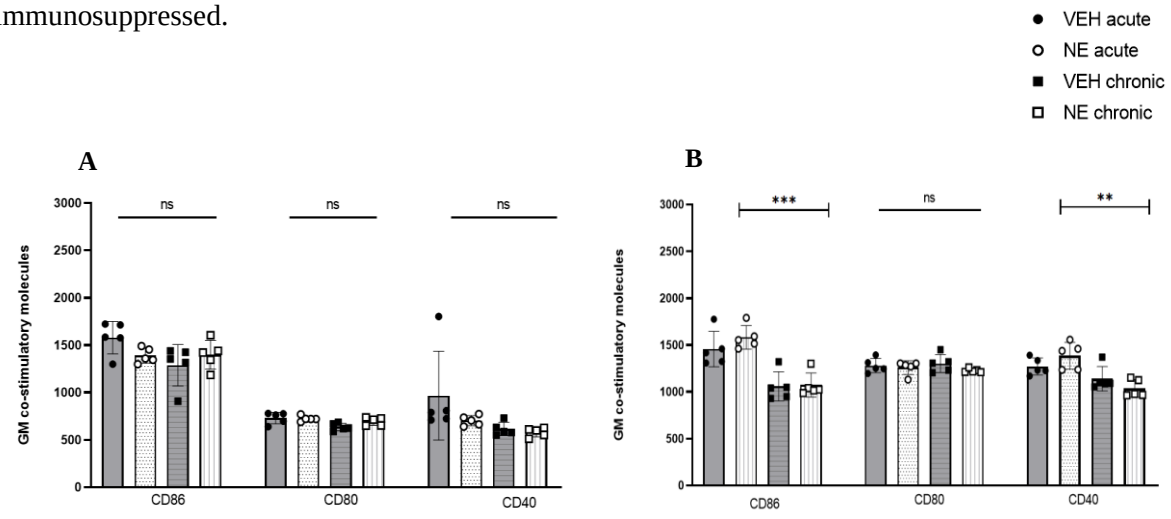

Figure 3.4. Co-stimulatory molecules expression following acute vs. chronic NE treatment in I **(A)** and II **(B)** experiments. *C57BL/6J* mice were i.p injected with an acute dose (4 mg /kg mice /day) of NE for 3 consecutive days representing acute NE or with a chronic dose (2 mg /kg mice /day) administered in 2 consecutive days with a resting period of 1 day in a total of 15 days simulating chronic stress. As control there are *C57BL/6J* mice i.p treated with a vehicle solution containing 0.1% ascorbic acid and 0.9 % NaCl following the same described kinetics as the NE acute or chronic mice. CD11c purified splenic DCs were then stained with extracellular antibodies depicted in Table 2.1. A total of 5 mice were utilized per condition in both experiments. The y-axis represents the Geometric mean. The analysis was performed by using FlowJo™ Software for Windows Version 10.8.1. Ashland, OR: Becton, Dickinson and Company; 2023. These values were obtained by using ordinary one-way ANOVA with multiple comparisons using GraphPad Prism version 8.4.3 for Windows (GraphPad Software, San Diego, California USA). ns- non-significant results (p-value >0.05).

Focusing on co-stimulatory molecules, as seen in Figure 3.4A there is a narrow trend to downregulate the expression levels of CD86 and CD40 in acute scenery thus hindering a more immunosuppressed cDC1. Likewise, this phenomenon also persists in chronic stress in CD40 since this molecule also has a tendency to reduce its expression levels as seen in Figure 3.4B, contradictory to the CD86 finding observed in both experiments. However, conversely as depicted by Figure 3.4B, acute stress condition induces a small upregulation of the expression levels of both CD86 and CD40 co-stimulatory molecules. CD80 expression levels did not change in both experiments in both acute and chronic scenarios therefore seems that this molecule is not affected by NE administration. Interestingly, as depicted by Figure 3.4B by comparing the NE acute vs. NE chronic columns there is a clear downregulation in the chronic stress group in CD86 and CD40. Nevertheless, overall, these results indicate that there is not a clear impact of NE administration on co-stimulatory molecule expression.

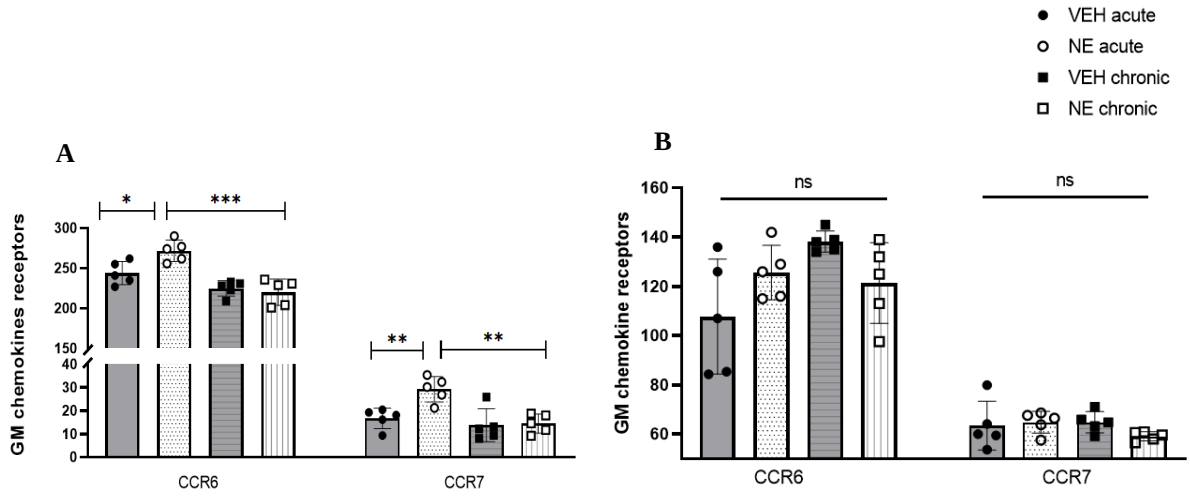

Figure 3. 5. Chemokine receptors values following acute vs. chronic NE treatment in I **(A)** and II **(B)** experiments. *C57BL/6J* mice were i.p injected with an acute dose (4 mg /kg mice /day) of NE for 3 consecutive days representing acute NE or with a chronic dose (2 mg /kg mice /day) administered in 2 consecutive days with a resting period of 1 day in a total of 15 days simulating chronic stress. As control there are *C57BL/6J* mice i.p treated with a vehicle solution containing 0.1% ascorbic acid and 0.9 % NaCl following the same described kinetics as the NE acute or chronic mice. CD11c purified splenic DCs were then stained with extracellular antibodies depicted in Table 2.2. A total of 5 mice were utilized per condition in both experiments. The y-axis represents the Geometric mean. The analysis was performed by using FlowJo™ Software for Windows Version 10.8.1. Ashland, OR: Becton, Dickinson and Company; 2023. These values were obtained by using ordinary one-way ANOVA with multiple comparisons using GraphPad Prism version 8.4.3 for Windows (GraphPad Software, San Diego, California USA). ns- non-significant results (p-value >0.05).

The chemokine receptors are crucial for the migration of cDC into the draining lymph node, in a CCR7-dependent manner, or to the skin, in a CCR6-dependent fashion, as stated in the 1.2.3 introduction section. Interestingly, there is a clear and robust upregulation of both chemokine receptors in the NE acute stress when compared with the vehicle group. This upregulation was experienced in both experiments performed being the first statistically significant for both CCR6 (*) and CCR7(**) while in the second experiment besides being non-significant there is also evidence of upregulation as seen in

Figures 3.5A and 3.5B, respectively. Intriguingly, in NE chronic scenarios the results are not as transparent as the acute findings, nonetheless in the second experiment there are traces of a small downregulation of the chemokines receptors, a finding that the first experiment didn't replicate. Furthermore, by comparison of NE acute vs. NE chronic in the I experiment, the latter has less expression of both CCR6 and CCR7 than the former group.

Overall, these results indicate that sympathetic-derived signaling prevents the migration capability of cDC1 and thereafter the development of an immunological action. In acute stress, by upregulating both chemokine receptors responsible for the migration to the skin (CCR6) or LN (CCR7), it is suggestive of promoting DC tissue retention in their current location. In chronic scenarios, due to lower amounts of chemokine receptors, also lead to less migration of DCs since they are less able to recognize the specific chemokine ligands to induce their migration.

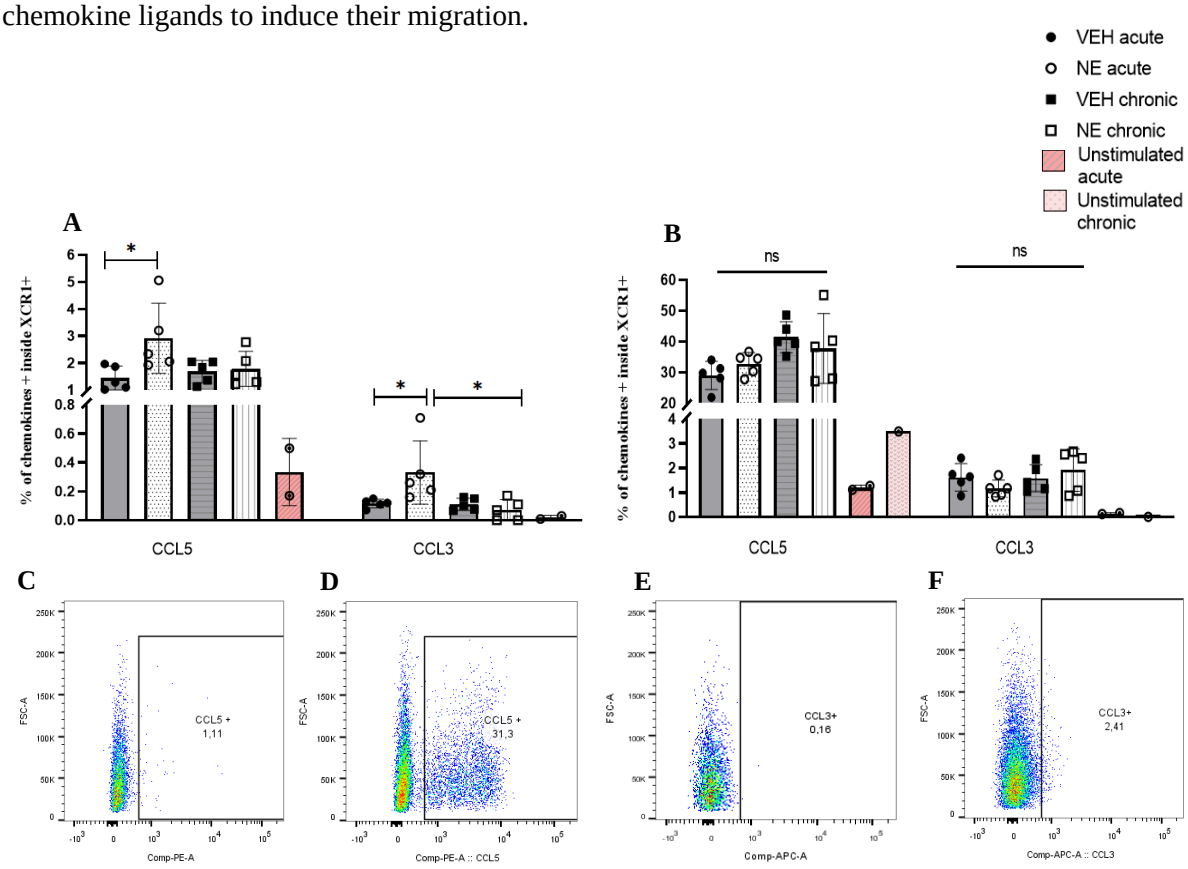

Figure 3.6. Chemokine values following acute vs. chronic NE treatment in I **(A)** and II **(B)** experiments. *C57BL/6J* mice were i.p injected with an acute dose (4 mg /kg mice /day) of NE for 3 consecutive days representing acute NE or with a chronic dose (2 mg /kg mice /day) administered in 2 consecutive days with a resting period of 1 day in a total of 15 days simulating chronic stress. As control there are *C57BL/6J* mice i.p treated with a vehicle solution containing 0.1% ascorbic acid and 0.9 % NaCl following the same described kinetics as the NE acute or chronic mice. After CD11c purification, the splenic DCs were then stimulated with a mix of CpG/Poly(I:C), apart from the unstimulated controls. Following *in vitro* stimulation, the cells were stained with CCL3 and CCL5 intracellular antibodies (Table 2.3), and their chemokine expression was assessed by flow cytometry. A total of 5 mice were utilized per condition in both experiments**. C–** Representative unstimulated values of $CCL5^+$. **D–** Representative stimulated value of $CCL5^+$. **E–** Representative unstimulated values of $CCL3^+$. **F–** Representative stimulated value of $CCL3^+$. The analysis was performed by using FlowJo™ Software for Windows Version 10.8.1. Ashland, OR: Becton, Dickinson and Company; 2023. These values were generated using ordinary one-way ANOVA with multiple comparisons using GraphPad Prism version 8.4.3 for Windows (GraphPad Software, San Diego, California USA). ns- non-significant results (p-value >0.05).

DCs are known to produce CCL3 and CCL5 chemokines[174]. Following acute stress, the cDC1 releases more CCL3 and CCL5 than non-stress groups, being the CCL5 produced with higher amounts (Figure 3.6A). Furthermore, as Figure 3.6B indicates, there is a tendency to produce more CCL5 after in acute stressful conditions, however, unlike the first experiment, this finding is not statistically significant. Conversely, there is a trend of CCL3 to decrease after acute NE dosage (Figure 3.6B). In the case of chronic stress, there are no clear differences in changes in the production of both chemokines, with CCL5 suffering a tiny decrease in experiment II and CCL3 showing reverse findings. However, in experiment I, NE chronic has less amounts of chemokines than NE acute.

Additionally, it is important to note that both experiments are valid as the stimulation protocol was successfully executed as visualized by the FlowJo plots in Figures 3.6C-E. Since stimulated cells, with the mix of CpG/Poly(I:C), produce more cytokines than the cells that were not stimulated with TLR agonists (salmon and pink color), although the differences are more defined in the second experiment than the first, due to higher amounts of chemokines released as visualized by the 3.6A and 3.6B plots.

All of these joint findings indicate that following acute but not chronic stress the cDC1 has a trend to promote production of mainly CCL5 but also CCL3 chemokines.

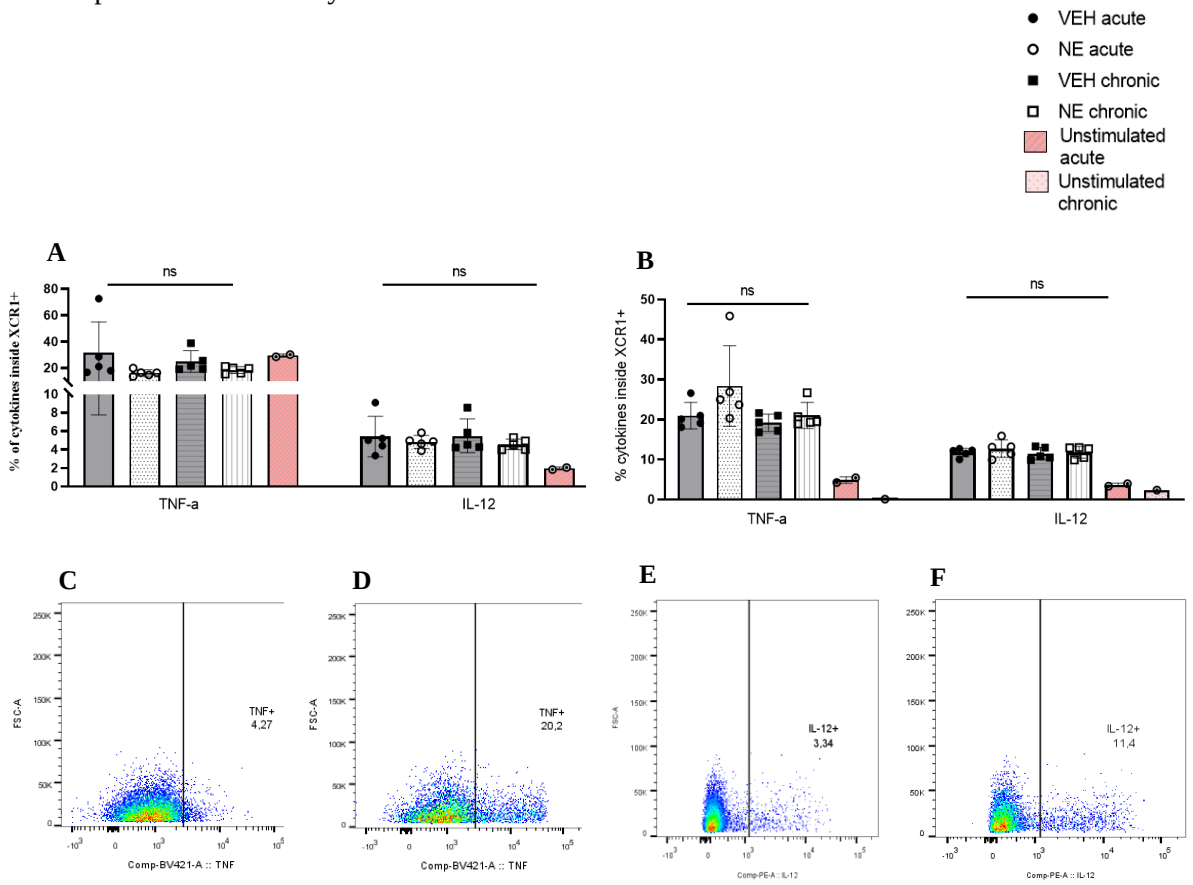

Figure 3.7. Cytokines values following acute vs. chronic NE treatment in I (**A**) and II (**B**) experiments. *C57BL/6J* mice were i.p injected with an acute dose (4 mg /kg mice /day) of NE for 3 consecutive days representing acute NE or with a chronic dose (2 mg /kg mice /day) administered in 2 consecutive days with a resting period of 1 day in a total of 15 days simulating chronic stress. As control there are *C57BL/6J* mice i.p treated with a vehicle solution containing 0.1% ascorbic acid and 0.9 % NaCl following the same described kinetics as the NE acute or chronic mice. After CD11c purification, the splenic DCs were stimulated with a mix of CpG/Poly(I:C), apart from the unstimulated controls. Following *in vitro* stimulation, the cells were stained with TNFα and IL-12 intracellular antibodies (Table 2.4), and their cytokine expression was assessed by flow cytometry. A total of 5 mice were utilized per condition in both experiments. **C** – Representative unstimulated values of $TNF\alpha^{+}$. **D**– Representative stimulated value of $TNF\alpha^{+}$. **E**– Representative unstimulated values of $IL\text{-}12^{+}$. **F**– Representative stimulated value of $IL\text{-}12^{+}$. The analysis was conducted by using FlowJo™ Software for Windows Version 10.8.1. Ashland, OR: Becton, Dickinson and Company; 2023. These values were calculated using ordinary one-way ANOVA with multiple comparisons using GraphPad Prism version 8.4.3 for Windows (GraphPad Software, San Diego, California USA). ns- non-significant results (p-value >0.05).

As indicated by Figure 3.7A there is a trend to have less production of TNFα in the acute NE group compared to acute vehicle groups although this finding is non-significant. However, the findings of the next experiment, Figure 3.7B, contradict this since acute NE stressed cells tend to produce more TNFα, although again this feature is non-significant. In chronically NE-stressed mice, the TNFα follows the same trend as the described NE acute findings, although the differences observed are less robust. Furthermore, in the I experiment the stimulation assay was not conducted properly since unstimulated cells produce similar amounts of TNFα as TLR-stimulated cDC1. However, in the II experiment, the stimulation protocol was successful as depicted by the graphs in Figure 3.7C-E. Resorting now to the Th1-polarizing cytokine, it seems that its production is unaffected by NE, since in both experiments and in both acute and chronic kinetics, the expression levels of IL-12 remain tightly constant.

All of the functionality results pooled, there are contradictory findings between experiments and values. Therefore, there is no clear indication of how adrenergic signaling is affecting the functional aspects of cDC1 phenotype. However, since NE was i.p administered, there is no guarantee that NE is reaching the cDC1s, this being the main limitation of this experiment. Henceforth, follow-up experiments with the $Xcr1^{Cre}Adr\beta2^{fl}$ genetic mouse model could provide more robust and precise results in how the sympathetic innervation is affecting cDC1 functionality. The findings of these experiments are displayed in the next chapter.

3.4 The loss of *Adrβ2* receptor promotes an immunologically active state of cDC1.

In line with the previous chapter, the impact of the loss of *adrβ2* in cDC1 functionality was investigated. The findings can be visualized in Figures 3.8-3.12

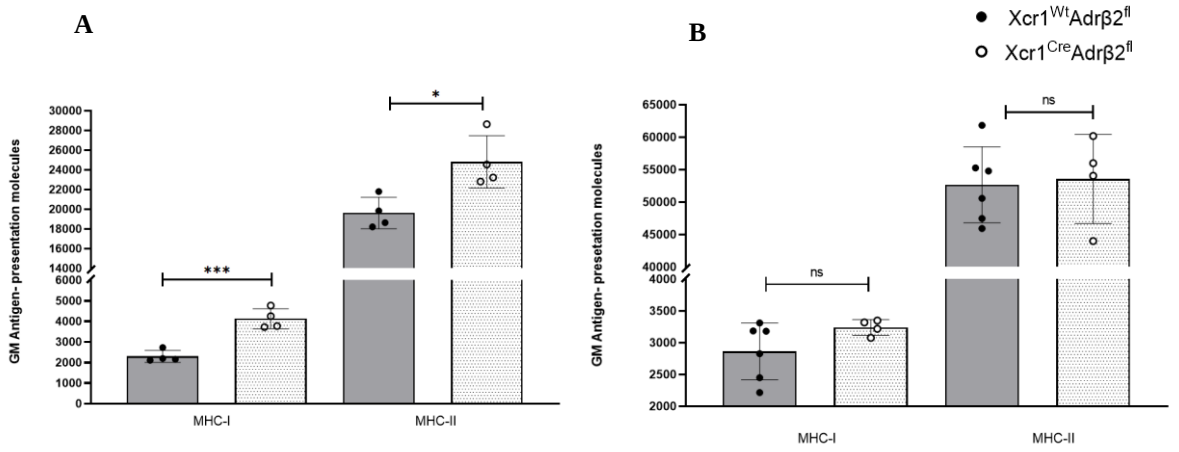

Figure 3.8. MHC presentation molecules values in *Xcr1*^{Wt}*Adrβ2*^{fl} or *Xcr1*^{Cre}*Adrβ2*^{fl} splenic cDC1 in I **(A)** and II **(B)** experiments. Steady-state splenic cDC from *Xcr1*^{Wt}*Adrβ2*^{fl} and *Xcr1*^{Cre}*Adrβ2*^{fl} were purified with CD11c Microbeads and stained with extracellular antibodies depicted in Table 2.1. In the first experiment, it was utilized 4 mice per group. In the second experiment, a total of 6 *Xcr1*^{Wt}*Adrβ2*^{fl} and 4 *Xcr1*^{Cre}*Adrβ2*^{fl} were used. The y-axis represents the Geometric mean. The analysis was performed by using FlowJo™ Software for Windows Version 10.8.1. Ashland, OR: Becton, Dickinson and Company; 2023. These values were obtained by unpaired t-test using GraphPad Prism version 8.4.3 for Windows (GraphPad Software, San Diego, California USA). ns- non-significant results (p-value >0.05).

As Figure 3.8 demonstrates, in steady-state *adrβ2*-depleted cDC1 there is a general tendency to upregulate both MHC-I and MHC-II antigen-presentation molecules in both conducted experiments (3.8A and 3.8B), being these findings are statistically significant in the first performed experiment. However, despite being non-significant in the second experiment, there is a clear predisposition to upregulate the MHC-I complex. Also, it is visible a small increase in MHC-II expression. These findings clearly corroborate that cDC1s lacking *adrβ2* receptor tend to become more immunologically active, likely being more able to prime naive T cells. Therefore *adrβ2*-signalling likely promotes an immunosuppressive cDC1 phenotype.

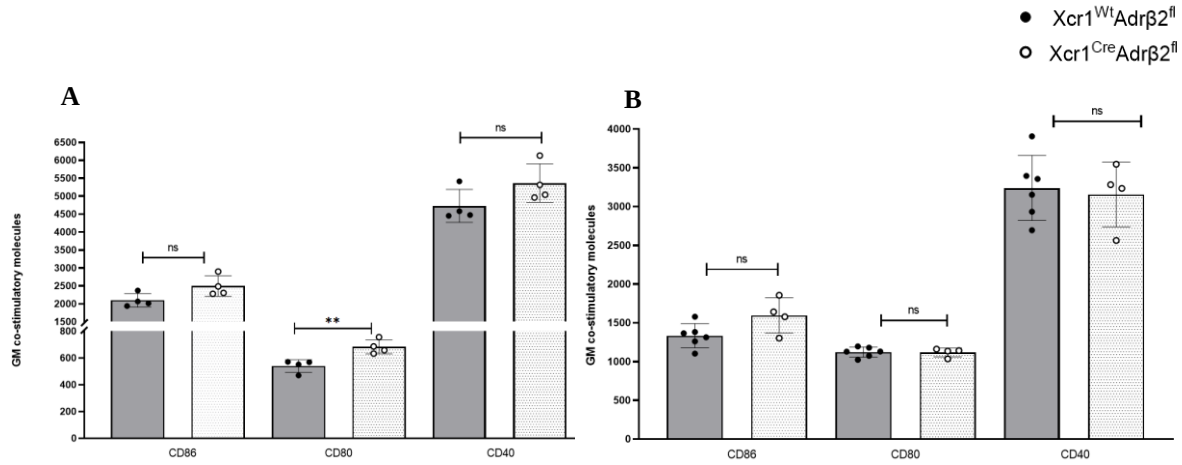

Figure 3.9 Co-stimulatory values in *Xcr1*^{Wt}*Adrβ2*^{fl} or *Xcr1*^{Cre}*Adrβ2*^{fl} splenic cDC1 in I (**A**) and II (**B**) experiments. Steady-state splenic cDC from *Xcr1*^{Wt}*Adrβ2*^{fl} and *Xcr1*^{Cre}*Adrβ2*^{fl} were purified with CD11c Microbeads and stained with extracellular antibodies depicted in Table 2.1. In the I experiment it was utilized 4 mice per group. In the second experiment, a total of 6 *Xcr1*^{Wt}*Adrβ2*^{fl} and 4 *Xcr1*^{Cre}*Adrβ2*^{fl} were used. The y-axis represents the Geometric mean. The analysis was performed by using FlowJo™ Software for Windows Version 10.8.1. Ashland,

OR: Becton, Dickinson and Company; 2023. These values were obtained by unpaired t-test using GraphPad Prism version 8.4.3 for Windows (GraphPad Software, San Diego, California USA). ns- non-significant results (p-value >0.05).

As visualized by Figure 3.9 there is a clear shift in upregulation of the expression levels of all co-stimulatory molecules in *Xcr1*^{Cre}*Adrβ2*^{fl} compared with *Xcr1*^{Wt}*Adrβ2*^{fl}. Although CD80 alterations in the first experiment (3.9A) are the only statistically significant outcome, both CD86 and CD40 also increased their expression in the surface of steady state *Xcr1*^{Cre}*Adrβ2*^{fl} cDC1. However, in the second experiment (3.9B) CD86 was the only visible co-stimulatory molecule that suffered an augmentation compared to *Xcr1*^{wt}*Adrβ2*^{fl} mice, since CD80 didn't change and CD40 experienced a slight decrease in the total expression. Nonetheless, the clear findings of the first experiment and CD86 of the second experiment, when joined with the shift in upregulation of MHC antigen-presentation outcomes, as discussed in the previous figure, further promotes the notion that the adrenergic signaling leads to an anergy state of cDC1 displaying reduced functionality.

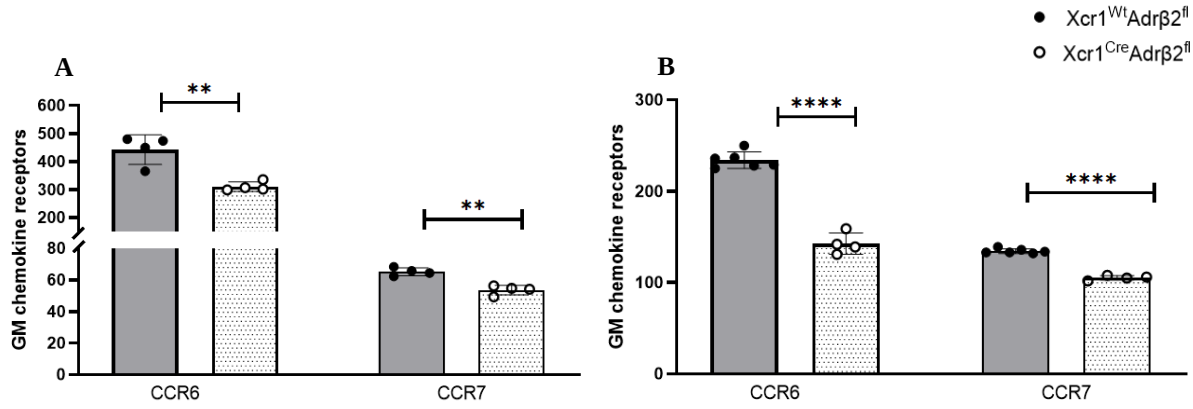

Figure 3.10. Chemokine receptors values in *Xcr1*^{Wt}*Adrβ2*^{fl} or *Xcr1*^{Cre}*Adrβ2*^{fl} splenic cDC1 in I **(A)** and II **(B)** experiments. Steady-state splenic cDC from *Xcr1*^{Wt}*Adrβ2*^{fl} and *Xcr1*^{Cre}*Adrβ2*^{fl} were purified with CD11c Microbeads and stained with extracellular antibodies depicted in Table 2.2. In the I experiment, it was utilized 4 mice per group. In the second experiment, a total of 6 *Xcr1*^{Wt}*Adrβ2*^{fl} and 4 *Xcr1*^{Cre}*Adrβ2*^{fl} were used. The y-axis represents the Geometric mean. The analysis was conducted by using FlowJo™ Software for Windows Version 10.8.1. Ashland, OR: Becton, Dickinson and Company; 2023. These values were obtained by unpaired t-test using GraphPad Prism version 8.4.3 for Windows (GraphPad Software, San Diego, California USA).

Focusing on the chemokine receptors responsible for the migration event of cDC, it was observed a clear reduction in both CCR6 and CCR7 in both experiments (3.10A and 3.10B) of *Xcr1*^{Cre}*Adrβ2*^{fl} mice. Furthermore, in both experiments the results obtained are statistically significant, further providing strong confirmation value of the findings observed. These pooled outcomes lead to the conclusion that the loss of *adrβ2* receptor-induced sympathetic signaling could influence the migratory capacity of cDC1, retaining this immune population in the original tissue they are encountered, preventing migration to either draining lymph node or to the skin. These results are compatible with the previous finding, as Figure 3.5 indicates that following NE, both chemokine receptors increased their expression. Hence, the migration event by cDC1 can be manipulated in an *adrβ2*-dependent fashion.

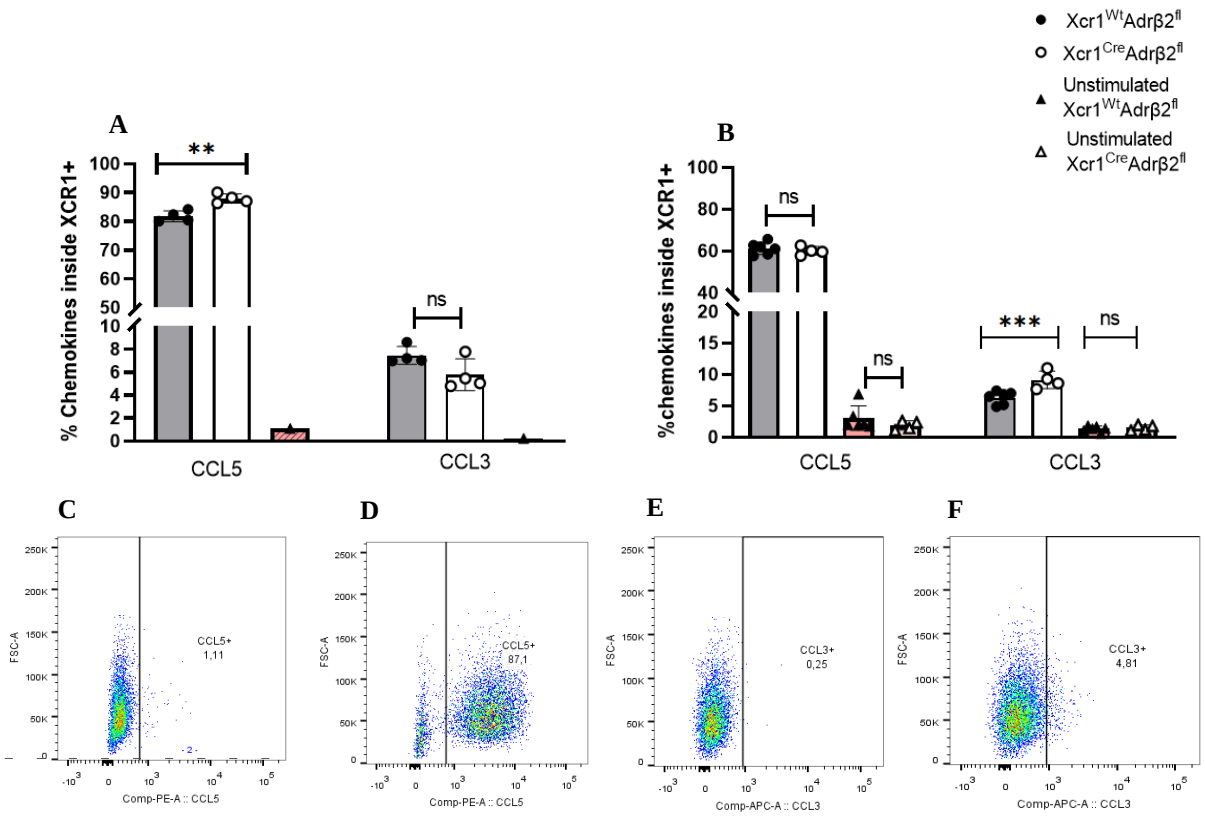

Figure 3.11. Chemokine values of *Xcr1*^{Wt}*Adrβ2*^{fl} or *Xcr1*^{Cre}*Adrβ2*^{fl} splenic cDC1in I **(A)** and II **(B)** experiments. After CD11c purification, the splenic DCs undergo *in vitro* stimulation with CpG/Poly(I:C), apart from the unstimulated controls. Following stimulation, the cells were stained with CCL3 and CCL5 intracellular antibodies (Table 2.3), and their chemokine expression was assessed by flow cytometry. In the I experiment, it was utilized 4 mice per group. In the second experiment, a total of 6 *Xcr1*^{Wt}*Adrβ2*^{fl} and 4 *Xcr1*^{Cre}*Adrβ2*^{fl} were used. **C–** Representative unstimulated values of CCL5^{+}. **D–** Representative stimulated value of CCL5^{+}. **E–** Representative unstimulated values of CCL3^{+}. **F–** Representative Stimulated value of CCL3^{+}. The analysis was performed by using FlowJo™ Software for Windows Version 10.8.1. Ashland, OR: Becton, Dickinson and Company; 2023 These values were obtained by unpaired t-test in the first experiment and an ordinary one-way ANOVA with multiple comparisons in the second experiment using GraphPad Prism version 8.4.3 for Windows (GraphPad Software, San Diego, California USA). ns- non-significant results (p-value >0.05).

Regarding the chemokines released by cDC1 after stimulation, in the first experiment, despite *Xcr1*^{Wt}*Adrβ2*^{fl} CCL5 values are already high, it further increased in *adrβ2*-depleted cDC1 as visualized by Figure 3.11A, being this alteration statistically significant. Contradictory to CCL5 results, the same excepted result was not observed with the CCL3 chemokine, since the amount of the production of this molecule slightly decreased in *Xcr1*^{Cre}*Adrβ2*^{fl} mice compared with *Xcr1*^{Wt}*Adrβ2*^{fl} in the same experiment, nonetheless this observed conversely is non-significant. However, as depicted in Figure 3.11B, in the second experiment the CCL3 production significantly increased in *adrβ2*-deficient cDC1, although the CCL5 readout in the same experiment didn't change between groups.

Additionally, as Figure 3.11B suggests, there were no observed differences in the production of both chemokines in steady-state conditions, by the *Xcr1*^{Wt}*Adrβ2*^{fl} or *Xcr1*^{Cre}*Adrβ2*^{fl} mice, indicating that the previous phenomenon only occurs after a stimulation event. Moreover, as visualized in Figure 3.11C-

E, the stimulation protocol was successfully executed, although CCL3 is poorly produced by cDC1 when compared with the CCL5 values, the latter produced in higher amounts.

The pool of the findings highlighted indicates that cDC1 that are insensitive to the *adrβ2* signaling cascade, after stimulation with TLR agonists, promotes a higher production of chemokines, since both CCL5 and CCL3 substantially increased, in the first and second experiment, respectively.

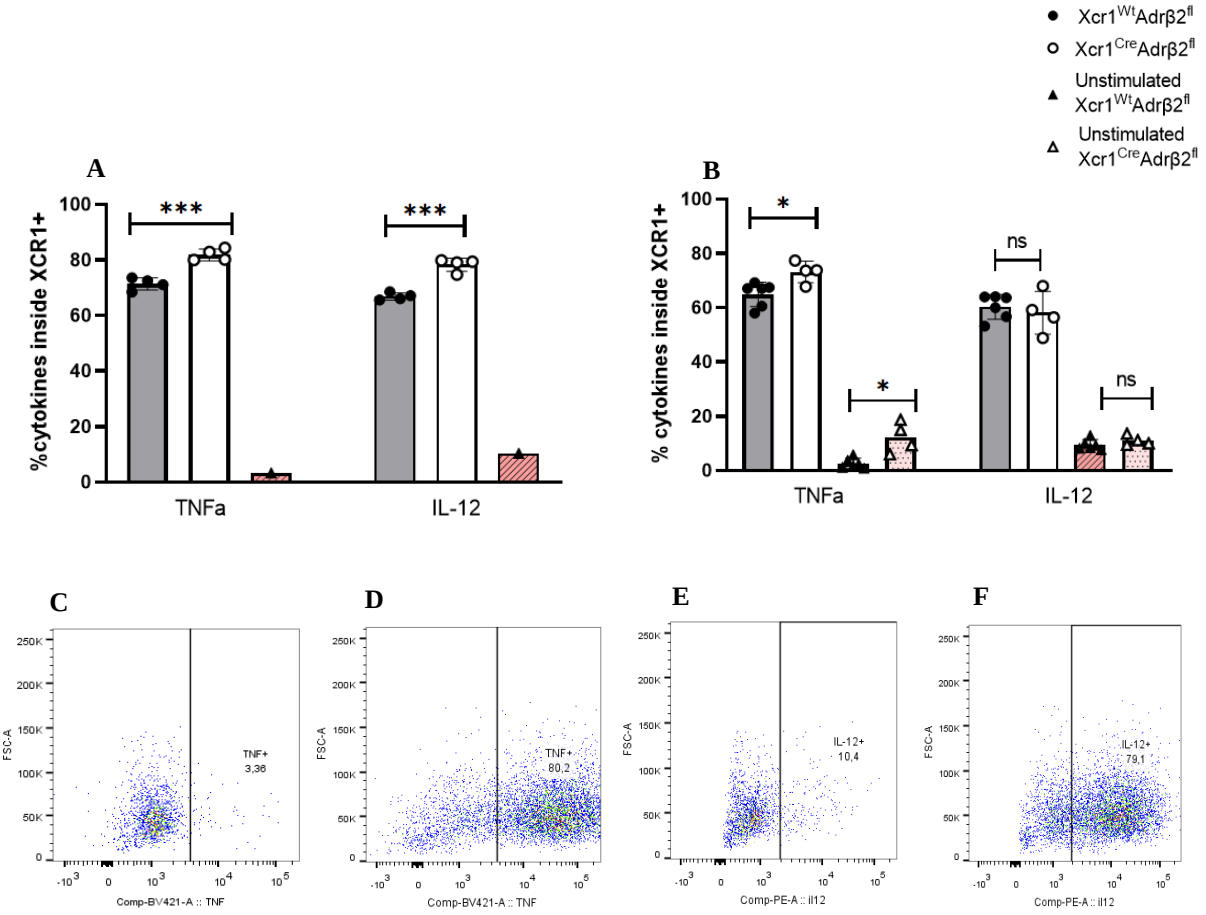

Figure 3.12. Cytokine values of *Xcr1*^{Wt}*Adrβ2*^{fl} or *Xcr1*^{Cre}*Adrβ2*^{fl} splenic cDC1in I **(A)** and II **(B)** experiments. After CD11c purification, the splenic DCs undergo *in vitro* stimulation with CpG/Poly(I:C), apart from the unstimulated controls. Following stimulation, the cells were stained with IL-12 and TNFα intracellular antibodies (Table 2.4), and their cytokine expression was assessed by flow cytometry. In the I experiment it was utilized 4 mice per group. In the second experiment, a total of 6 *Xcr1*^{Wt}*Adrβ2*^{fl} and 4 *Xcr1*^{Cre}*Adrβ2*^{fl} were used. **C–** Representative unstimulated values of TNFα^{+}. **D–** Representative stimulated value of TNFα^{+}. **E–** Representative unstimulated values of IL-12^{+}. **F–** Representative stimulated value of IL-12^{+}. The analysis was performed by using FlowJo™ Software for Windows Version 10.8.1. Ashland, OR: Becton, Dickinson and Company; 2023. These values were obtained by unpaired t-test using GraphPad Prism version 8.4.3 for Windows (GraphPad Software, San Diego, California USA). ns- non-significant results (p-value >0.05).

As Figure 3.12A represents, despite stimulated *Xcr1*^{Wt}*Adrβ2*^{fl} cDC1 produces high amounts of both TNFα and IL-12, *Xcr1*^{Cre}*Adrβ2*^{fl} cDC1 produces even higher levels of these cytokines, being the observed results statistically significant for both cytokines. Moreover, as Figure 3.12B demonstrates, in the repetition of the experiment, the same tendency was observed regarding the TNFα cytokine, further

promoting the robustness of the result. However, contrary to the previous experiment, the IL-12 production by *adrβ2*-floxed cDC1 did not increase.

Interestingly, as Figure 3.12B illustrates, $Xcr1^{Cre}Adr\beta2^{fl}$ cDC1 that were not submitted to a stimulation protocol produced more basal TNFα than $Xcr1^{Wt}Adr\beta2^{fl}$ cDC1 being these observed results statistically significant. However, the same phenomenon was not observed for the IL-12 cytokine, since steady-state *adrβ2*-cleaved cDC1 produces similar amounts of the Th1-polarizing cytokine than Wt cDC1, nonetheless, a very slight trend towards greater production can be observed. Additionally, as Figures 3.12C-F indicate, the stimulation event was successfully conducted, and both TNFα and IL-12 are produced in similar amounts.

All of these observations lead to the conclusion that NE-signaling via *adrβ2* receptor induces an anergic state of cDC1, evidenced by the higher production of cytokines by $Xcr1^{Cre}Adr\beta2^{fl}$ cDC1 in both stimulated and unstimulated conditions.

3.5 *Adrβ2* antagonists' effects on DC1 migration

The migration event is crucial for the development of the adaptive immunological response. Previous studies of the laboratory observed that intradermal administrations in the ear with NE induce less migration of the cDC1 to the ear-draining lymph node (unpublished) (Figure 7.4). In this experiment, 2 *Adrβ2* blockers (propranolol and ICI-118,551) were administered intradermally in the ear and after stimulating the cells with CpG/Poly(I:C), the ears were topically painted with a FITC fluorophore, prepared in an inflammatory stimulating solution of acetone and DBP. The DBP compound is an irritant molecule that promotes the migration of cDC. The effects of the 2 *Adrβ2* antagonists can be seen in Figure 3.13.

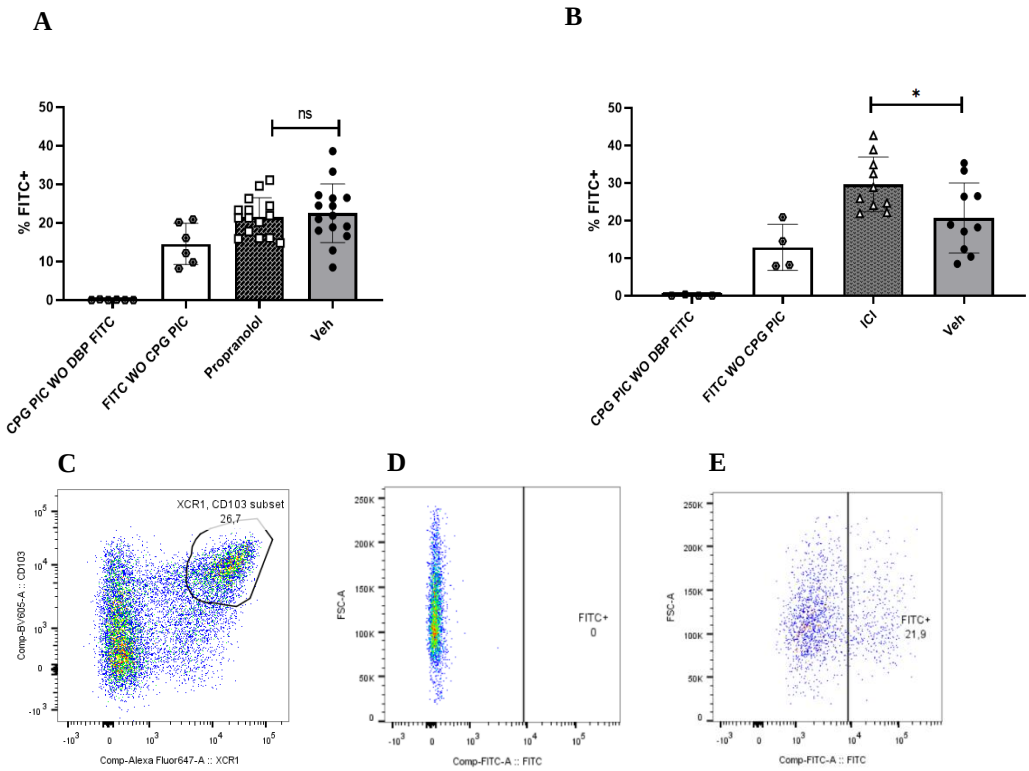

Figure 3.13. Migration capability of cDC1 following propranolol (**A**) or ICI-118,551 treatment (**B**). *C57BL/6J* mice were i.d injected for 3 consecutive days with propranolol or ICI-118,551 in the ear. As control, there are *C57BL/6J* mice treated with a vehicle solution containing 0.1% ascorbic acid and 0.9 % NaCl. Afterward, on the last day, the mice suffered i.d injections in the ear with a stimulation mix containing CpG/Poly(I:C). 2-3 hours after, the mice suffered skin sensitization with topical administration of 1% FITC prepared in an inflammatory stimulating solution of acetone and DBP. The removed LNs were then stained with extracellular antibodies (Table 2.5). The propranolol plots are a pool of 3 independent experiments with 15 *C57BL/6J* mice for both vehicle and propranolol groups. ICI-118,551 results derive from a pool of 2 independent experiments with 10 *C57BL/6J* mice for both vehicle and ICI groups. For every experiment, there were 2 control mice for both without FITC and without CpG/Poly(I:C) conditions. **C**- Representative plot displaying $XCR1^+$ $CD103^+$ double positive cells. **D**- Representative plot displaying negative $FITC^+$ positive cells. **E**- Representative plot in which it is possible to distinguish migratory cells derived from the ear ($FITC^+$). Abbreviations: PIC- Poly(I:C); WO- without; ns- non-significant results (p-value >0.05). The analysis was performed by using FlowJo™ Software for Windows Version 10.8.1. Ashland, OR: Becton, Dickinson and Company; 2023. These values were obtained by unpaired t-test using GraphPad Prism version 8.4.3 for Windows (GraphPad Software, San Diego, California USA).

Firstly, it is important to point out that both controls of the experiment are what was expected and validate the data generated, since mice that lack painting with the FITC fluorophore have 0% $FITC^+$ cells, and the mice in which the ear cDC1 were not stimulated with CpG/Poly(I:C) display reduced migration than all experimental mice (still have migration due to presence of the DBP irritant and FITC). As visualized by Figure 3.13A the migration capacity of cDC1 following mice treatment with propranolol did not change when compared with cDC1 from mice treated with the standard ascorbic acid solution. However, as Figure 3.13B suggests following application of ICI-118,551, cDC1 increased migration into the ear-draining LN when compared to vehicle-treated mice being this finding statistically significant. Hence, treatment with this *Adrβ2* antagonist promotes higher migration of these specialized

APCs. These findings correlate with previous depicted results, since i.d administration of NE leads to reduced migration of cDC1(unpublished) (Figure 7.4).

3.6 The NE mediated inhibition of cDC1 migration is *Adrβ2* signaling-dependent

In order to fully comprehend how the NE-mediated inhibition of migration of cDC1 is dependent on *Adrβ2* signaling, FITC painting experiments with the Xcr1^{Cre}*Adrβ2*^{fl} genetic mice model with or without NE were conducted. The alterations in migration can be assessed in Figure 3.14.

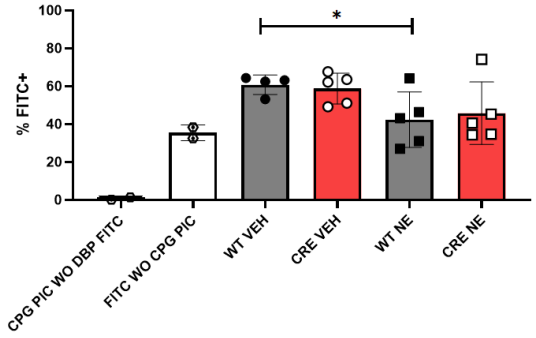

Figure 3.14. Migration capability of cDC1 from *Xcr1*^{Wt}*Adrβ2*^{fl} (Wt) or *Xcr1*^{Cre}*Adrβ2*^{fl} (CRE) following treatment with vehicle (VEH) or NE solutions. *Xcr1*^{Wt}*Adrβ2*^{fl} (Wt) or *Xcr1*^{Cre}*Adrβ2*^{fl} mice were i.d injected for 3 consecutive days with either vehicle solution containing 0.1% ascorbic acid and 0.9 % NaCl or NE in the ear. Posteriorly, on the last day the mice suffered i.d injections in the ear with a stimulation mix containing CpG/Poly(I:C). 2-3 hours after, the mice suffered skin sensitization with topical administration of 1% FITC prepared in an inflammatory stimulating solution of acetone and DBP. The removed LNs were then stained with extracellular antibodies (Table 2.5). The analysis was performed by using FlowJo™ Software for Windows Version 10.8.1. Ashland, OR: Becton, Dickinson and Company; 2023. These values were obtained by unpaired t-test using GraphPad Prism version 8.4.3 for Windows (GraphPad Software, San Diego, California USA).

As Figure 3.14 suggests, comparing migration values of cDC1 of Wt and CRE mice with vehicle solution there were no observed differences. However, following NE administration, it was observed NE mediated inhibition, being this finding statistically significant. This result is compatible with the already described previous results in which application of an *Adrβ2* antagonist the cDC1 migration increased. Interestingly, despite visualizing a small decrease in CRE mice treated with NE, this reduction when compared with the CRE vehicle group is statistically not significant. Therefore, it indicates that the observed reduced migration with the NE is dependent on the presence of *adrβ2* protein.

3.7 Chemical adrenergic deletion reduces chemokine content in the ear-draining LN

As previously addressed, 6-OHDA is a chemical adrenergic ablator widely used by researchers to promote selective degeneration of sympathetic innervation[171]. In this experiment, the chemokine content of the ears and the ears-draining LN were investigated following 6-OHDA intraperitoneal administration

and how this can contribute to differences in cDC migration. The findings of the chemokines responsible for the migration can be visualized in Figure 3.15.

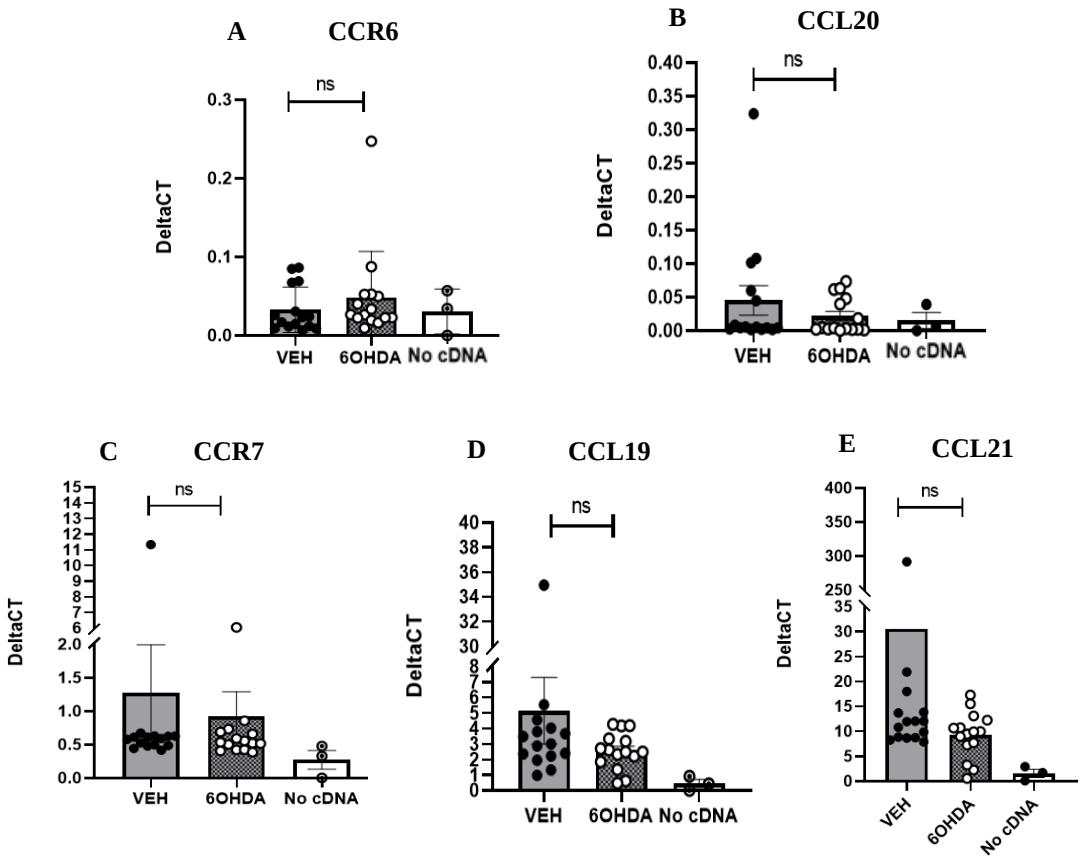

Figure 3. 15. Chemokine content in the ears (**A, B**) and LN (**C, D, E**) following i.p treatment with 6-OHDA. *C57BL/6J* mice were i.p injected with 100mg/kg of 6-OHDA for 5 consecutive days. The ears and LN were removed and their whole chemokine content was checked by qPCR. These findings are a pool of 3 independent experiments accounting for 15 mice in both groups. The selected probes for qPCR reaction are illustrated in Table 2.7B. *gadph* and *hprt* were the chosen housekeeping genes. These values were obtained by unpaired t-test using GraphPad Prism version 8.4.3 for Windows (GraphPad Software, San Diego, California USA. Abbreviations: ns-non-significant result (p-value>0.05). No cDNA values represent a control group, in which instead of cDNA plus RNAse-free, only RNAse-free were incubated with RT enzyme in the cDNA synthesis step.

As previously said, the cDC migration is dependent on the CCR7-CCL19/CC21 chemokine axis into the draining LN and CCR6-CCL20 chemokine axis into the skin. As Figure 3.15 A suggests, there is a tendency to increase the expression of CCR6 amount in the ears following treatment with 6-OHDA. However, CCL20 values decreased after such treatment despite the values being very low. On the other hand, in the LN, despite all results being non-statistically non-significant there is a tendency to downregulate all responsible chemokines (CCR7, CCL19, CCL21) required for the migration of cDC into the LN as visualized by the Figures 3.15 C, D and E respectively, following 6-OHDA administration.

These findings pooled hint that by chemically depleting the sympathetic innervation and therefore ablating NE release by adrenergic neurons, the cDC migration into the lymph node is affected since there are fewer chemokines guiding its migration. Furthermore, likely, since CCR6 values increased, it is also possible that cDCs retain in the ears and therefore won´t migrate into the LN.

Further experiments should be focused on i.d administration of 6-OHDA and check how the chemokine levels are really affected, instead of a systematic 6-OHDA injection. Additionally, these cells are at steady-state conditions, one possibility is to apply, after the 6-OHDA injections, CpG/Poly(I:C) and infer the chemokine content in the same organs. Finally, another possibility is to conduct FITC painting experiments with i.d administration of 6-OHDA. However, there are no papers indicating a dose for i.d administration of 6-OHDA.

3.8 6-OHDA i.d administration depletes adrenergic innervation

Since 6-OHDA is a widely used compound by researchers to deplete any sympathetic neurons, experiments with this compound are crucial to assess the importance of NE-signaling in the cDC1 functionality. As debated in the last section, one future experiment is to perform FITC painting with i.d injections utilizing this molecule, however, there are no papers establishing a dose for injections of 6-OHDA in the ear. Therefore, prior to performing the assay, it is needed to assess that the adrenergic innervation in the ears is indeed deleted. Hence, 6-OHDA i.d injections were performed on TH-CRE-dependent endogenous tdTomato and YFP fluorescence mice following the kinetics described in the materials and methods section. The results can be visualized in Figures 3.16 and 3.17.

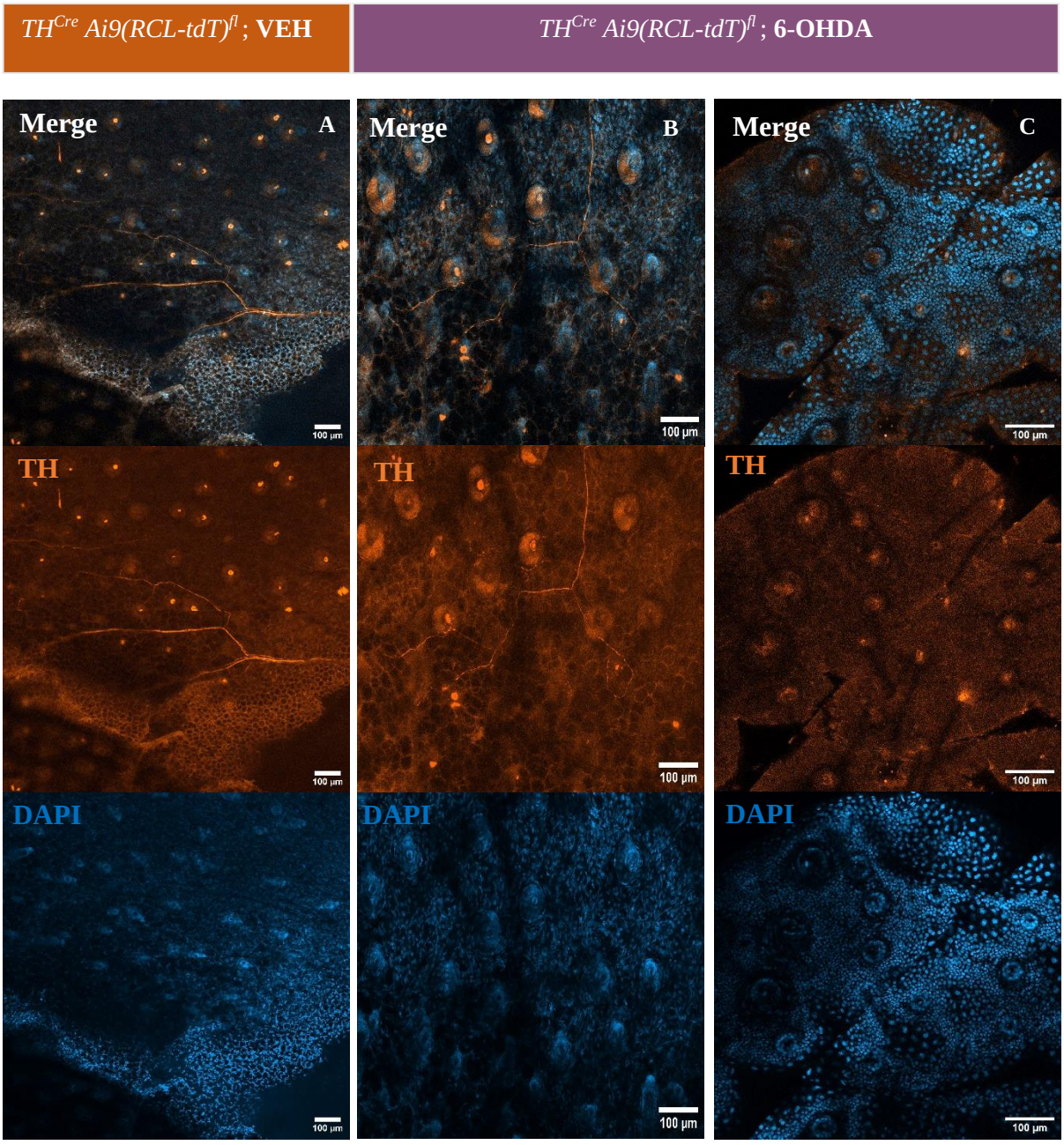

Figure 3.16. Whole mount ears acquisition following 2-day i.d injection in the ears with 25µL of 0.1% ascorbic acid and 0.9% NaCl (VEH) (**A**) or 6-OHDA at 12mg/mL (**B, C**) in *TH^{Cre} Ai9(RCL-tdT)^{fl}* genetic mice. Images generated by ZEISS LSM 980 inverted confocal microscopy with magnification 20x; scale bar, 100 µm. **A, B** and **C** are representative images. TH^{+} neurons express Cre-dependent Tdtomato endogenous fluorescence (red). The nuclei were stained with DAPI (blue).

As controls of the experiment and fluorescence signal, besides using *TH^{Cre} Ai9(RCL-tdT)^{fl}* reporter mice, *TH^{Wt}Ai9(RCL-tdT)^{fl}* were utilized and treated with both vehicle and 6-OHDA i.d injections. In these mice, as expected, the ears displayed no visible innervation of both groups of *TH^{Wt} Ai9(RCL-tdT)^{fl}*, as visualized by Figure 7.5.

As clearly depicted in Figure 3.16A, the ears of *TH^{Cre} Ai9(RCL-tdT)^{fl}* genetic mice that were i.d treated with vehicle solution exhibit neurons in a tdtomato endogenous fluorescence. Conversely, as Figure 3.16B illustrates, following i.d injections with 6-OHDA at 12mg/mL for 2 consecutive days, the

innervation is still present. However, as Figure 3.16C represents, there are some determined locations in the ears in which innervation is totally absent. Since i.d injections form a bubble in the site of injection, it is possible that in the local place of 6-OHDA administration restricts an area in which the adrenergic neurons are depleted, however in the whole ear remains areas in which the chemical ablator did not reach hence the sympathetic innervation in those areas is unaffected. Therefore, it was decided to advance in a follow-up experiment with double the dose of 6-OHDA (24mg/mL) and with two injections in two separate areas in the ear instead of a single injection to fully cover the ear. The results can be visualized in Figure 3.17.

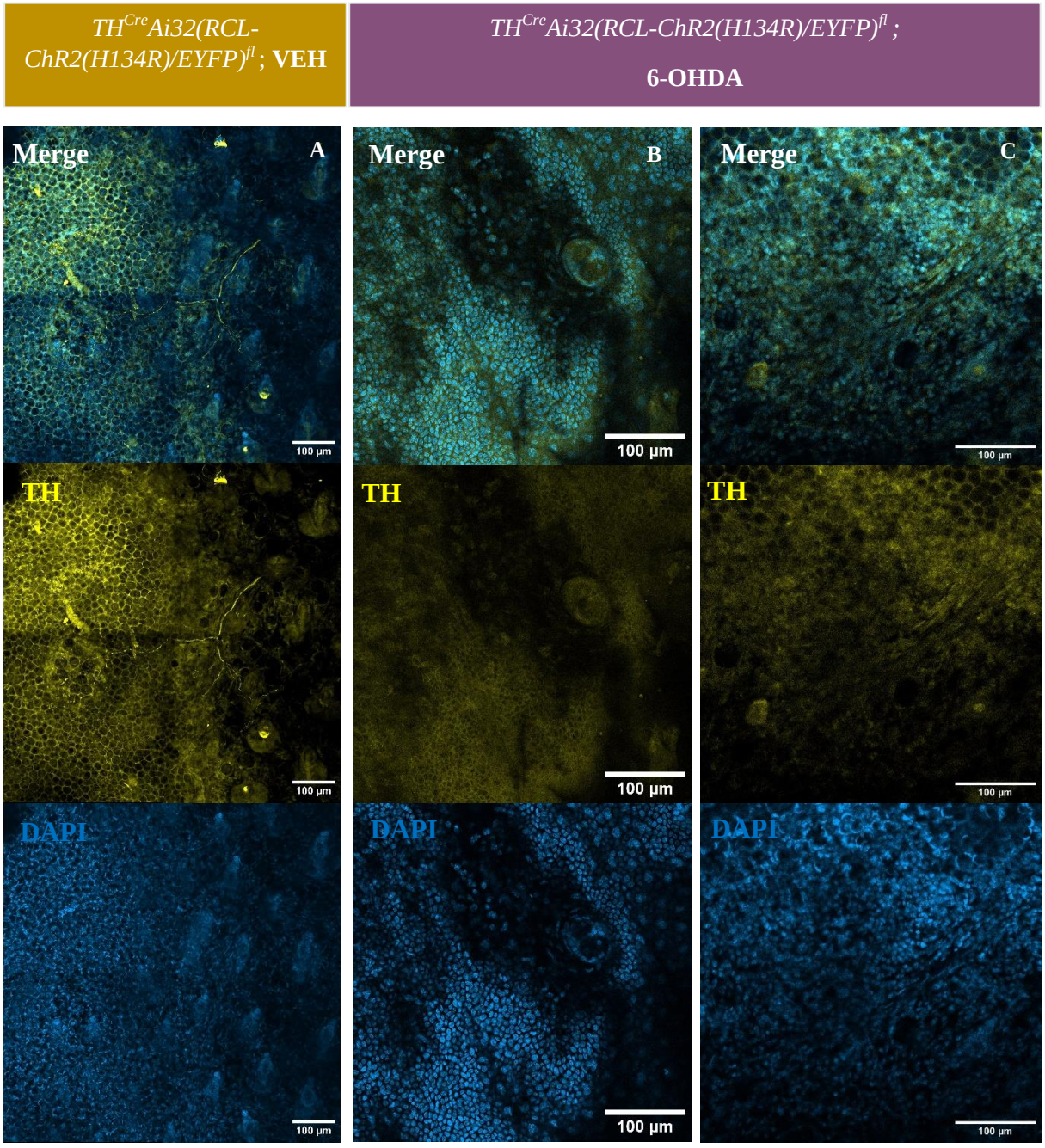

Figure 3.17. Whole mount ears acquisition following 2-day i.d injection in two separate regions of the ears with 25µL of 0.1% ascorbic acid and 0.9% NaCl (VEH) (**A**) or 6-OHDA at 24mg/mL (**B, C**) in *TH^{Cre}Ai32(RCL-ChR2(H134R)/EYFP)^{fl}* genetic mice. Images generated by ZEISS LSM 980 inverted confocal microscopy with magnification 20x; scale bar, 100 µm. **A, B,** and **C** are representative images. TH^{+} neurons express Cre-dependent YFP endogenous fluorescence (yellow). The nuclei were stained with DAPI (blue).

As visible by Figure 3.17A, the ears of *TH^{Cre}Ai32(RCL-ChR2(H134R)/EYFP)^{fl}* genetic mice that were i.d treated with vehicle solution exhibit TH^{+} neurons with yellow-fluorescence protein (YFP) intrinsic fluorescence. In addition, and contradictory to the findings of Figure 3.16, following i.d 6-OHDA treatment the adrenergic innervation of these mice is completely eliminated (Figure 3.17B and C). Since these animals were treated with two injections of 25µL in two separated regions of the ear with 24mg/mL (double the dose of the last experiment), these changes were sufficient to promote the killing of whole ear innervation. Therefore, for future experiments involving i.d injections of 6-OHDA, the assays should reproduce the same conditions of this experiment. Again, the endogenous fluorescence of control mice, *TH^{Wt}Ai32(RCL-ChR2(H134R)/EYFP)^{fl}* , treated with both VEH and 6-OHDA are represented by Figure 7.6.

3.9 6-OHDA effect's in cDC1 migration

As debated in the previous section, since the results observed indicated that following a 2-day i.d injection with 24mg/mL of 6-OHDA in two separate regions of the ear with 25µL each, this was sufficient to eliminate the sympathetic neurons, it was decided to conduct a FITC painting experiment with 6-OHDA following those kinetics to discuss how the migration of ear cDC1 is affected following absence of NE-releasing neurons. The results are illustrated in Figure 3.18.

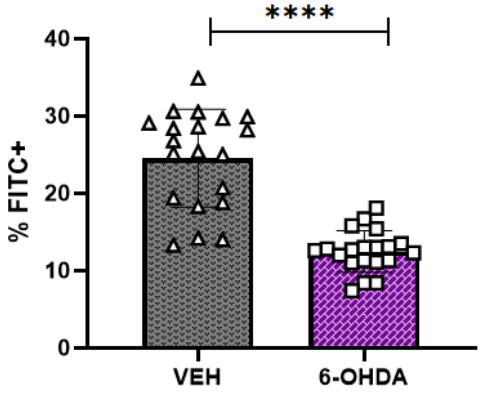

Figure 3.18. Migration capability of cDC1 following i.d 6-OHDA treatment. *C57BL/6J* mice were i.d injected for 2 consecutive days with 24mg/mL of 6-OHDA in 2 separate ear regions. As control there are *C57BL/6J* mice i.d treated with a vehicle solution containing 0.1% ascorbic acid and 0.9 % NaCl. Afterward, on the next day, the mice suffered i.d injections in the ear with a stimulation mix containing CpG/Poly(I:C). 2-3 hours after, the mice suffered skin sensitization with topical administration of 1% FITC prepared in an inflammatory stimulating solution of acetone and DBP. The removed LNs were then stained with extracellular antibodies (Table 2.5). For both 6-OHDA and VEH conditions a total of 20 mice were utilized. The analysis was performed by using FlowJo™ Software for Windows Version 10.8.1. Ashland, OR: Becton, Dickinson and Company; 2023. These values were obtained by unpaired t-test using GraphPad Prism version 8.4.3 for Windows (GraphPad Software, San Diego, California USA).

As observed in Figure 3.18 following i.d administration of 6-OHDA, a chemical ablator of sympathetic neurons, the migration of ear cDC1 decreased when compared with the vehicle-treated mice. This finding thus suggests that following elimination of adrenergic input the migration of cDC1 is severely downregulated.

3.10 Evidence of NICUs in several organs

As stated alongside the dissertation, NICUs are defined anatomical locations in which both different neurons and immune cells interact modulating each other's function. Through confocal microscopy, we can identify these regions in different lymphoid and non-lymphoid tissue through the use of a *XCR1*^{Cre} *Ai9(RCL-tdT)*^{fl} reporter mice that specifically marks cDC1 with tdTomato endogenous fluorescence, and a secondary anti-TH antibody targeting adrenergic innervation. Furthermore, mice were also i.p treated with either 0.1% ascorbic acid and 0.9% NaCl (VEH) or 6-OHDA solutions with the aim of assessing if the sympathetic innervation was depleted. The images can be visualized in Figure 3.19 and 7.7-7.8.

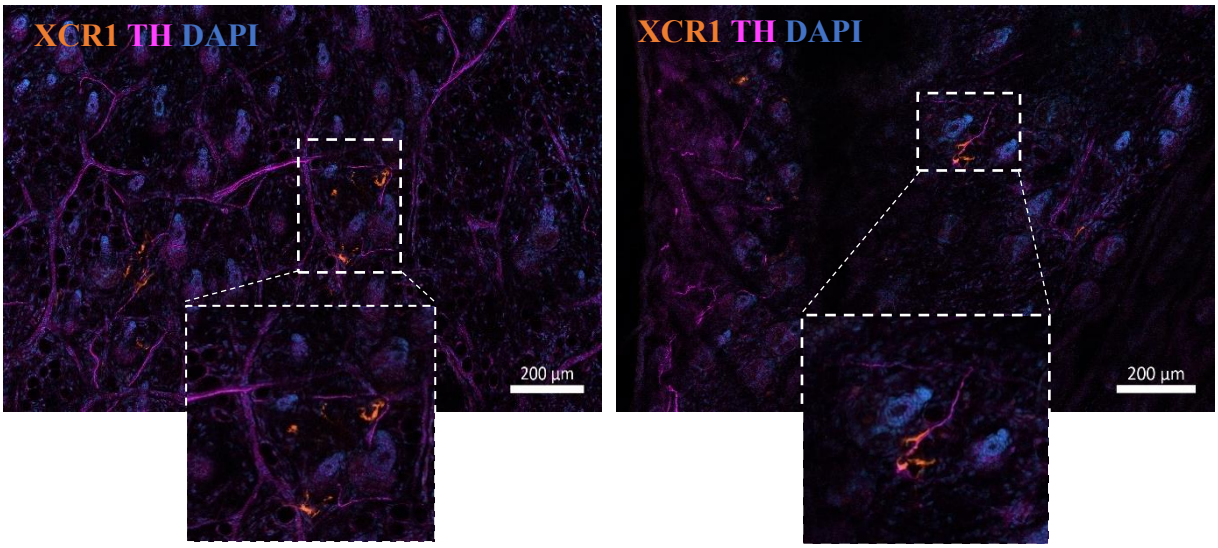

Figure 3.19. Confocal Microscopy acquisitions of whole mount ear of *XCR1^{Cre}Ai9(RCL-tdT)^{fl}* mice. cDC1s are labeled with tdTomato-endogenous fluorescence. Neurons are labeled with rabbit anti-mouse Tyrosine hydroxylase + anti-rabbit AF647 to identify sympathetic peripherical neurons. DAPI stains the nuclei of cells with blue fluorescence. Images generated by ZEISS LSM 980 inverted confocal microscopy with magnification 20x; scale bar, 200 μm.

With the representative images of Figure 3.19, with the whole mount ears, we can see the proximity between the cDC1 and the sympathetic neurons, further supporting that bidirectional interactions persist and both cell types can alter their functionality following this crosstalk. Furthermore, both the spleen and the mesenteric lymph node confocal acquisitions also suggest the same principle as represented by Figures 7.7A and 7.8A respectively. Moreover, following 6-OHDA i.p administration, the adrenergic innervation is totally absent, as visualized by Figures 7.7C, D and 7.8C, D validating the 6-OHDA conducted experiments depicted elsewhere. Furthermore, this also validates the stain of the TH antibody observed. As control of the experiment, *XCR1^{Wt}Ai9(RCL-tdT)^{fl}* VEH-treated displays no cDC1 endogenous fluorescence with visible sympathetic neurons (Figure 7.7B and 7.8B).

4. Discussion

A wide range of different neurons and immune populations have been shown to modulate each other cell function in a bidirectional fashion in defined anatomical locations reassembly NICUs. This highly complex crosstalk has been implicated in several key physiological and pathological processes thus fine-tuning the organism's health and disease. Therefore, modulating these mechanisms and unraveling novel molecular and cellular intervenients, could promote the development of new therapeutic approaches against vast immune and neurological disorders. Henceforth, following this process of thought, the main goal of this thesis is to uncover how the effects of sympathetic signaling affect the functionality of cDC1. Deciphering this communication can thus promote cDC1-based immunotherapies via manipulating adrenergic-derived signaling. However, advances in this research area are mainly derived from *in vitro* assays with non-specific targeting of cDC, thus does not represent the crosstalk between adrenergic neurons and cDC and how would this modulation affect the host physiology. Therefore, to fully deduct and comprehend how the sympathetic-derived cues affects the functionality aspect of cDC1, ranging from alterations of the expression of MHC-molecules, co-stimulatory markers, chemokines and, cytokines to migration experiments, this dissertation provides both *in vitro* and *in vivo* assays, with administration of NE and different *Adrβ2* agonist and antagonist. Furthermore, with the use of a specific genetic mice model targeting *Adrβ2* ablation in the surface of cDC1($Xcr1^{Cre}Adr\beta2^{fl}$), it is possible to infer how the absence of the receptor impacts the cDC1 functionality molecules.

However, due to some possible germline deletion problems of $Xcr1^{Cre}$, it was ordered a similar genetic construct mice ($Xcr1/ksho^{Cre}$) derived from Osaka University Suita, Japan, being later crossed with $Adr\beta2^{fl}$ mice. However, this genetic mouse mutant has severe germline deletion, since the *adrβ2* gene is floxed in the surface of the immune populations tested (B, T, MF, cDC1, and cDC2), a finding that in theory should only occur in cDC1, the only immune population expressing the XCR1. Hence these mice experience unspecified recombination. Furthermore, the expression of the adr*β1* gene has a tendency to be upregulated, compensating for the loss of the *adrβ2* gene. This finding confirms that the *adrβ2* receptor is absent in every immune cell thus these mice are not a proper specific model for targeting *adrβ2* depletion on cDC1, therefore it cannot be used for *in vivo* assays.

It was observed that upon administration of *Adrβ2* agonist, clenbuterol, the cDC1 has a tendency to produce less TNFα, however, it seems that is not *adrβ2*-dependent since $Xcr1/ksho^{Cre}Adr\beta2^{fl}$ mice treated with clenbuterol also reduced this cytokine production. Interestingly, the cDC1 that lacks *adrβ2* receptor produces slightly higher amounts of TNFα than Wt littermates in both treatment without or with clenbuterol. The former findings suggest that the solely the absence of *adrβ2* receptor leads to a more immunologically active cDC1 hence producing more TNFα than the cDC1-expressing *adrβ2* while the latter finding indicates that cDC1 lacking *adrβ2* receptor are less sensitive to clenbuterol inhibition.

Additionally, the clenbuterol inhibitory effects of TNFα production were only visible on cDC1 since cDC2 that were treated with clenbuterol displayed similar values to untreated cells. Nonetheless, the up-regulation of cDC1 without *adrβ2* receptor in eliciting higher amounts of TNFα was also replicated in cDC2 in both with or without clenbuterol scenarios, clearly indicating that cDC that lacks *adrβ2* receptor (as visualized by the RT-qPCR, both cDC1 and cDC2 lack *adrβ2*) tend to become more immunologically active. Therefore, this indicates that *adrβ2* signaling promotes an anergic cDC state. However, conversely to expected IL-12 production by cDC1 increased after *in vitro* clenbuterol administration.

The TNFα finding is compatible with the described literature, since as already previously stated NE sensing by DCs dampens down TNFα production[124], although here the same feature was not observed with IL-12 in this experiment as seen by previous papers already described in 1.6 section[124,154,159,161]. This could indicate that the IL-12 antibody used is worse than the TNFα antibody, in fact, it was used a titration of 1:50 in the former and 1:200 in the latter.

However, looking at the total percentage of TNFα and IL-12 production by the cells, this experiment was classified as sub-optimal due to the low amounts of cytokine release. Furthermore, and contributing to the low percentage numbers, the clenbuterol was supplied at a concentration of 0.5mg/mL, such amount for cDC could be toxic, hence the cytokine released by cDC is severely affected and cannot be robustly debated, thus the right pharmacokinetics of the compound should be investigated.

Overall, all the findings polled indicate that clenbuterol, an *Adrβ2* agonist, downregulates TNFα production by cDC1, hence triggering *Adrβ2* signaling could lead to decreased functional ability of cDC1.

To assess the effects of NE impact on cDC1 functionality, the mice were treated with two different kinetics and dosages of NE mimicking acute and chronic stress. We observed that MHC molecules tend to increase following acute NE and decrease after chronic scenarios. Nonetheless, as the co-stimulatory findings suggest, there is a very slight tendency that cDC1 are less able to prime naive T cells, being this compatible with antigen presentation experiments in which it is observed a tendency to have less IFN-y and proliferation of OT cells in previous data generated by María Martinéz-López and Raquel Silva (unpublished) (Figure 7.9). However, the results obtained upon this treatment were not robust enough between experiments replicates and we did not find a way to control that the delivered NE was acting as supposed. This could be due to the low half-life of NE (2.4 minutes[175]), therefore since this molecule is in systemic circulation for a such low period we cannot guarantee that it is reaching the DCs. Moreover, the splenic cDC also has a very low half-life (1.5-2.9 days[176]) being entirely replenished by novel cDC after their turnover. Since chronic NE treatment is 15 days long, we are losing some cDC that were treated in the earlier days with NE hence influencing the overall findings. One future idea is to repeat with the $Xcr1^{Cre}$ *Adrβ2* mouse model. With this approach, by supplying or not NE to both

Xcr1^{Cre} *Adrβ2* and *Xcr1*^{Wt}*Adrβ2* we can be sure that the observed downregulation of cDC functionality is *Adrβ2*-dependent.

Moreover, NE can bind to either α1, α2, and the 3β-adrenergic receptors, and since every receptor has its own associated g-couple protein with differences in cascade signaling, depicted in 1.3.2 chapter, thus resulting in different biological responses, the effects could not be derived entirely from specific activation of any type of adrenergic receptors, hence the findings observed could be a sum of all interactions. However, as previously addressed, *Adrβ2* is the main type of sympathetic receptor expressed in the surfaces of DCs. Henceforth, follow-up experiments with the *Xcr1*^{Cre}*Adrβ2*^{fl} genetic mouse model could provide more robust and precise results in how the sympathetic input is affecting cDC1 functionality via *adrβ2* receptor. Therefore, experiments utilizing mutant mice in steady-state were conducted, being these readouts much more clarifying and robust, as it was observed increased expression of MHC-molecules, co-stimulatory molecules, and higher production of cytokines and chemokines.

As said previously in the 1.6 section in the introduction chapter, IL-12 production is severely affected after NE administration in an *Adrβ2* signaling-dependent fashion as this paper stipulates[159]. Moreover, the same paper observed that inefficient antigen degradation was the reason for the reduced cross-presentation ability, as expression of the MHC-I and co-stimulatory molecules barely altered. However, we demonstrated that steady-state cDC1 lacking *Adrβ2* signaling has increased expression of such molecules and MHC-II, hence likely enhancing their ability to prime naïve CD8 and CD4 T cells. Therefore, providing more intel that cDC1 are more immunologically active following absence of sympathetic-neuron derived cues. Moreover, after stimulation, the production of CCL3 and CCL5 chemokines and TNFα and IL-12 further increased in splenic cDC1 from mice lacking the g-couple receptor. Interestingly, these cDC1s produce more TNFα in both steady-state scenarios and inflammation events, further proving that cDC1s respond negatively to NE signaling by *Adrβ2* triggering. Thereafter, if we pooled all functionality readouts of cDC1 observed in these two experiments, since *Xcr1*^{Cre}*Adrβ2*^{fl} cDC1 have higher expression amounts of both MHC complexes, co-stimulatory molecules, increased production of both chemokines and cytokines, it is possible to conclude that *Adrβ2* triggering promotes an immunosuppressive state of cDC1, which subsequently leads to a tolerogenic immunological response.

Intriguingly, the CCR7 and CCR6 chemokine receptors, responsible for the migration of cDC1 into LN and skin respectively both significantly reduced in both experiments. This loss was replicated in what was observed after administration of acute NE, in which both increased. Moreover, it is further compatible with previous experiments generated by María Martinéz-López and Raquel Silva in which after clenbuterol, an upregulation of the migration-responsible molecules was observed (unpublished) (Figure 7.10).

The increase of both chemokine receptors in acute stress scenarios is a debated topic. One possibility is that by upregulating both chemokines, the NE signal is blocking the cDC in the current location, thus resulting in decreased migration ability of cDCs. Hence, sympathetic signaling, by trapping the cDC, influences and dampens down the immunological response in a stressful event. However, the downregulation of both chemokine receptors observed also indicates reduced migration of cDC1 by having less amount of each receptor hence can no longer perceive the chemotactic gradient, crucial for the migration of cDC1. Hence, how the cDC1 responds to the NE-derived signaling and how it influences the migration into the LN is complex, therefore the rest of the dissertation is mainly focused on this issue.

Moreover, as previously said, how the migration can be influenced by different neuron-derived cues seems to be very ambiguous, since for instance, the neuropeptides derived from nociceptors, CGRP and VIP mainly reduce the migration of DC in the lung and intestine respectively, while SP promotes migration from the skin into the LN promoting Th2 immunity[134,145]. Additionally, to add more complexity, the sensory input that DCs receive are not restrictively immunosuppressive or immunostimulatory and experiences a duality of different functions that can either induce an inflammatory or anergy scenario. For example, and as previously depicted, VIP in the intestines mainly induces an anti-inflammatory phenotype in matured DCs but inflammatory in immature DCs[137]. Moreover, CGRP-treated DCs can reduce or promote airway inflammation by electing Tregs and Th2 responses[123], and in the skin it can activate DCs, promoting Th17 responses[144]. Moreover, their impact on DC phenotype could be receptor-dependent, in which the different nociceptor-derived neuropeptides can bind to different subtypes of the same receptor on the surface of DCs, possibly influencing the subsequent outcome, either being stimulatory or inhibitory.

Importantly to note is that in an inflammatory or even steady-state scenario, the DCs can receive several inputs, either sensory neuron-derived, cholinergic, or adrenergic cues, and also chemokines from other immune cells and epithelial cells, which all together severely influence the outcome of the DC migratory pool, and if the merge of signals indicate that they should be retained in the tissue or migrate into secondary lymphoid organs, to either promote tissue immunity or tolerance. Furthermore, the same inputs that DCs receive can be perceived by other third-party immune cells that trigger several unknown mediators that can influence the phenotypic characteristics of DCs. The full range of how DCs can perceive such signals is still far from complete understanding.

Resorting in the FITC painting *in vivo* migration experiments with *Adrβ2* antagonists, it was observed that propranolol administration did not influence the migration outcome of cDC1 in the pooled of the 3 experiments realized, however, it was observed an increase in the migration capacity of cDC1 following ICI-118,551 injections. Propranolol, despite being an *Adrβ2* antagonist, also has affinity to bind *Adrβ1*, being a non-selective beta receptor antagonist[177]. Therefore, it is less specific than ICI-118,551, hence

could indicate that the no differences in the migration observed are not strictly correlated with the blocking of *Adrβ2*. Furthermore, it is known that propranolol also promotes IL-8 mediated neutrophil chemotaxis recruitment in the skin while reducing their inflammatory phenotype[178], hence, this immune population can influence the findings by promoting a more immunosuppressive surrounding environment.

Nonetheless, following ICI-118,551, a highly-specific *Adrβ2* antagonist[179,180], it was observed increased migration of cDC1, being this effect solely by blocking the adrenergic receptor. Furthermore, this data is reproductive of other papers already listed, in which the propranolol displayed no differences in migration compared to control[158] while ICI-118,551 induces higher migration into the LN[163]. However, these authors are resorting to the migration of $CD11c^{+}$ Langerhans cells, and not specifically targeting cDC. Furthermore, ICI-118,551 result matches previous experiments conducted by María Martínez-López and Raquel Silva in which they observed that local administration of NE severely reduces migration of ear cDC1 into ear-draining LN (unpublished) (Figure 7.4). Therefore, all these findings merged it can be concluded that *Adrβ2* signaling reduces the migration ability of cDC1. As previously addressed, there are papers suggesting that *Adrα1* triggering leads to increased migration of DC[102,124,153,158]. However, we showed that *Adrβ2* activation displays a role in suppressing specifically cDC1 migration. Additionally, this migration is also dependent on *Adrβ2* signaling since when applying NE to $Xcr1^{Cre}Adr\beta2^{fl}$ mice, the downregulation of migration of cDC1 of these mice is not significant, contrary to the findings of $Xcr1^{Wt}Adr\beta2^{fl}$ mice when subjected to NE. Therefore, the findings of all these FITC painting experiments clearly represent that the cDC1 migratory capacity is significantly reduced following *Adrβ2* activation. This reduction in migration capability also correlates with the previous findings indicating that cDC1s become more immunosuppressed after sensing and perceiving sympathetic-derived molecules, therefore the initiation of an adaptive immunological response is compromised.

To further inquire how the migration is affected, all chemokines responsible for the migration from the ear to the ear-draining LN suffered downregulation in total LN tissue following 6-OHDA treatment. Moreover, the CCR6 content in the total ears increased, further supporting the notion that the migration to the LN is suppressed or that the cDC1s are retained in the skin. These findings are contradictory to the expected, since previously depicted experiments displayed that NE signaling suppressed ear cDC1 migration and treatment with a highly specific *Adrβ2* antagonist it was observed an increase in cDC1 migration. Nonetheless, despite being opposite to the excepted outcome, it is compatible with previous María Martínez-López and Raquel Silva FITC painting with i.p 6-OHDA data, in which they observe a tendency of less migration of cDC1 following treatment with 6-OHDA (unpublished) (Figure 7.11).

Further experiments should be focused on i.d administration of 6-OHDA and to conduct FITC painting experiments. The first experiment with $TH^{Cre}Ai9(RCL\text{-}tdT)^{fl}$ reporter mice, following i.d 6-OHDA

administered indicated that in some regions of the ear the innervation persists, and in other spots the sympathetic innervation was depleted. Therefore, it was conducted a follow-up experiment in which *TH^{Cre}Ai32(RCL-ChR2(H134R)/EYFP)^{fl}* were i.d injected in two different ear regions with double the dose. We observed by confocal microscopy total denervation of sympathetic neurons. Therefore, with this kinetics we can move forward for a future FITC painting assay with i.d 6-OHDA to provide more precise information on how the migration of cDC1 is affected following absence of NE-derived signaling.

After discovering the right kinetics to perform a FITC painting assay with i.d 6-OHDA, we conducted this experiment, and it was observed reduced migration of cDC1 following administration of the adrenergic chemical ablator. This finding is not consistent with the previous described results, since blocking the *Adrβ2* receptor with a highly specific antagonist and triggering this receptor with NE led to improved and reduced migration, respectively (Figure 3.13 and 7.4). Since 6-OHDA is a potent chemical ablator, it cannot be ruled out other unspecific effects in the surrounding environment, likely influencing other unknown mediators, moreover the observed finding can also be derived from the high toxicity of this compound. However, despite contradictory data, it is compatible with previous finding of FITC painting with i.p 6-OHDA, in which María Martínez-López and Raquel Silva also discover a tendency of reduced migration of cDC (unpublished) (Figure 7.11). Furthermore, since the i.d treatment is localized and not systematic, like i.p, these results are more specific and hence, translates into more robust findings. Moreover, it also correlates with the reduced expression levels of chemokines in the LN following 6-OHDA administration (Figure 3.15), thereafter since there is less amount of the chemokines responsible the cDC1 migration is reduced, further indicating that upon 6-OHDA, the migratory capacity of cDC1 is affected.

5. Conclusion and future experiments

DCs are potent APCs, being key players in the initiation of an immunological response against a specific antigen. These cells are highly versatile and dynamic, displaying different specialized receptors that can perceive and integrate all types of surrounding environmental cues, ranging from pathogenic agents and commensal microorganisms to neuron-derived signals.

Every human being at one point in their life experiences stress, being modulated by SyNS in a "fight or flight" response. This process alters major physiological components in the organism's whole body, including the immune system. Evidence of how cDC functionality is altered following recognition of NE and its impact on host immunity is still completely misunderstood.

Thereafter, to answer the thesis hypothesis, all the findings observed pooled point out that sympathetic neuron-derived signals promote an immunodeficient state of cDC1. This is corroborated by the downregulation of the expression of all functionality molecules that assess the cDC1 functionality, like decreased expression of MHC-antigen presentation complexes, reduced expression of the co-stimulatory molecules needed to prime naïve T cells, and less amounts of soluble molecules released by cDC1, including chemokines and cytokines observed (Figure 5.1A). Furthermore, the migration studies performed indicate that cDC1 migrates less after triggering of *Adrβ2* specific signaling, visible by increase migration with *Adrβ2* antagonist (ICI-118,551) and less with the *Adrβ2* natural ligand (NE), although 6-OHDA also decreased (Figure 5.1B). Therefore, cDC1s after sensing adrenergic-derived cues lead to a change in phenotype into a more immunosuppressive cell. This further implies in reduced ability to prime naïve T-cells, hence dampening down any consecutive adaptive immunological responses.

Altogether these new findings are going to help to develop novel cDC-based immunotherapies to either enhance an immunological response for instance against cancer, or help an immunocompromised individual, by interrupting *Adrβ2* signaling on cDC1. Additionally, it also has high potential for targeting autoimmunological disorders, by providing activation of *Adrβ2* on cDC1, to prevent excess inflammation and prevent a subsequential adaptive immune response. Notwithstanding, further experiments should be conducted to further clarify all these findings at the cellular and molecular level. Additionally, studies should also be performed on cDC1 derived from human cells, considering all these results are mice-derived. Furthermore, these mice are in perfect health, being constantly monitored with perfect environmental surroundings in sterile conditions, which couldn't be further from reality in the outside world. Therefore, standardized studies on human cDC1 should be conducted to infer if the same outputs on cDC1 phenotype are observed before loading this ideology into new rounds of clinical trials. Following this, a very promising experiment conducted by the research group already demonstrated that blood-derived human cDC1 after clenbuterol, leads to reduced expression of CD80 and CD40 co-

stimulatory molecules and reduced production of cytokines. Therefore, more promising results regarding human cDC1 after activation/inhibition of *Adrβ2* should be experimented.

To conclude, sympathetic neuron-derived signals trend to target cDC1 affecting their functionality making them more immunosuppressive. In-depth studies should be performed to deeper understand the molecular and cellular basis of this interaction, however, it shouldn't be overlooked the immense potential of these findings into improving both science and human health.

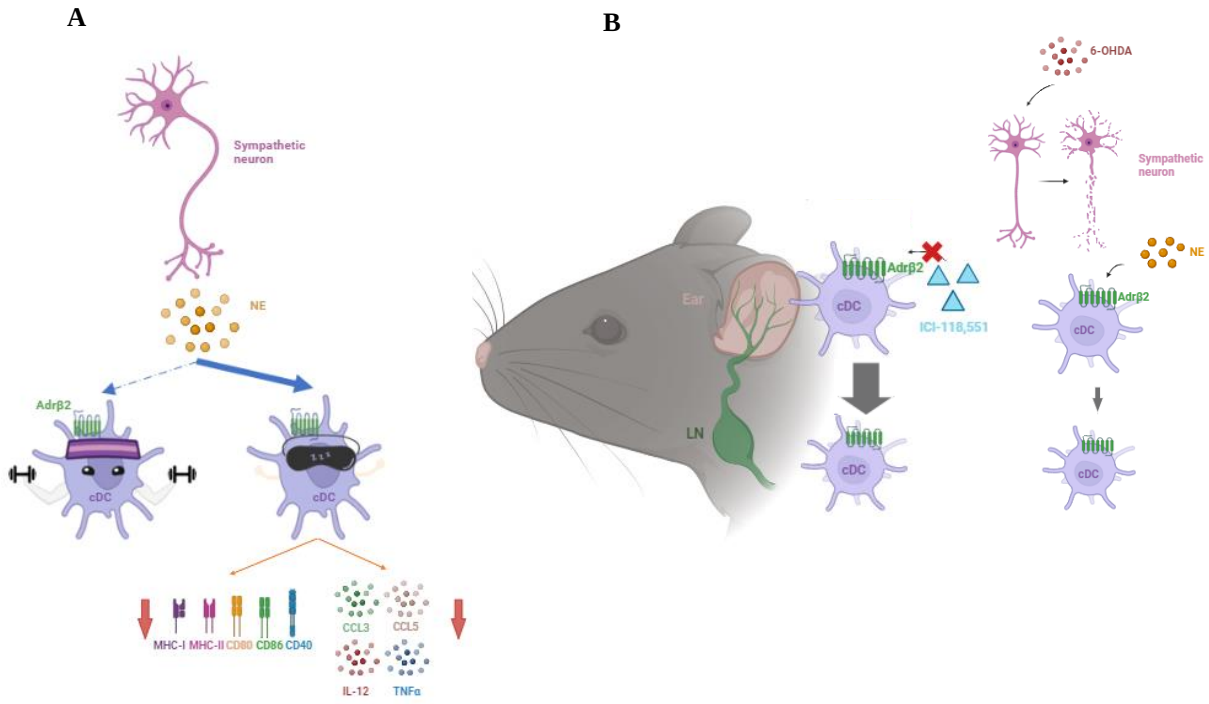

Figure 5.1. The cDC1 functionality following sympathetic-derived signaling cues. (**A**)- The cDCs after sensing the NE released by sympathetic neurons suffer a phenotypical shift into an immunosuppressive cDC, characterized by downregulation of MHC and co-stimulatory molecules expression as well as reduced chemokine and cytokine production. (**B**)- Changes in cDC migration. Following ICI-118,551, an *Adrβ2* antagonist, the ear cDC1s migrate more to the LN, however following NE the migration of cDC is downregulated. It was also observed less cDC1 migration upon or 6-OHDA, a chemical ablator of sympathetic neurons. All images were created by using Biorender.

6. References

1. Chaplin, D. D. Overview of the immune response. *J. Allergy Clin. Immunol.* **125**, S3–S23 (2010).
2. Alberts B, Johnson A, Lewis J, et al. *Innate Immunity - Molecular Biology of the Cell - NCBI Bookshelf*. (New York: Garland Science, 2002).
3. Kumar, H., Kawai, T. & Akira, S. Pathogen recognition by the innate immune system. *Int. Rev. Immunol.* **30**, 16–34 (2011).
4. Marshall, J. S., Warrington, R., Watson, W. & Kim, H. L. An introduction to immunology and immunopathology. *Allergy, Asthma Clin. Immunol.* **14**, 1–10 (2018).
5. Alberts B, Johnson A, Lewis J, et al. The Adaptive Immune System - Molecular Biology of the Cell - NCBI Bookshelf. in (New York: Garland Science, 2002).
6. Worbs, T., Hammerschmidt, S. I. & Förster, R. Dendritic cell migration in health and disease. *Nat. Rev. Immunol.* **17**, 30–48 (2017).
7. Balan, S., Saxena, M. & Bhardwaj, N. Dendritic cell subsets and locations. *Int. Rev. Cell Mol. Biol.* **348**, 1–68 (2019).
8. Cabeza-Cabrerizo, M., Cardoso, A., Minutti, C. M., Pereira Da Costa, M. & Reis E Sousa, C. Dendritic Cells Revisited. *Annu. Rev. Immunol.* **39**, 131–166 (2021).
9. Ardavín, C. *et al.* Origin and differentiation of dendritic cells. *Trends Immunol.* **22**, 691–700 (2001).
10. Merad, M., Sathe, P., Helft, J., Miller, J. & Mortha, A. The Dendritic Cell Lineage: Ontogeny and Function of Dendritic Cells and Their Subsets in the Steady State and the Inflamed Setting. *Annu. Rev. Immunol.* **31**, 563–604 (2013).
11. Ye, Y., Gaugler, B., Mohty, M. & Malard, F. Plasmacytoid dendritic cell biology and its role in immune-mediated diseases. *Clin. Transl. Immunol.* **9**, (2020).
12. Ardavín, C. *et al.* Origin and differentiation of dendritic cells. *Trends Immunol.* **22**, 691–700 (2001).
13. Zhou, H. & Wu, L. The development and function of dendritic cell populations and their regulation by miRNAs. doi:10.1007/s13238-017-0398-2.
14. Sichien, D., Lambrecht, B. N., Guilliams, M. & Scott, C. L. Development of conventional dendritic cells: From common bone marrow progenitors to multiple subsets in peripheral tissues. *Mucosal Immunol.* **10**, 831–844 (2017).
15. Puhr, S., Lee, J., Zvezdova, E., Zhou, Y. J. & Liu, K. Dendritic cell development-History, advances, and open questions. *Seminars in Immunology* vol. 27 388–396 at https://doi.org/10.1016/j.smim.2016.03.012 (2015).
16. Miller, J. C. *et al.* Deciphering the transcriptional network of the dendritic cell lineage. *Nat. Immunol.* **13**, 888–899 (2012).
17. Macri, C., Pang, E. S., Patton, T. & O'Keeffe, M. Dendritic cell subsets. *Semin. Cell Dev. Biol.* **84**, 11–21 (2018).
18. Marzaioli, V. *et al.* Monocyte-Derived Dendritic Cell Differentiation in Inflammatory Arthritis Is Regulated by the JAK/STAT Axis via NADPH Oxidase Regulation. *Front. Immunol.* **11**, 1406 (2020).
19. Thomas, R. & Lipsky, E. Dendritic Cells : Origin and Differentiation. *Stem Cells* 196–206 (1996).
20. Santiago-Schwarz, F., Belilos, E., Diamond, B. & Carsons, S. E. TNF in combination with GM-CSF enhances the differentiation of neonatal cord blood stem cells into dendritic cells and macrophages. *J. Leukoc. Biol.* **52**, 274–281 (1992).
21. Schlitzer, A. *et al.* Identification of cDC1- and cDC2-committed DC progenitors reveals early lineage priming at the common DC progenitor stage in the bone marrow. *Nat. Immunol.* **16**, 718–728 (2015).
22. Satpathy, A. T. *et al.* Zbtb46 expression distinguishes classical dendritic cells and their committed

progenitors from other immune lineages. *J. Exp. Med.* **209**, 1135–1152 (2012).

23. Wu, J., Wu, H., An, J., Ballantyne, C. M. & Cyster, J. G. Critical role of integrin CD11c in splenic dendritic cell capture of missing-self CD47 cells to induce adaptive immunity. *Proc. Natl. Acad. Sci. U. S. A.* **115**, 6786–6791 (2018).

24. Cueto, F. J., del Fresno, C. & Sancho, D. DNGR-1, a Dendritic Cell-Specific Sensor of Tissue Damage That Dually Modulates Immunity and Inflammation. *Front. Immunol.* **10**, 3146 (2020).

25. Gurka, S., Hartung, E., Becker, M. & Kroczek, R. A. Mouse conventional dendritic cells can be universally classified based on the mutually exclusive expression of XCR1 and SIRPα. *Front. Immunol.* **6**, (2015).

26. Banchereau, J. & Steinman, R. M. Dendritic cells and the control of immunity. *Nature* vol. 392 245–252 at https://doi.org/10.1038/32588 (1998).

27. Lewis, K. L. & Reizis, B. Dendritic Cells: Arbiters of Immunity and Immunological Tolerance. doi:10.1101/cshperspect.a007401.

28. Dalod, M., Chelbi, R., Malissen, B. & Lawrence, T. Dendritic cell maturation: functional specialization through signaling specificity and transcriptional programming. *EMBO J.* **33**, 1104 (2014).

29. Cella, M. *et al.* Maturation, Activation, and Protection of Dendritic Cells Induced by Double-stranded RNA. *J. Exp. Med.* **189**, 821 (1999).

30. Fancke, B. & O'Keeffe, M. Monitoring dendritic cell activation and maturation. *Methods Mol. Biol.* **960**, 359–370 (2013).

31. Cui, J., Chen, Y., Wang, H. Y. & Wang, R. F. Mechanisms and pathways of innate immune activation and regulation in health and cancer. *http://dx.doi.org/10.4161/21645515.2014.979640* **10**, 3270–3285 (2015).

32. Diebold, S. S. Activation of dendritic cells by toll-like receptors and C-type lectins. *Handb. Exp. Pharmacol.* **188**, 3–30 (2009).

33. Joffre, O., Nolte, M. A., Spörri, R. & Sousa, C. R. E. Inflammatory signals in dendritic cell activation and the induction of adaptive immunity. *Immunol. Rev.* **227**, 234–247 (2009).

34. Dzopalic, T., Rajkovic, I., Dragicevic, A. & Colic, M. The response of human dendritic cells to co-ligation of pattern-recognition receptors. *Immunol. Res.* **52**, 20–33 (2012).

35. Lauterbach, H. *et al.* Mouse CD8alpha+ DCs and human BDCA3+ DCs are major producers of IFN-lambda in response to poly IC. *J. Exp. Med.* **207**, 2703–2717 (2010).

36. Hubert, M. *et al.* IFN-III is selectively produced by cDC1 and predicts good clinical outcome in breast cancer. *Sci. Immunol.* **5**, (2020).

37. Davey, G. M. *et al.* Cutting Edge: Priming of CD8 T Cell Immunity to Herpes Simplex Virus Type 1 Requires Cognate TLR3 Expression In Vivo . *J. Immunol.* **184**, 2243–2246 (2010).

38. Bianchi, F., Pretto, S., Tagliabue, E., Balsari, A. & Sfondrini, L. Exploiting poly(I:C) to induce cancer cell apoptosis. *Cancer Biol. Ther.* **18**, 747–756 (2017).

39. Martins, K. A. O., Bavari, S. & Salazar, A. M. Vaccine adjuvant uses of poly-IC and derivatives. *Expert Rev. Vaccines* **14**, 447–459 (2015).

40. Hafner, A. M., Corthésy, B. & Merkle, H. P. Particulate formulations for the delivery of poly(I: C) as vaccine adjuvant. *Adv. Drug Deliv. Rev.* **65**, 1386–1399 (2013).

41. Cance, J. C., Crozat, K., Dalod, M. & Mattiuz, R. Are conventional type 1 dendritic cells critical for protective antitomor immunity and how? *Front. Immunol.* **10**, (2019).

42. Tjwa, E. T. T. L. *et al.* Restoration of TLR3-activated myeloid dendritic cell activity leads to improved natural killer cell function in chronic hepatitis B virus infection. *J. Virol.* **86**, 4102–4109 (2012).

43. Kawasaki, T. & Kawai, T. Toll-like receptor signaling pathways. *Front. Immunol.* **5**, 461 (2014).

44. Jin, Y., Zhuang, Y., Dong, X. & Liu, M. Development of CpG oligodeoxynucleotide TLR9 agonists in anti-cancer therapy. *Expert Rev. Anticancer Ther.* **21**, 841–851 (2021).

45. Yazdani, M. *et al.* Ex vivo dendritic cell-based (DC) vaccine pulsed with a low dose of liposomal antigen and CpG-ODN improved PD-1 blockade immunotherapy. *Sci. Rep.* **11**, (2021).

46. Shirota, H. & Klinman, D. M. Recent progress concerning CpG DNA and its use as a vaccine adjuvant. *Expert Rev. Vaccines* **13**, 299–312 (2014).

47. Vollmer, J. & Krieg, A. M. Immunotherapeutic applications of CpG oligodeoxynucleotide TLR9 agonists. *Adv. Drug Deliv. Rev.* **61**, 195–204 (2009).

48. Alloatti, A. *et al.* Toll-like Receptor 4 Engagement on Dendritic Cells Restrains Phago-Lysosome Fusion and Promotes Cross-Presentation of Antigens. *Immunity* **43**, 1087–1100 (2015).

49. Biscari, L. *et al.* Immunization With Lipopolysaccharide-Activated Dendritic Cells Generates a Specific CD8+ T Cell Response That Confers Partial Protection Against Infection With Trypanosoma cruzi. *Front. Cell. Infect. Microbiol.* **12**, 966 (2022).

50. Reis E Sousa, C. Activation of dendritic cells: Translating innate into adaptive immunity. *Curr. Opin. Immunol.* **16**, 21–25 (2004).

51. Gallo, P. M. & Gallucci, S. The Dendritic Cell Response to Classic, Emerging, and Homeostatic Danger Signals. Implications for Autoimmunity. *Front. Immunol.* **4**, (2013).

52. Wesa, A. & Galy, A. Increased production of pro-inflammatory cytokines and enhanced T cell responses after activation of human dendritic cells with IL-1 and CD40 ligand. *BMC Immunol.* (2002).

53. Pyrillou, K., Burzynski, L. C. & Clarke, M. C. H. Alternative Pathways of IL-1 Activation, and Its Role in Health and Disease. *Front. Immunol.* **11**, (2020).

54. Feng, M. *et al.* Regulation of the Migration of Distinct Dendritic Cell Subsets. *Front. Cell Dev. Biol.* **9**, 1–13 (2021).

55. Tiberio, L. *et al.* Chemokine and chemotactic signals in dendritic cell migration review-article. *Cell. Mol. Immunol.* **15**, (2018).

56. Dieu, M. C. *et al.* Selective recruitment of immature and mature dendritic cells by distinct chemokines expressed in different anatomic sites. *J. Exp. Med.* **188**, 373–386 (1998).

57. Uguccioni, M. *et al.* Differential ccr7 Targeting in Dendritic cells by Three naturally Occurring cc-chemokines. **7**, 1 (2016).

58. Ohl, L. *et al.* CCR7 governs skin dendritic cell migration under inflammatory and steady-state conditions. *Immunity* **21**, 279–288 (2004).

59. Hong, W., Yang, B., He, Q., Wang, J. & Weng, Q. New Insights of CCR7 Signaling in Dendritic Cell Migration and Inflammatory Diseases. *Front. Pharmacol.* **13**, 1–14 (2022).

60. Li, B. *et al.* CCL19 and CCR7 Expression, Signaling Pathways, and Adjuvant Functions in Viral Infection and Prevention. (2019) doi:10.3389/fcell.2019.00212.

61. Schutyser, E., Struyf, S. & Van Damme, J. The CC chemokine CCL20 and its receptor CCR6. *Cytokine Growth Factor Rev.* **14**, 409–426 (2003).

62. Le Borgne, M. *et al.* Dendritic cells rapidly recruited into epithelial tissues via CCR6/CCL20 are responsible for CD8+ T cell crosspriming in vivo. *Immunity* **24**, 191–201 (2006).

63. Meitei, H. T., Jadhav, N. & Lal, G. CCR6-CCL20 axis as a therapeutic target for autoimmune diseases. *Autoimmun. Rev.* **20**, 102846 (2021).

64. Eisenbarth, S. C. Dendritic cell subsets in T cell programming: location dictates function. *Nat. Rev. Immunol.* **19**, 89 (2019).

65. Corthay, A. A three-cell model for activation of naïve T helper cells. *Scand. J. Immunol.* **64**, 93–96 (2006).

66. Kapsenberg, M. L. Dendritic-cell control of pathogen-driven T-cell polarization. *Nat. Rev. Immunol.* **3**, 984–993 (2003).

67. Blum, J. S., Wearsch, P. A. & Cresswell, P. *Pathways of antigen processing*. *Annual Review of*

Immunology vol. 31 (2013).

68. Kotsias, F., Cebrian, I. & Alloatti, A. Antigen processing and presentation. *Int. Rev. Cell Mol. Biol.* **348**, 69–121 (2019).

69. Noubade, R., Majri-Morrison, S. & Tarbell, K. V. Beyond CDC1: Emerging roles of DC crosstalk in cancer immunity. *Front. Immunol.* **10**, 1–13 (2019).

70. Gutiérrez-Martínez, E. *et al.* Cross-presentation of cell-associated antigens by MHC class I in dendritic cell subsets. *Front. Immunol.* **6**, 146579 (2015).

71. Belz, G. T., Shortman, K., Bevan, M. J. & Heath, W. R. CD8α+Dendritic Cells Selectively Present MHC Class I-Restricted Noncytolytic Viral and Intracellular Bacterial Antigens In Vivo. *J. Immunol.* 2–6 (2005).

72. Smith, C. M. *et al.* Cutting Edge: Conventional CD8α+ Dendritic Cells Are Preferentially Involved in CTL Priming After Footpad Infection with Herpes Simplex Virus-1. *J. Immunol.* **170**, 4437–4440 (2003).

73. Domenjo-Vila, E. *et al.* XCR1+ DCs are critical for T cell-mediated immunotherapy of chronic viral infections. *Cell Rep.* **42**, (2023).

74. Iborra, S. *et al.* Optimal Generation of Tissue-Resident but Not Circulating Memory T Cells during Viral Infection Requires Crosspriming by DNGR-1+ Dendritic Cells. *Immunity* **45**, 847–860 (2016).

75. Böttcher, J. P. & Reis e Sousa, C. The Role of Type 1 Conventional Dendritic Cells in Cancer Immunity. *Trends in Cancer* **4**, 784–792 (2018).

76. Sánchez-Paulete, A. R. *et al.* Cancer Immunotherapy with Immunomodulatory Anti-CD137 and Anti-PD-1 Monoclonal Antibodies Requires BATF3-Dependent Dendritic Cells. *Cancer Discov.* **6**, 71–79 (2016).

77. Kumar, S., Jeong, Y., Ashraf, M. U. & Bae, Y. S. Dendritic cell-mediated th2 immunity and immune disorders. *Int. J. Mol. Sci.* **20**, (2019).

78. Iborra, S. *et al.* Leishmania Uses Mincle to Target an Inhibitory ITAM Signaling Pathway in Dendritic Cells that Dampens Adaptive Immunity to Infection. *Immunity* **45**, 788–801 (2016).

79. Satpathy, A. T. *et al.* Notch2-dependent classical dendritic cells orchestrate intestinal immunity to attaching-and-effacing bacterial pathogens. *Nat. Immunol.* **14**, 937–948 (2013).

80. Eickhoff, S. *et al.* Robust Anti-viral Immunity Requires Multiple Distinct T Cell-Dendritic Cell Interactions. *Cell* **162**, 1322–1337 (2015).

81. Ferris, S. T. *et al.* cDC1 prime and are licensed by CD4+ T cells to induce anti-tumour immunity. *Nature* **584**, 624–629 (2020).

82. Martínez-López, M., Iborra, S., Conde-Garrosa, R. & Sancho, D. Batf3-dependent CD103+ dendritic cells are major producers of IL-12 that drive local Th1 immunity against Leishmania major infection in mice. *Eur. J. Immunol.* **45**, 119–129 (2015).

83. Liu, C.-H. *et al.* Cutting Edge: Dendritic Cells Are Essential for In Vivo IL-12 Production and Development of Resistance against Toxoplasma gondii Infection in Mice. *J. Immunol.* **177**, 31–35 (2006).

84. Collin, M. & Bigley, V. Human dendritic cell subsets: an update. *Immunology* **154**, 3–20 (2018).

85. Rizzitelli, A. *et al.* Switching from a restricted to an effective CD4 T cell response by activating CD8+ murine dendritic cells with a Toll-like receptor 9 ligand. *Eur. J. Immunol.* **35**, 3209–3220 (2005).

86. Bosteels, C. *et al.* Inflammatory Type 2 cDCs Acquire Features of cDC1s and Macrophages to Orchestrate Immunity to Respiratory Virus Infection. *Immunity* **52**, 1039-1056.e9 (2020).

87. Buchbinder, E. I. & Desai, A. CTLA-4 and PD-1 pathways similarities, differences, and implications of their inhibition. *Am. J. Clin. Oncol. Cancer Clin. Trials* **39**, 98–106 (2016).

88. Ma, D. Y. & Clark, E. A. The role of CD40 and CD40L in Dendritic Cells. *Semin Immunol* **21**, 265–272 (2009).

89. Hilligan, K. L. & Ronchese, F. Antigen presentation by dendritic cells and their instruction of CD4+ T helper cell responses. *Cell. Mol. Immunol.* **17**, 587–599 (2020).

90. Yin, X., Chen, S. & Eisenbarth, S. C. Dendritic Cell Regulation of T Helper Cells. *Annual Review of Immunology* vol. 39 759–790 at https://doi.org/10.1146/annurev-immunol-101819-025146 (2021).

91. Walsh, K. P. & Mills, K. H. G. Dendritic cells and other innate determinants of T helper cell polarisation. *Trends Immunol.* 1–10 (2013) doi:10.1016/j.it.2013.07.006.

92. Pereda, A. E. Electrical synapses and their functional interactions with chemical synapses. *Nat. Rev. Neurosci.* **15**, 250–263 (2014).

93. Catala, M. & Kubis, N. Gross anatomy and development of the peripheral nervous system. *Handb. Clin. Neurol.* **115**, 29–41 (2013).

94. Sheffler, Z. M., Reddy, V. & Pillarisetty, L. S. *Physiology, Neurotransmitters*. *StatPearls* (StatPearls Publishing, 2022).

95. Thau, L., Reddy, V. & Singh, P. *Anatomy, Central Nervous System*. *StatPearls* vol. 1 (StatPearls Publishing, 2022).

96. Pavlov, V. A., Chavan, S. S. & Tracey, K. J. Molecular and Functional Neuroscience in Immunity. *Annu. Rev. Immunol.* **36**, 783–812 (2018).

97. Basso, L., Serhan, N., Tauber, M. & Gaudenzio, N. Peripheral neurons: Master regulators of skin and mucosal immune response. *Eur. J. Immunol.* **49**, 1984–1997 (2019).

98. Waxenbaum, J. A., Reddy, V. & Varacallo, M. *Anatomy, Autonomic Nervous System*. *StatPearls* (StatPearls Publishing, 2022).

99. McCorry, L. K. Physiology of the Autonomic Nervous System. *Am. J. Pharm. Educ.* **71**, (2007).

100. Gibbons, C. H. Basics of autonomic nervous system function. *Handb. Clin. Neurol.* **160**, 407–418 (2019).

101. Cristina Godinho-Silva, Filipa Cardoso, and H. V.-F. Neuro–Immune Cell Units_ A New Paradigm in Physiology.pdf.

102. Takenaka, M. C., Guereschi, M. G. & Basso, A. S. Neuroimmune interactions: dendritic cell modulation by the sympathetic nervous system. *Semin. Immunopathol.* **39**, 165–176 (2017).

103. Chhatar, S. & Lal, G. Role of adrenergic receptor signalling in neuroimmune communication. *Curr. Res. Immunol.* **2**, 202–217 (2021).

104. Perez, D. M. α1-Adrenergic Receptors in Neurotransmission, Synaptic Plasticity, and Cognition. *Front. Pharmacol.* **11**, 1–22 (2020).

105. Kraus, A., Buckley, K. M. & Salinas, I. Sensing the world and its dangers: An evolutionary perspective in neuroimmunology. *Elife* **10**, 1–33 (2021).

106. Talbot, S., Foster, S. L. & Woolf, C. J. Neuroimmunity: Physiology and Pathology. *Annu. Rev. Immunol.* **34**, 421–447 (2016).

107. Kioussis, D. & Pachnis, V. Immune and Nervous Systems: More Than Just a Superficial Similarity? *Immunity* **31**, 705–710 (2009).

108. Veiga-Fernandes, H. & Mucida, D. Neuro-Immune Interactions at Barrier Surfaces. *Cell* **165**, 801–811 (2016).

109. Chavan, S. S., Pavlov, V. A. & Tracey, K. J. Mechanisms and Therapeutic Relevance of Neuro-immune Communication. *Immunity* **46**, 927–942 (2017).

110. Kawli, T., He, F. & Tan, M. W. It takes nerves to fight infections: insights on neuro-immune interactions from C. elegans. *Dis. Model. Mech.* **3**, 721 (2010).

111. Blake, K. J., Jiang, X. R. & Chiu, I. M. Neuronal Regulation of Immunity in the Skin and Lungs. *Trends Neurosci.* **42**, 537–551 (2019).

112. Huh, J. R. & Veiga-Fernandes, H. Neuroimmune circuits in inter-organ communication. *Nat. Rev. Immunol.* **20**, 217–228 (2020).

113. Veiga-Fernandes, H. & Pachnis, V. Neuroimmune regulation during intestinal development and homeostasis. *Nat. Immunol.* **18**, 116–122 (2017).

114. Pacheco, R. *et al.* Cells, Molecules and Mechanisms Involved in the Neuro-Immune Interaction. *Cell Interact.* (2012) doi:10.5772/48367.

115. Veiga-Fernandes, H. & Artis, D. Neuronal-immune system cross-talk in homeostasis. *Science (80-.).* **359**, 1465–1466 (2018).

116. Shurin, M. R., Shurin, G. V., Zlotnikov, S. B. & Bunimovich, Y. L. The Neuroimmune Axis in the Tumor Microenvironment. *J. Immunol.* **204**, 280–285 (2020).

117. Nutma, E., Willison, H., Martino, G. & Amor, S. Neuroimmunology – the past, present and future. *Clin. Exp. Immunol.* **197**, 278–293 (2019).

118. Nisticò, R. *et al.* Synaptoimmunology - roles in health and disease. *Mol. Brain 2017 101* **10**, 1–12 (2017).

119. Bucsek, M. J., Giridharan, T., MacDonald, C. R., Hylander, B. L. & Repasky, E. A. An overview of the role of sympathetic regulation of immune responses in infectious disease and autoimmunity. *Int. J. Hyperth.* **34**, 135–143 (2018).

120. Pavlov, V. A. & Tracey, K. J. Neural regulation of immunity: Molecular mechanisms and clinical translation. *Nat. Neurosci.* **20**, 156–166 (2017).

121. Bellocchi, C. *et al.* The Interplay between Autonomic Nervous System and Inflammation across Systemic Autoimmune Diseases. *Int. J. Mol. Sci. 2022, Vol. 23, Page 2449* **23**, 2449 (2022).

122. Klein Wolterink, R. G. J., Wu, G. S., Chiu, I. M. & Veiga-Fernandes, H. Neuroimmune Interactions in Peripheral Organs. *Annu. Rev. Neurosci.* (2022) doi:10.1146/annurev-neuro-111020.

123. Chesné, J., Cardoso, V. & Veiga-Fernandes, H. Neuro-immune regulation of mucosal physiology. *Mucosal Immunol.* **12**, 10–20 (2019).

124. Shouman, K. & Benarroch, E. E. Peripheral neuroimmune interactions: selected review and some clinical implications. *Clin. Auton. Res. 2021 314* **31**, 477–489 (2021).

125. Hoffman, C. & Aballay, A. Role of neurons in the control of immune defense. *Curr. Opin. Immunol.* **60**, 30–36 (2019).

126. Franco, R., Pacheco, R., Lluis, C., Ahern, G. P. & O'Connell, P. J. The emergence of neurotransmitters as immune modulators. *Trends Immunol.* **28**, 400–407 (2007).

127. Klose, C. S. N. & Veiga-Fernandes, H. Neuroimmune interactions in peripheral tissues. *Eur. J. Immunol.* **51**, 1602–1614 (2021).

128. Scanzano, A. & Cosentino, M. Adrenergic regulation of innate immunity: A review. *Front. Pharmacol.* **6**, (2015).

129. Fujii, T. *et al.* Physiological functions of the cholinergic system in immune cells. *J. Pharmacol. Sci.* **134**, 1–21 (2017).

130. Wang, F. & Kim, B. S. Itch: A Paradigm of Neuroimmune Crosstalk. *Immunity* **52**, 753–766 (2020).

131. Baral, P., Udit, S. & Chiu, I. M. Pain and immunity: implications for host defence. *Nat. Rev. Immunol.* **19**, 433–447 (2019).

132. Dubin, A. E. & Patapoutian, A. Nociceptors: the sensors of the pain pathway. *J. Clin. Invest.* **120**, 3760 (2010).

133. Pinho-Ribeiro, F. A., Verri, W. A. & Chiu, I. M. Nociceptor Sensory Neuron-Immune Interactions in Pain and Inflammation. *Trends Immunol.* **38**, 5 (2017).

134. Jean, E. E., Good, O., Rico, J. M. I., Rossi, H. L. & Herbert, D. R. Neuroimmune regulatory networks of the airway mucosa in allergic inflammatory disease. *J. Leukoc. Biol.* **111**, 209 (2022).

135. Le, D. D. *et al.* Allergic airway inflammation induces the migration of dendritic cells into airway sensory ganglia. *Respir. Res.* **15**, 1–12 (2014).

136. Voedisch, S., Rochlitzer, S., Veres, T. Z., Spies, E. & Braun, A. Neuropeptides Control the Dynamic Behavior of Airway Mucosal Dendritic Cells. **7**, 1–12 (2012).

137. Nijhuis, L. E. J., Olivier, B. J. & de Jonge, W. J. Neurogenic regulation of dendritic cells in the intestine. *Biochem. Pharmacol.* **80**, 2002–2008 (2010).

138. Jacobson, A., Yang, D., Vella, M. & Chiu, I. M. The intestinal neuro-immune axis: crosstalk between neurons, immune cells, and microbes. *Mucosal Immunol. 2021 143* **14**, 555–565 (2021).

139. Okumura, R. & Takeda, K. Maintenance of gut homeostasis by the mucosal immune system. *Proc. Jpn. Acad. Ser. B. Phys. Biol. Sci.* **92**, 423 (2016).

140. Brun, P., Akbarali, H. I. & Castagliuolo, I. Editorial: The Gut Microbiota Orchestrates the Neuronal-Immune System. *Front. Cell Dev. Biol.* **9**, 627 (2021).

141. Stagg, A. J. Intestinal Dendritic Cells in Health and Gut Inflammation. *Front. Immunol.* **9**, 1–10 (2018).

142. Delgado, M., Reduta, A., Sharma, V. & Ganea, D. VIP/PACAP oppositely affects immature and mature dendritic cell expression of CD80/CD86 and the stimulatory activity for CD4+ T cells. *J. Leukoc. Biol.* **75**, 1122–1130 (2004).

143. Kim, T. G. *et al.* Skin-Specific CD301b + Dermal Dendritic Cells Drive IL-17−Mediated Psoriasis-Like Immune Response in Mice. *J. Invest. Dermatol.* **138**, 844–853 (2018).

144. Kashem, S. W. *et al.* Nociceptive Sensory Fibers Drive Interleukin-23 Production from CD301b+ Dermal Dendritic Cells and Drive Protective Cutaneous Immunity. *Immunity* **43**, 515–526 (2015).

145. Perner, C. *et al.* Substance P Release by Sensory Neurons Triggers Dendritic Cell Migration and Initiates the Type-2 Immune Response to Allergens. *Immunity* **53**, 1063-1077.e7 (2020).

146. Riol-Blanco, L. *et al.* Nociceptive sensory neurons drive interleukin-23-mediated psoriasiform skin inflammation. *Nature* **510**, 157–161 (2014).

147. Salamone, G. *et al.* Cholinergic modulation of dendritic cell function. *J. Neuroimmunol.* **236**, 47–56 (2011).

148. Liu, D. *et al.* The effect of the cholinergic anti-inflammatory pathway on collagen-induced arthritis involves the modulation of dendritic cell differentiation. *Arthritis Res. Ther.* **20**, 1–11 (2018).

149. Gori, S. *et al.* Acetylcholine polarizes dendritic cells toward a Th2-promoting profile. *Allergy Eur. J. Allergy Clin. Immunol.* **72**, 221–231 (2017).

150. Gori, S. *et al.* Acetylcholine-treated murine dendritic cells promote inflammatory lung injury. *PLoS One* **14**, 1–14 (2019).

151. Teratani, T. *et al.* The liver–brain–gut neural arc maintains the Treg cell niche in the gut. *Nature* **585**, 591–596 (2020).

152. Maestroni, G. J. M. Sympathetic nervous system influence on the innate immune response. *Ann. N. Y. Acad. Sci.* **1069**, 195–207 (2006).

153. Bellinger, D. L. & Lorton, D. Autonomic regulation of cellular immune function. *Auton. Neurosci. Basic Clin.* **182**, 15–41 (2014).

154. Takenaka, M. C. *et al.* Norepinephrine Controls Effector T Cell Differentiation through β2-Adrenergic Receptor–Mediated Inhibition of NF-κB and AP-1 in Dendritic Cells. *J. Immunol.* **196**, 637–644 (2016).

155. Maestroni, G. Adrenergic Modulation of Dendritic Cells Function: Relevance for the Immune Homeostasis. *Curr. Neurovasc. Res.* **2**, 169–173 (2005).

156. Nijhuis, L. E. *et al.* Adrenergic β2 receptor activation stimulates anti-inflammatory properties of dendritic cells in vitro. *PLoS One* **9**, 2–3 (2014).

157. Yanagawa, Y., Matsumoto, M. & Togashi, H. Enhanced Dendritic Cell Antigen Uptake via α2 Adrenoceptor-Mediated PI3K Activation Following Brief Exposure to Noradrenaline. *J. Immunol.* **185**, 5762–5768 (2010).

158. Maestroni, G. J. M. Dendritic Cell Migration Controlled by α1b-Adrenergic Receptors. *J. Immunol.* **165**, 6743–6747 (2000).

159. Hervé, J. *et al.* β2-Adrenoreceptor Agonist Inhibits Antigen Cross-Presentation by Dendritic Cells. *J. Immunol.* **190**, 3163–3171 (2013).

160. Manni, M., Granstein, R. D. & Maestroni, G. β2-Adrenergic agonists bias TLR-2 and NOD2 activated dendritic cells towards inducing an IL-17 immune response. *Cytokine* **55**, 380–386 (2011).

161. Maestroni, G. J. M. Short exposure of maturing, bone marrow-derived dendritic cells to norepinephrine: Impact on kinetics of cytokine production and Th development. *J. Neuroimmunol.* **129**, 106–114 (2002).

162. Jakob, M. O., Murugan, S. & Klose, C. S. N. Neuro-Immune Circuits Regulate Immune Responses in Tissues and Organ Homeostasis. *Front. Immunol.* **11**, 1–17 (2020).

163. Maestroni, G. J. M. & Mazzola, P. Langerhans cells β2-adrenoceptors: Role in migration, cytokine production, Th priming and contact hypersensitivity. *J. Neuroimmunol.* **144**, 91–99 (2003).

164. Cells, D. *et al.* GM-CSF Mouse Bone Marrow Cultures Comprise a Resource GM-CSF Mouse Bone Marrow Cultures Comprise a Heterogeneous Population. 1197–1211 (2015) doi:10.1016/j.immuni.2015.05.018.

165. Mattiuz, R. *et al.* Novel Cre-Expressing Mouse Strains Permitting to Selectively Track and Edit Type 1 Conventional Dendritic Cells Facilitate Disentangling Their Complexity in vivo. *Front. Immunol.* **9**, 1–14 (2018).

166. Ohta, T., Sugiyama, M., Hemmi, H. & Yamazaki, C. Crucial roles of XCR1-expressing dendritic cells and the XCR1- XCL1 chemokine axis in intestinal immune homeostasis. *Nat. Publ. Gr.* 1–11 (2016) doi:10.1038/srep23505.

167. Savitt, J. M., Jang, S. S., Mu, W., Dawson, V. L. & Dawson, T. M. Bcl-x is required for proper development of the mouse: Substantia nigra. *J. Neurosci.* **25**, 6721–6728 (2005).

168. Madisen, L. *et al.* A robust and high-throughput Cre reporting and characterization system for the whole mouse brain. *Nat. Neurosci.* **13**, 133–140 (2010).

169. Madisen, L. *et al.* A toolbox of Cre-dependent optogenetic transgenic mice for light-induced activation and silencing. *Nat. Neurosci.* **15**, 793–802 (2012).

170. Hinoi, E. *et al.* The sympathetic tone mediates leptin's inhibition of insulin secretion by modulating osteocalcin bioactivity. *J. Cell Biol.* **183**, 1235–1242 (2008).

171. Thoenen, H. & Tranzer, J. P. Chemical sympathectomy by selective destruction of adrenergic nerve endings with 6-hydroxydopamine. *Naunyn. Schmiedebergs. Arch. Pharmakol. Exp. Pathol.* **261**, 271–288 (1968).

172. Wang, Y. *et al.* The role of somatosensory innervation of adipose tissues. *Nature* **609**, 569–574 (2022).

173. Yamazaki, T., Li, W. & Mukouyama, Y. S. Whole-mount confocal microscopy for adult ear skin: A model system to study neuro-vascular branching morphogenesis and immune cell distribution. *J. Vis. Exp.* **2018**, 1–5 (2018).

174. Proietto, A. I. *et al.* Differential production of inflammatory chemokines by murine dendritic cell subsets. **209**, 163–172 (2004).

175. Smith MD, Maani CV. Norepinephrine. In: StatPearls. Treasure Island (FL): StatPearls Publishing; May 8, 2023.

176. Kamath, A. T., Henri, S., Battye, F., Tough, D. F. & Shortman, K. Developmental kinetics and lifespan of dendritic cells in mouse lymphoid organs. *Blood* **100**, 1734–1741 (2002).

177. Bylund, D. B. & Gruetter, C. A. Propranolol. *xPharm Compr. Pharmacol. Ref.* 1–9 (2007) doi:10.1016/B978-008055232-3.62481-X.

178. Stüssel, P. *et al.* Propranolol Is an Effective Topical and Systemic Treatment Option for Experimental Epidermolysis Bullosa Acquisita. *J. Invest. Dermatol.* **140**, 2408–2420 (2020).

179. Jefferson, D., Wharrad, H., Birmingham, A. & Patrick, J. The comparative effects of ICI 118551 and propranolol on essential tremor. *Br. J. Clin. Pharmacol.* **24**, 729–734 (1987).

180. Bilski, A. J., Halliday, S. E., Fitzgerald, J. D. & Wale, J. L. The pharmacology of a beta 2-selective adrenoceptor antagonist (ICI 118,551). *J. Cardiovasc. Pharmacol.* **5**, 430–437 (1983).

7. Annexes

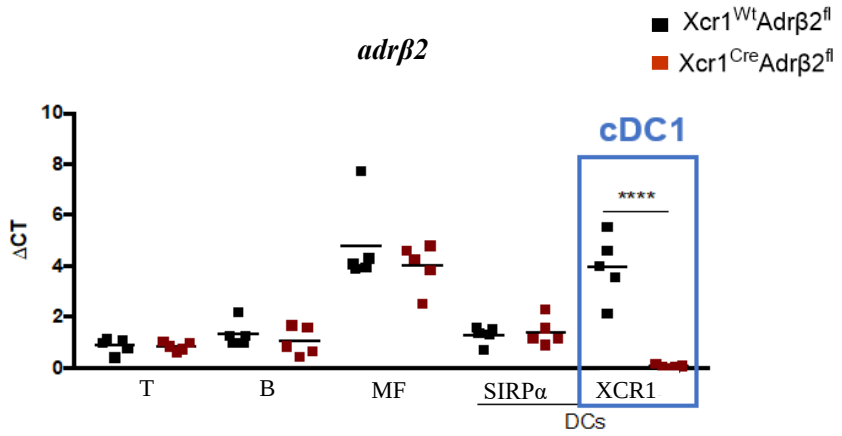

Figure 7.1. qPCR results of sorted splenic immune populations of *Xcr1*^{Cre}*Adrβ2*^{fl} mice. *adrβ2* expression levels values in each sorted immune population: cDC1(MHC-II$^+$ CD11c$^+$ XCR1$^+$); cDC2 (MHC-II$^+$ CD11c$^+$ SIRPα$^+$) macrophages (MF) (CD64$^+$), T (CD3$^+$) and B cells (CD19$^+$). The selected probes for qPCR reaction were obtained from Thermo Fisher Scientific illustrated in Table 2.7A. *gadph* and *hprt* were the chosen housekeeping genes. These plots were obtained by applying ordinary one-way ANOVA using GraphPad Prism 8.4.3 version for Windows (GraphPad Software, San Diego, Califórnia EUA). Data generated by María Martinéz-López and Raquel Silva.

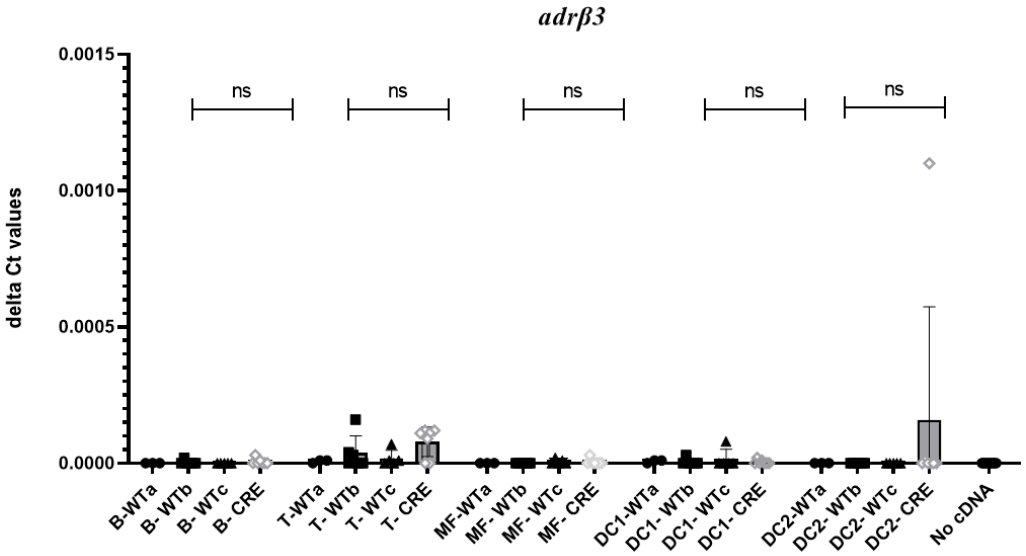

Figure 7.2. *adrβ3* expression level values in each immune population. The selected probes for qPCR reaction were obtained by Applied Biosystems™ TaqMan®, illustrated in Table 7A. *gadph* and *hprt* were the chosen housekeeping genes. These plots were obtained by applying ordinary one-way ANOVA with multiple comparisons per immune population using GraphPad Prism 8.4.3 version for Windows (GraphPad Software, San Diego, California EUA). Abbreviations: ns- non-significant result (p-value>0.05). Wta- *Xcr1/ksho*$^{Cre/Wt}$*Adrβ2*$^{Wt/Wt}$ mice. Wtb- *Xcr1/ksho*^{Wt}*Adrβ2*$^{fl/Wt}$ mice. WTc- *Xcr1/ksho*$^{Wt/Wt}$*Adrβ2*$^{fl/fl}$ mice. CRE- *Xcr1/ksho*$^{Cre/Wt}$*Adrβ2*$^{fl/Wt}$ mice. B- B immune cell; T- T immune cell. MF- macrophage immune cell. DC1- cDC1 immune cell; DC2- cDC2 immune cell. These results are derived from two independent experiments which account for 3Wta, 6Wtb, 5Wtc and, 7 CRE mice. No cDNA values represent a control group, in which instead of cDNA plus RNAse-free, only RNAse-free were incubated with RT enzyme in the cDNA synthesis step.

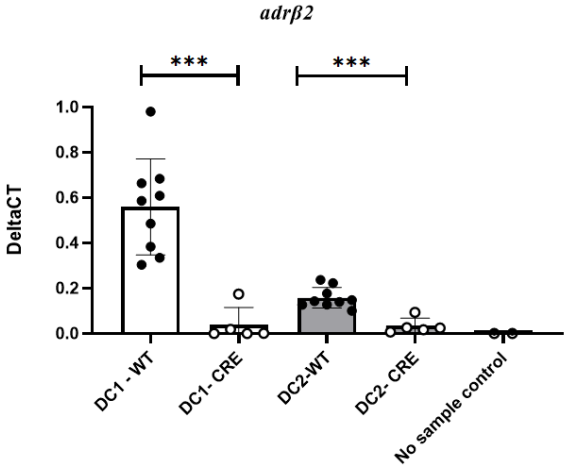

Figure 7.3. qPCR results of sorted cDC1 and cDC2 splenic immune populations of *Xcr1/ksho*^{Cre}*Adrβ2*^{fl} (CRE) and *Xcr1/ksho*^{Wt}*Adrβ2*^{fl}(Wt) mice to infer levels of *adrβ2* receptor. These statistical values were obtained by performing unpaired t-test for both cDC1 and cDC2 using GraphPad Prism version 8.4.3 for Windows (GraphPad Software, San Diego, California USA). Abbreviations: DC1- cDC1 immune cell; DC2- cDC2 immune cell. These results are derived from two independent experiments which account for 9 *Xcr1/ksho*^{Wt}*Adrβ2*^{fl} and 5 *Xcr1/ksho*^{Cre}*Adrβ2*^{fl} mice.

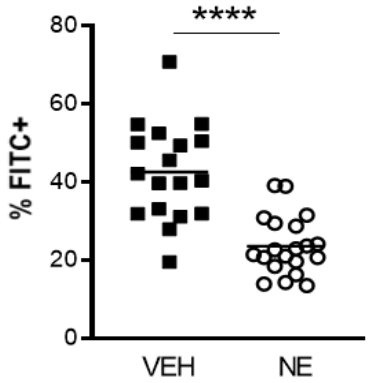

Figure 7.4. Migration capability of cDC1 following i.d NE treatment. *C57BL/6J* mice were i.d injected for 3 consecutive days with NE in the ear. As control, there are *C57BL/6J* mice treated with a vehicle solution containing 0.1% ascorbic acid and 0.9 % NaCl. Afterward, on the last, day the mice suffered i.d injections in the ear with a stimulation mix containing CpG/Poly(I:C). 2-3 hours after, the mice suffered skin sensitization with topical administration of 1% FITC prepared in an inflammatory stimulating solution of acetone and DBP. The removed LNs were then stained with extracellular antibodies (Table 2.5). The analysis was performed by using FlowJo™ Software for Windows Version 10.8.1. Ashland, OR: Becton, Dickinson and Company; 2023. These values were obtained by unpaired t-test using GraphPad Prism version 8.4.3 for Windows (GraphPad Software, San Diego, California USA). Data generated by María Martinéz-López and Raquel Silva.

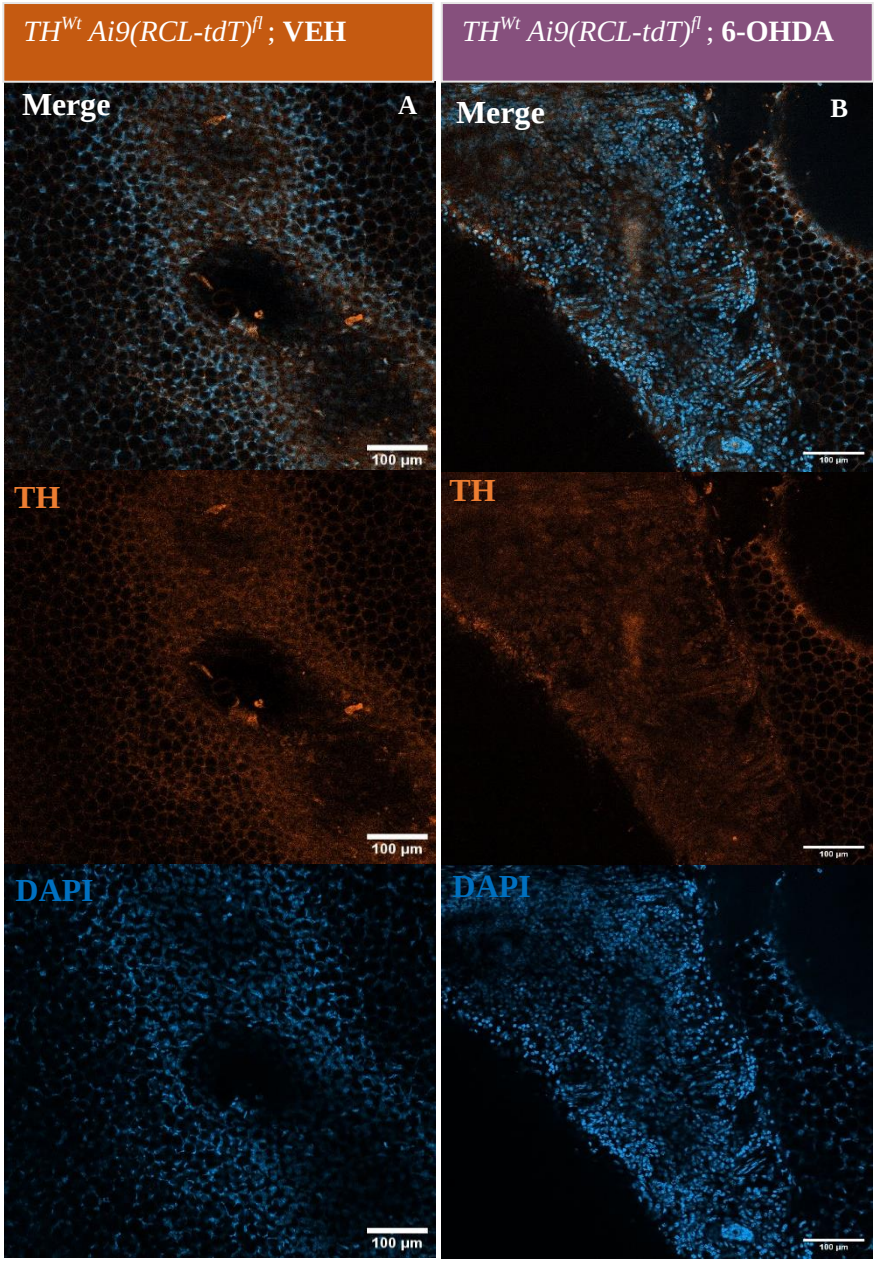

Figure 7.5. Whole mount ears acquisition following 2-day i.d injection in the ears with 25µL of 0.1% ascorbic acid and 0.9% NaCl (VEH) (**A**) or 6-OHDA at 12mg/mL (**B**) in *TH^{Wt} Ai9(RCL-tdT)^{fl}* genetic mice. Images generated by ZEISS LSM 980 inverted confocal microscopy with magnification 20x; scale bar, 100 µm. **A** and **B** are representative images. TH^{+} neurons express Cre-dependent tdtomato endogenous fluorescence (red). The nuclei were stained with DAPI (blue).

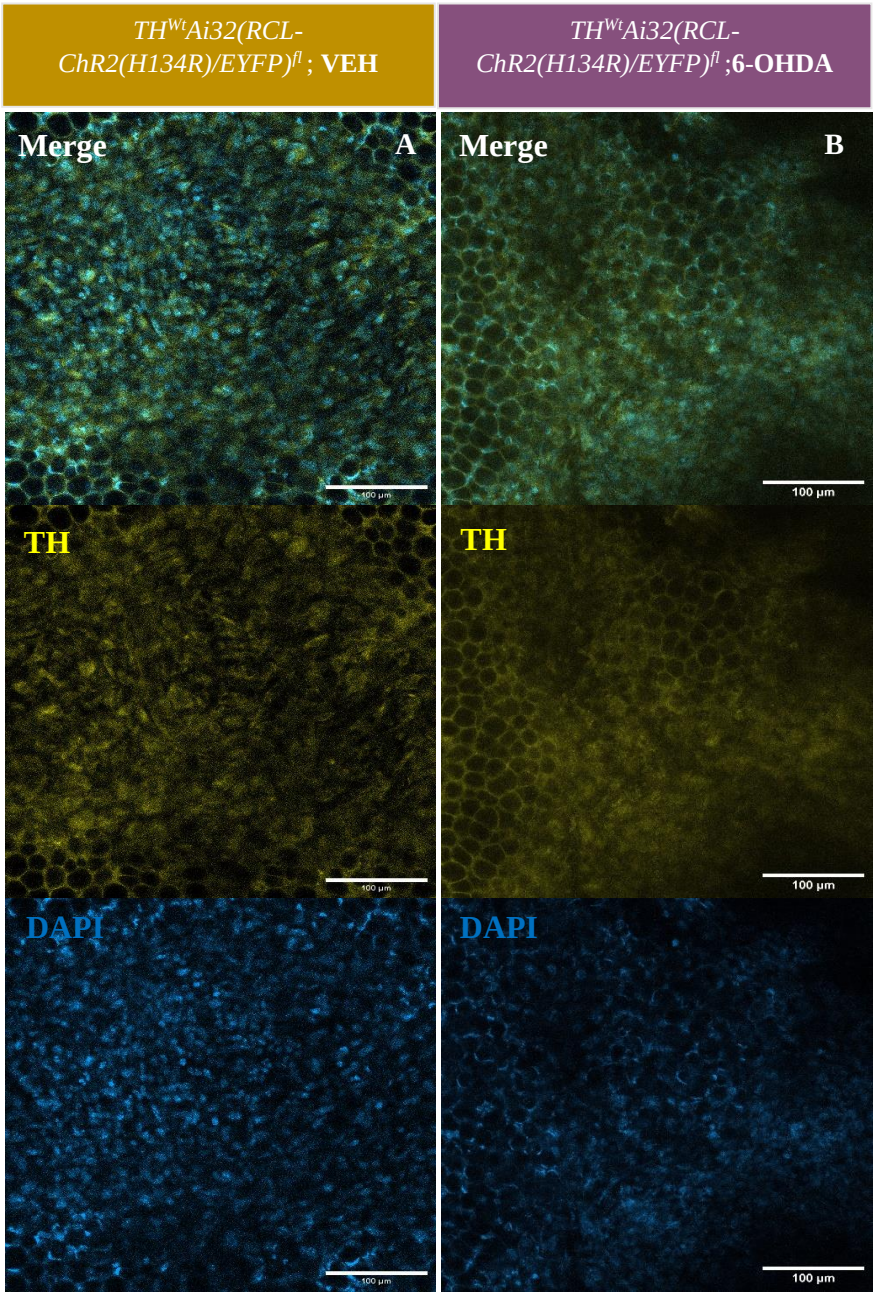

Figure 7.6. Whole mount ears acquisition following 2-day i.d injection in two separate regions of the ears with 25µL of 0.1% ascorbic acid and 0.9% NaCl (VEH) (**A**) or 6-OHDA at 24mg/mL (**B**) in *TH^{Wt}Ai32(RCL-ChR2(H134R)/EYFP)^{fl}* genetic mice. Images generated by ZEISS LSM 980 inverted confocal microscopy with magnification 20x; scale bar, 100 µm. **A** and **B** are representative images. TH^{+} neurons express Cre-dependent YFP endogenous fluorescence (yellow). The nuclei were stained with DAPI (blue).

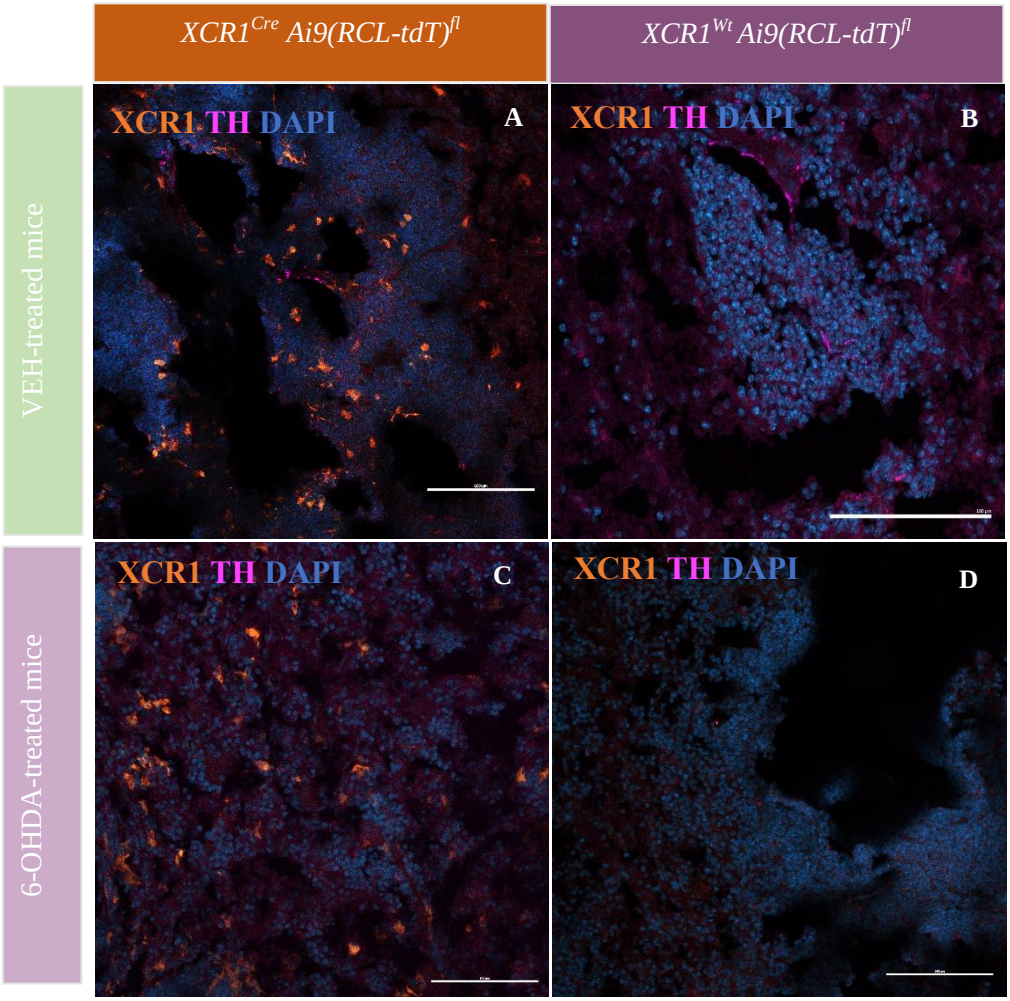

Figure 7.7. Confocal microscopy acquisitions of the spleen. **A-** *XCR1^{Cre}Ai9(RCL-tdT)^{fl}* mice treated with 0.1% ascorbic acid and 0.9% NaCl (VEH) solution. **B-** *XCR1^{Wt}Ai9(RCL-tdT)^{fl}* mice treated with VEH solution. **C-** *XCR1^{Cre}Ai9(RCL-tdT)^{fl}* mice treated with 6-OHDA solution. **D-** *XCR1^{Wt}Ai9(RCL-tdT)^{fl}* mice treated with 6-OHDA solution. The cDC1s are labeled with tdTomato-endogenous fluorescence. Neurons are labeled with rabbit anti-mouse Tyrosine hydroxylase + anti-rabbit AF647 to identify sympathetic peripherical neurons. DAPI stains the nuclei of cells with blue fluorescence. Images generated by ZEISS LSM 980 inverted confocal microscopy with magnification 20x; scale bar, 100 µm.

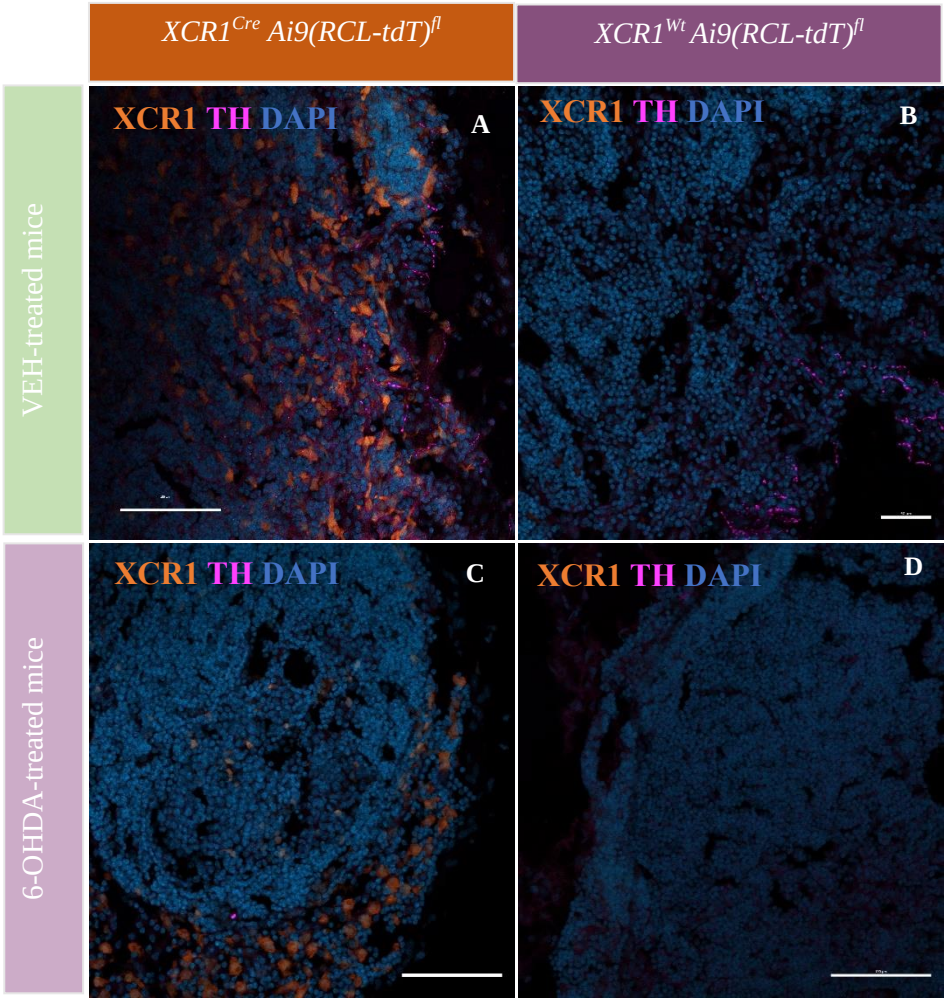

Figure 7.8. Confocal microscopy acquisitions of the mesenteric lymph node. **A-** *XCR1^{Cre}Ai9(RCL-tdT)^{fl}* mice treated with 0.1% ascorbic acid and 0.9% NaCl (VEH) solution. **B-** *XCR1^{Wt}Ai9(RCL-tdT)^{fl}* mice treated with VEH solution. **C-** *XCR1^{Cre}Ai9(RCL-tdT)^{fl}* mice treated with 6-OHDA solution. **D-** *XCR1^{Wt}Ai9(RCL-tdT)^{fl}* mice treated with 6-OHDA solution. The cDC1s are labeled with tdTomato-endogenous fluorescence. Neurons are labeled with rabbit anti-mouse Tyrosine hydroxylase + anti-rabbit AF647 to identify sympathetic peripherical neurons. DAPI stains the nuclei of cells with blue fluorescence. Images generated by ZEISS LSM 980 inverted confocal microscopy with magnification 20x; scale bar, 100 µm.

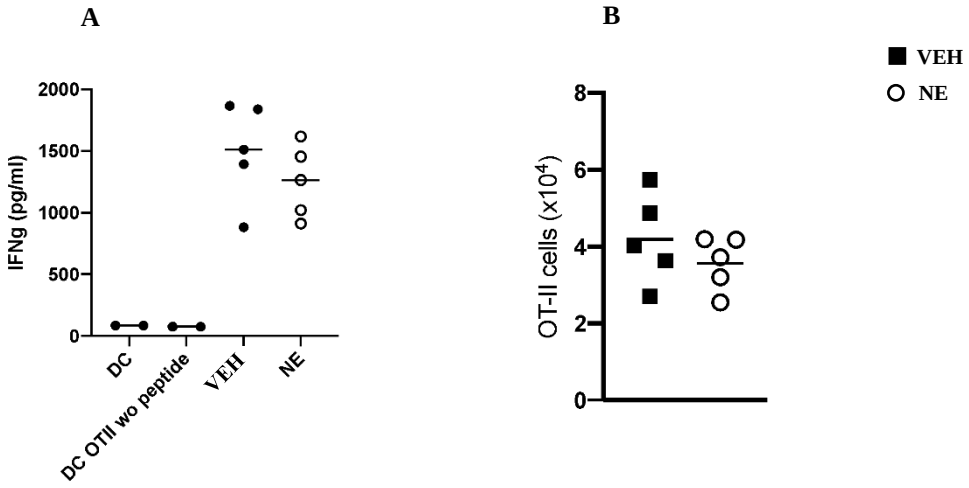

Figure 7.9. Antigen presentation following i.p NE treatment. *C57BL/6J* mice were i.p injected for 3 consecutive days with NE or vehicle (VEH) solution containing 0.1% ascorbic acid and 0.9% NaCl. Afterward, CD11c purified splenic cDC1s were sorted and plated with OT-II cells for 3 days. Posteriorly, the supernatant was collected to perform BD OptEIA™ Mouse IFN-γ Elisa Kit (BD Bioscience) to measure IFN-γ production **(A)**. Later, a stimulatory mix containing PMA and ionomycin was supplied together with Brefeldin A. After a 3-hour stimulation period, the cell pellet was stained and fixed to measure proliferation of OT-II cells **(B)**. The analysis was performed by using FlowJo™ Software for Windows Version 10.8.1. Ashland, OR: Becton, Dickinson and Company; 2023. These values were obtained by unpaired t-test using GraphPad Prism version 8.4.3 for Windows (GraphPad Software, San Diego, California USA). Data generated by María Martinéz-López and Raquel Silva.

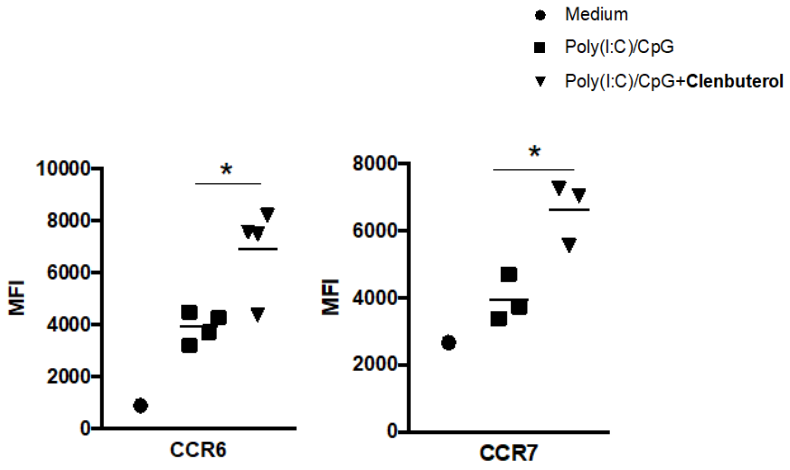

Figure 7.10. Chemokine receptors values following clenbuterol. Splenic cDC1 from *C57BL/6J* mice were sorted and stimulated with CpG/Poly(I:C), apart from the unstimulated controls, in the presence or not of clenbuterol. After stimulation, the cells were stained for extracellular antibodies depicted in Table 2.2. The analysis was conducted by using FlowJo™ Software for Windows Version 10.8.1. Ashland, OR: Becton, Dickinson and Company; 2023. These values were obtained by unpaired t-test using GraphPad Prism version 8.4.3 for Windows (GraphPad Software, San Diego, California USA). Data generated by María Martinéz-López and Raquel Silva.

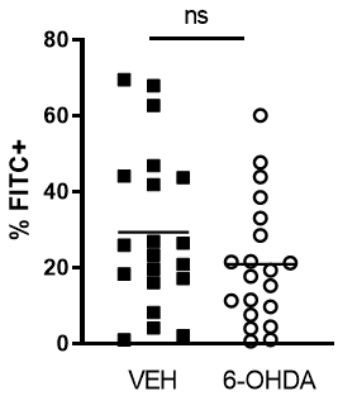

Figure 7.11. Migration capability of cDC1 following i.p 6-OHDA treatment. *C57BL/6J* mice were i.p injected for 5 consecutive days with 6-OHDA in the ear. As control there are *C57BL/6J* mice treated with a vehicle solution containing 0.1% ascorbic acid and 0.9 % NaCl. Afterward, in the next day the mice suffered i.d injections in the ear with a stimulation mix containing CpG/Poly(I:C). 2-3 hours after, the mice suffered skin sensitization with topical administration of 1% FITC prepared in an inflammatory stimulating solution of acetone and DBP. The removed LNs were then stained with extracellular antibodies (Table 2.5). The analysis was performed by using FlowJo™ Software for Windows Version 10.8.1. Ashland, OR: Becton, Dickinson and Company; 2023. These values were obtained by unpaired t-test using GraphPad Prism version 8.4.3 for Windows (GraphPad Software, San Diego, California USA). Data generated by María Martinéz-López and Raquel Silva.

2023

Miguel Ângelo Magalhães Patrício

Dendritic cells, bridging neuromodulation and immunity

NOVA SCHOOL OF SCIENCE & TECHNOLOGY